

SUPPORTING INFORMATION

A Polyketide Cyclase That Forms Medium-ring Lactones

De-Wei Gao,^{1,†‡} Cooper S. Jamieson,^{2,†} Gaoqian Wang^{3,†} Yan Yan,¹ Jiahai Zhou,^{3,*\$} K. N. Houk,^{2,*} Yi Tang^{1,2,*}

¹Department of Chemical and Biomolecular Engineering and ²Department of Chemistry and Biochemistry, University of California Los Angeles, Los Angeles, California 90095, United States ³State Key Laboratory of Bio-organic and Natural Products Chemistry, Center for Excellence in Molecular Synthesis, Shanghai Institute of Organic Chemistry, University of Chinese Academy of Sciences, Shanghai, China

TABLE OF CONTENTS

EXPERIMENTAL PROCEDURES

1. General methods	S5
2. Strains and culture conditions	S5
3. General DNA manipulation techniques	S5
4. Preparation of protoplast of <i>A. nidulans</i>	S6
5. Heterologous expression of the <i>PKS</i> gene cluster in <i>A. nidulans</i>	S6
6. Analysis of metabolites and isolation of compounds	S7
7. Expression and purification of DcsB from <i>E. coli</i> BL21 (DE3) for <i>in vitro</i> reaction	S7
8. Expression and purification of DcsB for protein crystallization	S8
9. Protein crystallization	S8
10. Data collection and structure determination	S9
11. Construction of expression plasmid of DcsB mutant	S9
12. Ultracentrifugation analysis of DcsB	S10
13. General procedure for the biocatalytic synthesis of cyclic polyketides by using DcsB as catalyst	S10
13.1 General procedure for the synthesis of substrates	S10
13.2 Small-scale <i>in vitro</i> characterization and kinetics study of DcsB	S20
13.3 Preparative scale <i>in vitro</i> reactions	S20
14. Computational methods	S24
14.1 Molecular docking methodology	S24
14.2 Density functional theory calculation methodology	S26

SUPPLEMENTARY TABLES

Table S1. Bioinformatics analysis of <i>dcs</i> gene cluster	S28
Table S2. Primers used in this project	S28
Table S3. Plasmids used in this study	S29
Table S4. Optimization of thioesterase-catalyzed lactonization	S30
Table S5. Spectroscopic data of 2a	S31
Table S6. Spectroscopic data of 1	S32
Table S7. Data collection and refinement statistics	S33

SUPPLEMENTARY FIGURES

Figure S1. Plasmids used for heterologous expression of <i>dcs</i> gene cluster in <i>A. nidulans</i> and protein expressions in <i>E. coli</i> .	S34
Figure S2. SDS-PAGE (6%) analysis of DcsB and mutants expressed and purified from <i>E. coli</i> .	S34
Figure S3. Kinetics study of DcsB-catalyzed conversion of 4a to 2a	S35
Figure S4. DcsB-catalyzed lactonization of 4f for the formation of 2f	S36

Figure S5. DcsB-catalyzed hydrolysis of 4e for the formation of 2e'	S37
Figure S6. Structures of <i>apo</i> DcsB and its complex with substrate analog	S38
Figure S7. Solution oligomerization state of DcsB	S40
Figure S8. Sequence alignment of DcsB with the closest structural homologs identified by DALI search.	S40
Figure S9. Structural comparison of DcsB with other homologs	S41
Figure S10. Comparison of the <i>apo</i> DcsB and its substrate analog 4a-2' complex	S42
Figure S11. Clip view of the active site cavity of DcsB and Pik TE.	S43
Figure S12. Calculated theozyme model for cyclization	S44
Figure S13. Covalent docking of 4d-h Ser114-bound acyl-intermediates	S45
Figure S14. Proposed catalytic mechanism of DcsB	S46
Figure S15. ¹ H NMR Spectra of compound 4a-1	S47
Figure S16. ¹³ C NMR Spectra of compound 4a-1	S47
Figure S17. ¹ H NMR Spectra of compound 4a-2	S48
Figure S18. ¹³ C NMR Spectra of compound 4a-2	S48
Figure S19. ¹ H NMR Spectra of compound 4a-3	S49
Figure S20. ¹³ C NMR Spectra of compound 4a-3	S49
Figure S21. ¹ H NMR Spectra of compound 4a	S50
Figure S22. ¹³ C NMR Spectra of compound 4a	S50
Figure S23. ¹ H NMR Spectra of compound 4b	S51
Figure S24. ¹³ C NMR Spectra of compound 4b	S51
Figure S25. ¹ H NMR Spectra of compound 4c	S52
Figure S26. ¹³ C NMR Spectra of compound 4c	S52
Figure S27. ¹ H NMR Spectra of compound 4d	S53
Figure S28. ¹³ C NMR Spectra of compound 4d	S53
Figure S29. ¹ H NMR Spectra of compound 4e	S54
Figure S30. ¹³ C NMR Spectra of compound 4e	S54
Figure S31. ¹ H NMR Spectra of compound 4f	S55
Figure S32. ¹³ C NMR Spectra of compound 4f	S55
Figure S33. ¹ H NMR Spectra of compound 4g	S56
Figure S34. ¹³ C NMR Spectra of compound 4g	S56
Figure S35. ¹ H NMR Spectra of compound 4h	S57
Figure S36. ¹³ C NMR Spectra of compound 4h	S57
Figure S37. ¹ H NMR Spectra of compound 4i	S58
Figure S38. ¹³ C NMR Spectra of compound 4i	S58
Figure S39. ¹ H NMR Spectra of compound 4j	S59
Figure S40. ¹³ C NMR Spectra of compound 4j	S59
Figure S41. ¹ H NMR Spectra of compound 4k	S60
Figure S42. ¹³ C NMR Spectra of compound 4k	S60
Figure S43. ¹ H NMR Spectra of compound 4l	S61
Figure S44. ¹³ C NMR Spectra of compound 4l	S61
Figure S45. ¹ H NMR Spectra of compound 1	S62

Figure S46. ^{13}C NMR Spectra of compound 1	S62
Figure S47. ^1H - ^1H COSY Spectra of compound 1	S63
Figure S48. ^1H - ^{13}C HSQC Spectra of compound 1	S64
Figure S49. ^1H - ^{13}C HMBC Spectra of compound 1	S65
Figure S50. ^1H NMR Spectra of compound 2a	S66
Figure S51. ^{13}C NMR Spectra of compound 2a	S66
Figure S52. ^1H - ^1H COSY Spectra of compound 2a	S67
Figure S53. ^1H - ^{13}C HSQC Spectra of compound 2a	S68
Figure S54. ^1H - ^{13}C HMBC Spectra of compound 2a	S69
Figure S55. ^1H NMR Spectra of compound 2b	S70
Figure S56. ^{13}C NMR Spectra of compound 2b	S70
Figure S57. ^1H NMR Spectra of compound 2c	S71
Figure S58. ^{13}C NMR Spectra of compound 2c	S71
Figure S59. ^1H NMR Spectra of compound 2d	S72
Figure S60. ^{13}C NMR Spectra of compound 2d	S72
Figure S61. ^1H NMR Spectra of compound 2g	S73
Figure S62. ^{13}C NMR Spectra of compound 2g	S73
Figure S63. ^1H NMR Spectra of compound 2h	S74
Figure S64. ^{13}C NMR Spectra of compound 2h	S74
Figure S65. ^1H NMR Spectra of compound 2i	S75
Figure S66. ^{13}C NMR Spectra of compound 2i	S75
Figure S67. ^1H NMR Spectra of compound 2j	S76
Figure S68. ^{13}C NMR Spectra of compound 2j	S76
Figure S69. ^1H NMR Spectra of compound 2k	S77
Figure S70. ^{13}C NMR Spectra of compound 2k	S77
Figure S71. ^1H NMR Spectra of compound 2l	S78
Figure S72. ^1H NMR Spectra of compound 2l	S78
References	S79

EXPERIMENTAL PROCEDURES

1. General methods

Unless stated otherwise, all solvents were purified and dried according to standard methods prior to use. NMR spectra were recorded on Bruker AV-400 and AV-500. ^1H NMR spectra were referenced relative to tetramethylsilane signals or residual solvent signals. Data for ^1H NMR are reported as follows: chemical shift (δ , ppm), multiplicity (s = singlet, d = doublet, t = triplet, q = quartet, p = pentet, sex = sextet, m = multiplet or unresolved, br = broad singlet, coupling constant (s) in Hz, integration). Data for ^{13}C NMR are reported in terms of chemical shift (δ , ppm). High-resolution mass spectra (HRMS) for new compounds were recorded on an Agilent LC/MSD TOF mass spectrometer.

2. Strains and culture conditions

Beauveria bassiana ARSEF 2860 was grown on PDA (potato dextrose agar, BD) at 28 °C for 3 days for cell proliferation or in liquid PDB medium (PDA medium without agar) for isolation of genomic DNA. *Aspergillus nidulans* A1145¹ was grown at 28 °C in CD media (1 L: 10 g Glucose, 50 mL 20 × Nitrate salts, 1 mL Trace elements, pH 6.5, and 20 g/L Agar for solid cultivation) for sporulation or in CD-ST media (1L: 20 g Starch, 20 g Casamino acids, 50 mL 20 × Nitrate salts, 1 mL Trace elements, pH 6.5) for heterologous expression of gene cluster, compound production and RNA extraction. For the preparation of 20 × Nitrate salts, 120 g NaNO_3 , 10.4 g KCl, 10.4 g $\text{MgSO}_4 \cdot 7\text{H}_2\text{O}$, 30.4 g KH_2PO_4 were dissolved in 1 L double distilled water. The 100 mL trace elements with pH 6.5 contained 2.20 g $\text{ZnSO}_4 \cdot 7\text{H}_2\text{O}$, 1.10 g H_3BO_3 , 0.50 g $\text{MnCl}_2 \cdot 4\text{H}_2\text{O}$, 0.16 g $\text{FeSO}_4 \cdot 7\text{H}_2\text{O}$, 0.16 g $\text{CoCl}_2 \cdot 5\text{H}_2\text{O}$, 0.16 g $\text{CuSO}_4 \cdot 5\text{H}_2\text{O}$, and 0.11 g $(\text{NH}_4)_6\text{Mo}_7\text{O}_{24} \cdot 4\text{H}_2\text{O}$.² All *Escherichia coli* strains were cultured in LB media at 37 °C, and yeast strains were cultured in YPD (yeast extract 1%, peptone 2%, glucose 2%) media at 28 °C.

3. General DNA manipulation techniques

All DNA manipulations in this study were conducted according to manufacturer's protocol. *E. coli* TOP10 and *E. coli* XL-1 were used for cloning, following standard recombinant DNA techniques. DNA restriction enzymes were used as recommended by the manufacturer (New England Biolabs, NEB). PCR was performed using Phusion High-Fidelity DNA Polymerase (NEB). The gene-specific primers are listed in Table S2. PCR products were confirmed by DNA sequencing. *E. coli* BL21 (DE3) (Novagen) was used for protein expression.

4. Preparation of protoplast of *A. nidulans*

A. nidulans A1145 was initially grown on CD agar plates containing 10 mM uridine, 5 mM uracil, 0.5 µg/ml pyridoxine HCl and 2.5 µg/ml riboflavin at 30 °C for 5 days. Fresh spores of *A. nidulans* A1145 were inoculated into 50 mL liquid CD media in 250 mL flask and germinated at 30 °C, 250 rpm for approximately 16 h. Mycelia were harvested by centrifugation at 3500 rpm for 10 min, and washed with 10 mL osmotic buffer (1.2 M MgSO₄, 10 mM sodium phosphate, pH 5.8). Then the mycelia were transferred into 10 mL of osmotic buffer containing 30 mg Lysing enzymes from *Trichoderma* and 20 mg Yatalase in a 125 mL flask. The flask was kept in shaker at 80 rpm for 4–6 h at 30 °C. Cells were collected in a 30 mL Corex tube and overlaid gently by 10 mL of trapping buffer (0.6 M sorbitol, 0.1 M Tris-HCl, pH 7.0). After centrifugation at 3500 rpm for 15 min at 4 °C, protoplasts were collected in the interface of the two buffers. The protoplasts were then transferred to a sterile 15 mL falcon tube and washed by 10 mL STC buffer (1.2 M sorbitol, 10 mM CaCl₂, 10 mM Tris-HCl, pH 7.5). The protoplasts were then resuspended in 1 mL STC buffer for transformation.³

5. Heterologous expression of the *PKS* gene cluster in *A. nidulans*

To construct pDWG1001 plasmid, full length *dcsA* was amplified by PCR with three sets of primers of pDWG1001-F1/R1, pDWG1001-F2/R2, pDWG1001-F3/R3. *GpdA* (pYTP) was amplified by PCR with primers of pDWG1001-F4/R4. Full length *dcsB* was amplified by PCR with one pair of primers of pDWG1001-F5/R5. These five overlapping DNA fragments and *PacI/SwaI*-digested pYTP expression vector⁴ were transformed into yeast for homologous recombination. The correct colonies checked by PCR were combined, and subjected to yeast miniprep to obtain a small amount of plasmids. The plasmids obtained from yeast miniprep were introduced into *Escherichia coli* XL-1-Blue by electroporation. Single *E. coli* colony was cultured and minipreped to obtain pDWG1001, which was confirmed by sequencing. pDWG1002, pDWG1003 and pDWG1004 were generated following the same protocol of pDWG1001. DNA sequencing was used to confirm the identities of the expression plasmids. The plasmids used for the heterologous expression are illustrated in Table S3 and Figure S1.

After obtaining the plasmids, the plasmids were added to 60 µL *A. nidulans* A1145 protoplast suspension prepared above and the mixture was incubated for 60 min on ice. Then 600 µL of PEG solution at pH 7.5 (60% PEG, 50 mM calcium chloride and 50 mM Tris-HCl) was added to the protoplast mixture, followed by additional incubation at room temperature for 20 min. The mixture was spread on the regeneration medium (CD solid

medium with 1.2 M sorbitol and appropriate supplements: 10 mM uridine, 5 mM uracil or/and 0.5 µg/mL pyridoxine HCl or/and 2.5 µg/mL riboflavin according to the transformed plasmids) and incubated at 30 °C for 2-3 days.

6. Analysis of metabolites and isolation of compounds

For small scale analysis, the transformants of *A. nidulans* strains were grown in CD-ST for 3 days and then extracted with ethyl acetate. The extract was evaporated to remove ethyl acetate and dissolved in methanol for LC-MS analysis.

For isolation of compounds (diplodialide-B **2a** and decarestrictine C1 **1**), the transformants of *A. nidulans* strains were grown for 4-5 days in 4 L liquid CD-ST and then filtered to collect the cells from liquid culture. The cells were extracted with 1 L acetone, filtered and acetone was evaporated. The remaining residue was extracted with ethyl acetate three times followed by removal of the organic solvent by evaporation. The crude extracts were subjected to silica gel column purification. Fractions containing pure target component were evaporated and dried. **2a** and **1** were dissolved in chloroform-*d*₁ or methanol-*d*₄ for NMR analysis. A single crystal of **1** was obtained through slow evaporation from its solution in ethyl acetate and hexane. The structure and absolute configuration were determined by X-ray crystallography.

7. Expression and purification of DcsB from *E. coli* BL21 (DE3) for *in vitro* reaction

The gene encoding DcsB was amplified by PCR from cDNA with a pair with primer pDWG1005-F/R. The PCR product of target genes and pET28a (+) vector (N-his tag) were assembled using GeneArt Seamless Cloning and Assembly kit according to the manufacturer's instructions. The resulting recombinant plasmid (See Table S3) was confirmed by sequencing. The plasmid was transferred into *E. coli* BL21 (DE3) for protein overexpression. The single colony was grown overnight in 5 mL LB with 50 µg/mL kanamycin at 37 °C. Then 5 mL of the inoculum was used as seed culture to 1 L of LB medium with 50 µg/mL of kanamycin and grown at 37 °C to an OD₆₀₀ of 0.6~0.8 and protein expression was induced by the addition of isopropyl-β-D-thiogalactopyranoside (IPTG) at a final concentration of 100 µM, followed by further incubation for 18-24 h at 16 °C. The cultures were centrifuged for 15 min at 5000 rpm at 4 °C, and the cell pellet was resuspended in 40 mL of lysis buffer (50 mM Tris-HCl, 300 mM NaCl, 5% glycerol, pH 8.0) and lysed on ice by sonication. The lysate was centrifuged at 15000 rpm for 25 min at 4 °C to remove the cellular debris. One-step purification of the recombinant His6-tagged

fusion DcsB from soluble protein by affinity chromatography with Ni-NTA agarose resin (Qiagen) was carried out according to the manufacturer's instructions. Purified DcsB was concentrated and exchanged into storage buffer (50 mM Tris-HCl, 300 mM NaCl, 5% glycerol, pH 8.0, wash at least four times) with Centriprep filters (Amicon). The purified DcsB was checked by SDS-PAGE. Bradford Protein Assay (Bio-Rad) was used to calculate protein concentration and stored at -80°C in buffer (50 mM Tris-HCl, 300 mM NaCl, 5% glycerol, pH 8.0).

8. Expression and purification of DcsB for protein crystallization

The recombinant plasmid pDWG1005 was transferred into *E. coli* BL21 (DE3) for overexpression. The single colony was grown overnight in 5 mL LB with 50 µg/mL kanamycin at 37 °C. Then 5 mL of the inoculum was used as seed culture to 1 L of LB medium with 50 µg/mL of kanamycin and grown at 37 °C to an OD₆₀₀ of 0.6~0.8 and protein expression was induced by the addition of isopropyl-β-D-thiogalactopyranoside (IPTG) to a final concentration of 200 µM, followed by further incubation for 18 h at 16 °C. The selenomethionine-derivatized (Se-Met) DcsB was overexpressed in *E. coli* B834 (DE3) in M9 medium with 50 µg/mL of kanamycin and grown at 37 °C to an OD₆₀₀ of 0.6~0.8. After supplementation with 50 mg/L L-(+)-selenomethionine (J&K Scientific), Se-Met protein expression was induced by the addition of 0.2 mM IPTG, followed by further incubation for 18 h at 16 °C. The cultures were centrifuged for 5 min at 8000 rpm at 4 °C, and the cell pellets were resuspended in buffer (25 mM Tris-HCl, 500 mM NaCl, 5 mM β-mercaptoethanol, pH 8.0) and lysed by French press with a high-pressure homogenizer (60-100 MPa). The lysate was centrifuged at 15000 rpm for 25 min at 4 °C to remove the cellular debris. Soluble protein was loaded onto a Ni-NTA affinity column (GE) and eluted with a buffer containing 25 mM Tris-HCl, 500 mM NaCl, 300 mM imidazole, 5 mM β-mercaptoethanol, pH 8.0. Purified DcsB was concentrated with Amicon Ultracel-30 and was then subjected to a HiLoad Superdex 200 column (GE Healthcare) in a buffer containing 25 mM Tris-HCl, 150 mM NaCl, 5 mM DTT, pH 8.0. Fractions that contained DcsB were collected and concentrated for crystallization and activity assay. Mutants of DcsB were purified by the same method.

9. Protein crystallization

Crystal screening was performed at 16 °C by the sitting-drop vapor diffusion method in 2 µL drops containing an 1:1 mixture of the protein solution (10 mg/mL) and a reservoir solution and equilibrated against 50 µL

reservoir solution. Native DcsB crystals were obtained under conditions of 0.1M MIB, 25% PEG 1500, pH 7.0 after 2~3 days.

Crystals of the Se-Met DcsB were produced under conditions of 10 % (w/v) PEG 4000, 20 % (w/v) isopropanol after 2~3 days. The DcsB-substrate complexes were crystallized using the sitting drop vapor diffusion method at 16 °C. Purified DcsB (10 mg/mL) was incubated with 3.0 mM compound dissolved with DMSO in buffer containing 25 mM Tris-HCl, 150 mM NaCl, 5 mM DTT, pH 8.0 on ice for 30 min. The DcsB-**4a-2'** complex crystals were obtained under conditions of 0.1M MMT, 25% PEG 1500, pH 7.0 after 2~3 days.

All crystals were flash-frozen in liquid nitrogen by using reservoir solution containing 10% (v/v) glycerol as cryo-protectant.

10. Data collection and structure determination

All X-ray diffraction data were collected at the Shanghai Synchrotron Radiation Facility (SSRF). For Se-Met DcsB and DcsB-**4a-2'** complex, data were collected at beamline BL19U1 ($\lambda = 0.97855 \text{ \AA}$). For native DcsB, data were collected at beamline BL18U1 ($\lambda = 0.97930 \text{ \AA}$). The diffraction data of native DcsB and DcsB-**4a-2'** were indexed integrated and scaled using the HKL3000 package⁵ while others were processed with XDS,⁶ and scaled and merged using AIMLESS from the CCP4 program suite.⁷

Structure of Se-Met-DcsB was determined by single-wavelength anomalous dispersion (SAD). 45 selenium positions were located in one asymmetric unit by Autosol with the PHENIX package and an initial model was built automatically using Autobuild.⁸ The structures of native DcsB and other DcsB complexes were determined by molecular replacement with the program Phaser⁹ using the structure of SeDcsB as the search model. Iterative cycles of model rebuilding and refinement were achieved using PHENIX⁸ and COOT.¹⁰

Detailed statistics for data collection and refinement are presented in Supplementary Table S7. All protein structure figures were prepared using the program PyMol 1.3 (Schrödinger, LLC).¹¹

11. Construction of expression plasmid of DcsB mutant

To construct the expression plasmid pDWG1006 of S114C mutant, the plasmid pDWG1005 containing the wild-type *dcsB* gene was used as the template for PCR-based site-directed mutagenesis. The primers of pDWG1006-F1/F2 were used for S114C (Table S2), and the resulting fragments were then digested by Dpn I to remove the parental DNA, and the digested products were directly used to transform *E. coli* DH5a. The correct

mutations were confirmed by sequencing. The procedures are the same for other mutants.

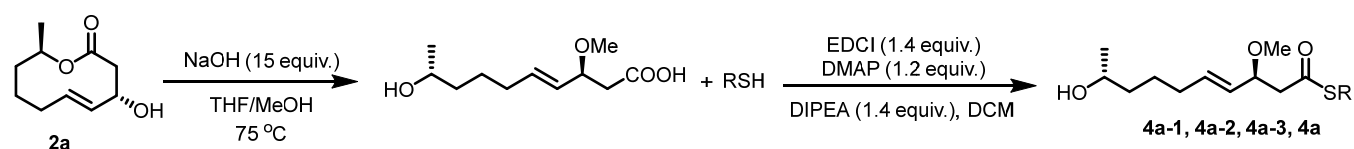
12. Ultracentrifugation analysis of DcsB

The sedimentation velocity data were collected on a Beckman Optima AUC analytical ultracentrifuge equipped with an eight-cell rotor under 35000 rpm at 4 °C. The partial specific volume of different protein samples and the buffer density were calculated using the program SEDNTERP (<http://www.rasmb.bbri.org/>). Data were analyzed and fitted to a continuous sedimentation coefficient distribution model using the program SEDFIT.¹²

13. General procedure for the biocatalytic synthesis of cyclic polyketides by using DcsB as catalyst

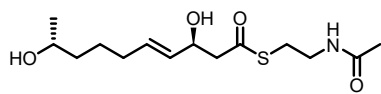
13.1 General procedure for the synthesis of substrates^{13,14}

Synthesis of 4a, 4a-1, 4a-2, 4a-3



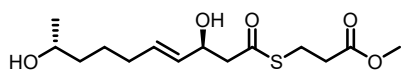
THF (3.0 mL/mmol) was added to a vial containing of **2a** (1 equiv.) followed by addition of NaOH solution (4.7 mM, dissolved in water, 15 equiv.). Methanol and THF (1:1) were added dropwise until a homogeneous solution was obtained. The reaction mixture was refluxed at 76 °C for 12 hours and then allowed to room temperature. The reaction was quenched by the addition of 1M HCl to a pH of 2 and extracted with EtOAc three times, the combined organic extracts were dried over Na₂SO₄ and concentrated under reduced pressure. The crude residue was used directly in the next step without further purification.

A reaction vial containing a Teflon-coated magnetic stir bar and the crude residue from the previous step (1 equiv.) was charged with CH₂Cl₂ (0.01 mM) and cooled to 0 °C. Thiol (1.4 equiv.), EDCI (1.4 equiv.), DMAP (1.2 equiv.) and DIPEA (1.4 equiv.) were then added to the reaction mixture in succession. The reaction mixture was stirred at room temperature overnight and then water was added. The aqueous layer was extracted with CH₂Cl₂ three times. The combined organic layers were dried over Na₂SO₄, filtered and concentrated under reduced pressure. Purification using flash silica gel column chromatography (ethyl acetate/hexanes or methanol = 1/2 to 1/1 or 15/1, v/v) gave the product **4** as a colorless oil.



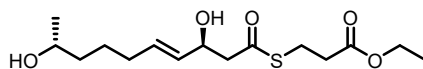
(2-acetamidoethyl)-(3*S*,9*R*,*E*)-3,9-dihydroxydec-4-enethioate (**4a-1**):

Purification using preparative TLC (ethyl acetate/methanol = 15/1, v/v) gave the product as a colorless oil (11.0 mg, 38% yield in overall two steps). $[\alpha]_D^{22} = -10.8$ ($c = 1.0$ Chloroform). **¹H NMR** (500 MHz, CDCl₃) δ 6.13 (br, 1H), 5.77–5.67 (m, 1H), 5.48 (ddt, $J = 15.4, 6.6, 1.4$ Hz, 1H), 4.60–4.50 (m, 1H), 3.83–3.73 (m, 1H), 3.49–3.38 (m, 2H), 3.10–2.98 (m, 2H), 2.85–2.72 (m, 2H), 2.29 (s, 2H), 2.10–2.00 (m, 2H), 1.97 (s, 3H), 1.52–1.36 (m, 4H), 1.18 (d, $J = 6.2$ Hz, 3H). **¹³C NMR** (125 MHz, CDCl₃) δ 198.6, 170.7, 132.6, 130.7, 69.6, 67.9, 51.1, 39.3, 38.6, 32.0, 28.8, 25.1, 23.5, 23.1. **HRMS** (ESI-TOF) calcd for C₁₄H₂₅NNaO₄S [M+Na]⁺: 326.1397, Found: 326.1404.



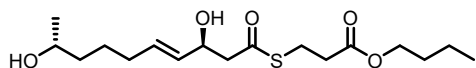
Methyl 3-[(3*S*,9*R*,*E*)-3,9-dihydroxydec-4-enoyl]thio}propanoate (**4a-2**):

Purification using preparative TLC (ethyl acetate/hexanes = 1/2 to 1/1, v/v) gave the product as a colorless oil (6.0 mg, 18% yield in overall two steps). $[\alpha]_D^{22} = -10.2$ ($c = 1.0$ Chloroform). **¹H NMR** (500 MHz, CDCl₃) δ 5.76–5.58 (m, 1H), 5.41 (ddt, $J = 15.4, 6.6, 1.5$ Hz, 1H), 4.47 (q, $J = 6.3$ Hz, 1H), 3.78–3.68 (m, 1H), 3.63 (s, 3H), 3.08 (t, $J = 6.9$ Hz, 2H), 2.74–2.67 (m, 2H), 2.57 (t, $J = 7.0$ Hz, 2H), 1.99 (q, $J = 6.9$ Hz, 2H), 1.77 (s, 2H), 1.47–1.29 (m, 4H), 1.12 (d, $J = 6.2$ Hz, 3H). **¹³C NMR** (125 MHz, CDCl₃) δ 198.3, 172.0, 132.7, 130.6, 69.5, 68.0, 52.0, 50.8, 38.7, 34.1, 32.0, 25.1, 24.1, 23.5. **HRMS** (ESI-TOF) calcd for C₁₄H₂₄NaO₅S [M+Na]⁺: 327.1237, Found: 327.1251.



Ethyl 3-[(3*S*,9*R*,*E*)-3,9-dihydroxydec-4-enoyl]thio}propanoate (**4a-3**):

Purification using preparative TLC (ethyl acetate/hexanes = 1/2 to 1/1, v/v) gave the product as a colorless oil (20.5 mg, 34% yield in overall two steps). $[\alpha]_D^{22} = -10.8$ ($c = 0.5$ Chloroform). **¹H NMR** (500 MHz, CDCl₃) δ 5.74–5.59 (m, 1H), 5.41 (ddt, $J = 15.3, 6.6, 1.5$ Hz, 1H), 4.47 (q, $J = 6.2$ Hz, 1H), 4.09 (q, $J = 7.1$ Hz, 2H), 3.77–3.67 (m, 1H), 3.08 (t, $J = 7.0$ Hz, 2H), 2.73–2.67 (m, 2H), 2.56 (t, $J = 7.0$ Hz, 2H), 2.48 (s, 1H), 1.99 (q, $J = 6.9$ Hz, 2H), 1.49–1.29 (m, 4H), 1.20 (t, $J = 7.1$ Hz, 3H), 1.12 (d, $J = 6.2$ Hz, 3H). **¹³C NMR** (125 MHz, CDCl₃) δ 198.3, 171.6, 132.6, 130.6, 69.5, 68.0, 60.9, 50.8, 38.7, 34.3, 32.0, 25.1, 24.1, 23.6, 14.2. **HRMS** (ESI-TOF) calcd for C₁₅H₂₆NaO₅S [M+Na]⁺: 341.1393, Found: 341.1393.

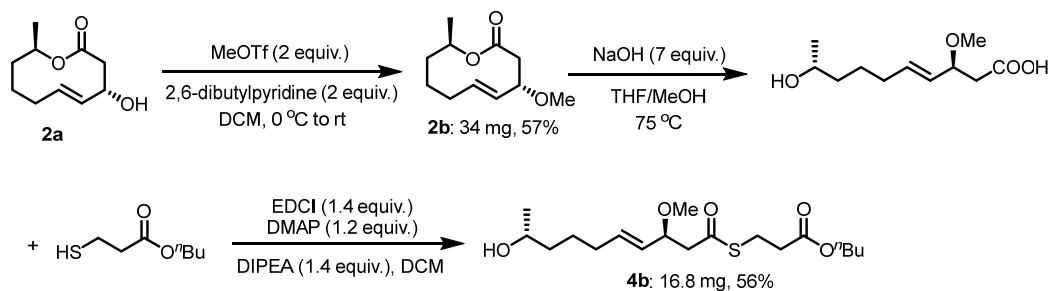


Butyl 3-[(3*S*,9*R*,*E*)-3,9-dihydroxydec-4-enoyl]thio}propanoate

(**4a**): Purification using preparative TLC (ethyl acetate/hexanes = 1/2 to 1/1, v/v) gave the product as a colorless oil (22.7 mg, 31% yield in overall two steps). $[\alpha]_D^{22} = -16.2$ ($c = 0.5$

Chloroform). $^1\text{H NMR}$ (500 MHz, CDCl_3) δ 5.72–5.58 (m, 1H), 5.41 (ddt, $J = 15.4, 6.6, 1.5$ Hz, 1H), 4.47 (q, $J = 6.6$ Hz, 1H), 4.03 (t, $J = 6.7$ Hz, 2H), 3.78–3.65 (m, 1H), 3.07 (t, $J = 7.0$ Hz, 2H), 2.71–2.69 (m, 2H), 2.56 (t, $J = 7.0$ Hz, 3H), 2.03–1.93 (m, 2H), 1.59–1.49 (m, 2H), 1.47–1.25 (m, 6H), 1.12 (d, $J = 6.2$ Hz, 3H), 0.87 (t, $J = 7.4$ Hz, 3H). $^{13}\text{C NMR}$ (125 MHz, CDCl_3) δ 198.3, 171.7, 132.6, 130.6, 69.5, 67.9, 64.8, 50.8, 38.7, 34.3, 32.0, 30.6, 25.1, 24.1, 23.5, 19.1, 13.7. **HRMS** (ESI-TOF) calcd for $\text{C}_{17}\text{H}_{30}\text{NaO}_5\text{S}[\text{M}+\text{Na}]^+$: 369.1706, Found: 369.1707.

Synthesis of 4b



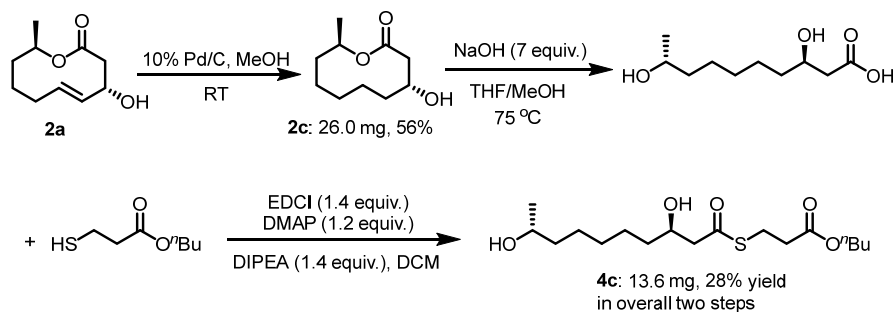
To a reaction tube containing a Teflon-coated magnetic stir bar were added **2a** (54 mg, 0.30 mmol, 1.0 equiv.), $\text{CH}_2\text{Cl}_2/\text{PhMe}$ (2:1, 3 mL) and cooled to 4 °C under N_2 atmosphere. 2,6-Di-*t*-butylpyridine (114.8 mg, 0.60 mmol, 2.0 equiv.) was added followed by methyl trifluoromethanesulfonate (98.5 mg, 0.60 mmol, 2.0 equiv) and stirred for 72 h at 4 °C. The reaction was quenched with saturated NH_4Cl solution and extracted with CH_2Cl_2 three times. The combined organic extracts were washed with brine, then filtered through a pad of celite and concentrated under reduced pressure. Purification using silica gel column chromatography (ethyl acetate/hexanes = 1/10, v/v) gave the product **2b** as a colorless oil (34 mg, 57% yield).

0.5 mL THF was added to a vial containing 34 mg of **2b** followed by addition of NaOH solution (48.1 mg, dissolved in 0.26 mL water, 7.0 equiv.). Methanol and THF (1:1) were added dropwise until a homogeneous solution was obtained. The reaction mixture was refluxed at 75 °C for 12 hours and then allowed to room temperature. The reaction was quenched by the addition of 1M HCl to a pH of 2 and extracted with EtOAc three times, the combined organic extracts were dried over Na_2SO_4 and concentrated under reduced pressure. The crude residue was used directly in the next step without further purification.

A reaction vial containing a Teflon-coated magnetic stir bar and the crude residue from the previous step (18.0 mg, 0.083 mmol, 1 equiv.) was charged with CH_2Cl_2 (8.0 mL) and cooled to 0 °C. Butyl 3-mercaptopropanoate (18.9 mg, 0.117 mmol, 1.4 equiv.) was added to the flask. EDCI (22.4 mg, 0.117 mmol, 1.4

equiv.), DMAP (12.2 mg, 0.1 mmol, 1.2 equiv.) and DIPEA (15.0 mg, 0.116 mmol, 1.4 equiv.) were then added to the reaction mixture in succession. The reaction mixture was stirred at room temperature overnight and then water (15 mL) was added. The aqueous layer was extracted with CH₂Cl₂ (3 x 15 mL). The combined organic layers were dried over Na₂SO₄, filtered and concentrated under reduced pressure. Purification using flash silica gel column chromatography (ethyl acetate/hexanes = 1/2, v/v) gave the product **4b** as a colorless oil (16.8 mg, 56% yield over two steps). $[\alpha]_D^{22} = -7.2$ (c = 1.0 Chloroform). ¹H NMR (400 MHz, CDCl₃) δ 5.79–5.58 (m, 1H), 5.27 (ddt, *J* = 15.4, 8.2, 1.4 Hz, 1H), 4.08 (t, *J* = 6.7 Hz, 2H), 4.04–3.95 (m, 1H), 3.84–3.73 (m, 1H), 3.23 (s, 3H), 3.11 (td, *J* = 7.0, 1.8 Hz, 2H), 2.83 (dd, *J* = 14.8, 7.9 Hz, 1H), 2.68–2.55 (m, 3H), 2.15–1.96 (m, 2H), 1.68–1.54 (m, 3H), 1.53–1.28 (m, 6H), 1.17 (d, *J* = 6.1 Hz, 3H), 0.92 (t, *J* = 7.4 Hz, 3H). ¹³C NMR (100 MHz, CDCl₃) δ 196.4, 171.7, 135.1, 128.6, 78.7, 67.8, 64.7, 56.1, 50.0, 38.6, 34.4, 32.0, 30.6, 25.1, 24.0, 23.5, 19.1, 13.7. HRMS (ESI-TOF) calcd for C₁₈H₃₂NaO₅S[M+Na]⁺: 383.1863, Found: 383.1865.

Synthesis of 4c



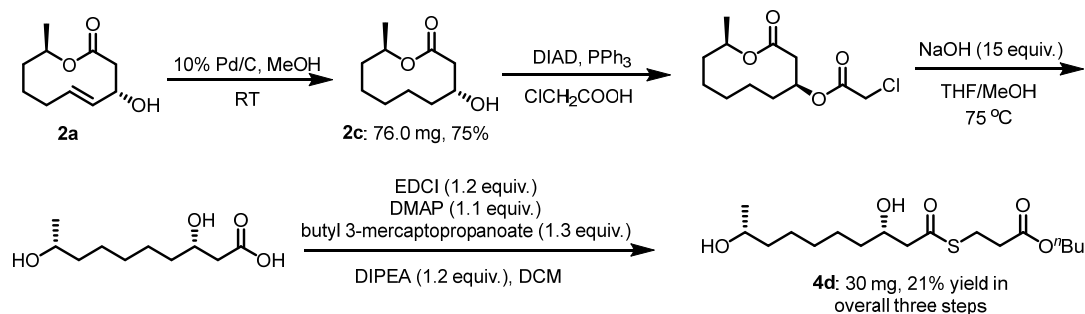
Diploidalide-B **2a** (46 mg, 0.25 mmol, 1.0 equiv.) was added to a reaction tube containing a Teflon-coated magnetic stir bar. Methanol (2 mL) and Pd/C (26.7 mg, 10% on activated carbon) were added successively. The resulting mixture was stirred at room temperature under 1 atm H₂ atmosphere until full conversion (as monitored by LC-MS). The reaction mixture was filtered through a pad of celite, and concentrated under reduced pressure. Purification using flash silica gel column chromatography (ethyl acetate/hexanes = 1/2, v/v) gave the product **2c** as a colorless oil (26.0 mg, 56% yield).

0.31 mL THF was added to a vial containing 26.0 mg of **2c** followed by addition of NaOH solution (39.1 mg, dissolved in 0.22 mL water, 7.0 equiv.). Methanol and THF (1:1) were added dropwise until a homogeneous solution was obtained. The reaction mixture was refluxed at 75 °C for 12 hours and then allowed to room

temperature. The reaction was quenched by the addition of 1M HCl to a pH of 2 and extracted with EtOAc three times, the combined organic extracts were dried over Na₂SO₄ and concentrated under reduced pressure. The crude residue was used directly in the next step without further purification.

A reaction vial containing a Teflon-coated magnetic stir bar and the crude residue from the previous step (25.0 mg, 0.16 mmol, 1 equiv.) was charged with CH₂Cl₂ (8.0 mL) and cooled to 0 °C. Butyl 3-mercaptopropanoate (35.5 mg, 0.22 mmol, 1.4 equiv.) was added to the flask. EDCI (42.0 mg, 0.22 mmol, 1.4 equiv.), DMAP (23.1 mg, 0.19 mmol, 1.2 equiv.) and DIPEA (28.3 mg, 0.22 mmol, 1.4 equiv.) were then added to the reaction mixture in succession. The reaction mixture was stirred at room temperature overnight and then water (15 mL) was added. The aqueous layer was extracted with CH₂Cl₂ (3 x 15 mL). The combined organic layers were dried over Na₂SO₄, filtered and concentrated under reduced pressure. Purification using flash silica gel column chromatography (ethyl acetate/hexanes = 1/2, v/v) gave the product **4c** as a colorless oil (13.6 mg, 28% yield over two steps). [α]_D²² = -17.8 (c = 1.0 Chloroform). ¹H NMR (500 MHz, CDCl₃) δ 4.10–3.87 (m, 3H), 3.80–3.61 (m, 1H), 3.15–2.99 (m, 2H), 2.75–2.46 (m, 4H), 1.90 (s, 2H), 1.61–1.49 (m, 2H), 1.48–1.18 (m, 10H), 1.15–1.03 (m, 3H), 0.94–0.70 (m, 3H). ¹³C NMR (125 MHz, CDCl₃) δ 199.2, 171.7, 68.6, 68.1, 64.8, 50.7, 39.2, 36.4, 34.3, 30.6, 29.4, 25.7, 25.4, 24.1, 23.5, 19.1, 13.7. HRMS (ESI-TOF) calcd for C₁₇H₃₂NaO₅S [M+Na]⁺: 371.1863, Found: 371.1863.

Synthesis of **4d**



Dipodialide-B **2a** (100 mg, 0.54 mmol, 1.0 equiv.) was added to a reaction tube containing a Teflon-coated magnetic stir bar. Methanol (3 mL) and Pd/C (58.0 mg, 10% on activated carbon) were added successively. The resulting mixture was stirred at room temperature under 1 atm H₂ atmosphere until full conversion (as monitored by LC-MS). The reaction mixture was filtered through a pad of celite, and concentrated under reduced pressure.

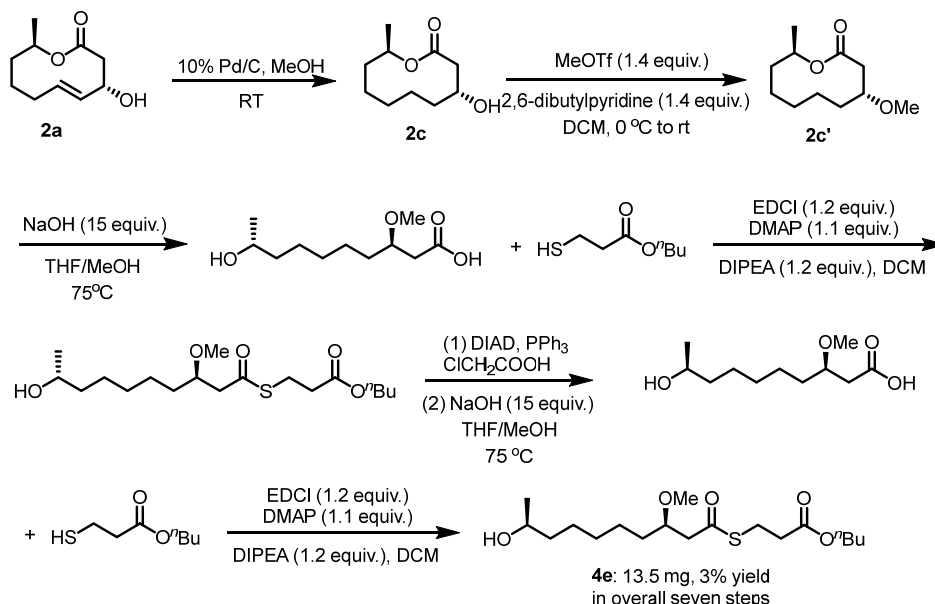
Purification using flash silica gel column chromatography (ethyl acetate/hexanes = 1/2, v/v) gave the product **2c** as a colorless oil (76.0 mg, 75% yield).

2c (76 mg, 0.41 mmol, 1.0 equiv.) was added to a reaction tube containing a Teflon-coated magnetic stir bar. Toluene (4 mL) and ClCH₂COOH (191.7 mg, 2.04 mmol, 5.0 equiv.) and PPh₃ (534.7 mg, 2.04 mmol, 5.0 equiv.) were added successively. The reaction mixture was cooled to 0 °C and DIAD (412.5 mg, 2.04 mmol, 5 equiv.) was added dropwise. Then allowed to room temperature and stir overnight. After 20 h, quenched with 8 mL water, extracted with EtOAc three times, the combined organic extracts were dried over Na₂SO₄ and concentrated under reduced pressure. The crude residue was used directly in the next step without further purification.

1.0 mL THF was added to a vial containing the crude mixture obtained above followed by addition of NaOH solution (275 mg, dissolved in 1.58 mL water, 15 equiv.). Methanol and THF (1:1) were added dropwise until a homogeneous solution was obtained. The reaction mixture was refluxed at 75 °C for 12 hours and then allowed to room temperature. The reaction was quenched by the addition of 1M HCl to a pH of 2 and extracted with EtOAc three times, the combined organic extracts were dried over Na₂SO₄ and concentrated under reduced pressure. The crude residue was used directly in the next step without further purification.

A reaction vial containing a Teflon-coated magnetic stir bar and the crude residue from the previous step (66.0 mg, 0.32 mmol, 1 equiv.) was charged with CH₂Cl₂ (8.0 mL) and cooled to 0 °C. Butyl 3-mercaptopropanoate (68.1 mg, 0.42 mmol, 1.3 equiv.) was added to the flask. EDCI (73.6 mg, 0.38 mmol, 1.2 equiv.), DMAP (43.0 mg, 0.35 mmol, 1.1 equiv.) and DIPEA (49.6 mg, 0.38 mmol, 1.2 equiv.) were then added to the reaction mixture in succession. The reaction mixture was stirred at room temperature overnight and then water (15 mL) was added. The aqueous layer was extracted with CH₂Cl₂ (3 x 15 mL). The combined organic layers were dried over Na₂SO₄, filtered and concentrated under reduced pressure. Purification using flash silica gel column chromatography (ethyl acetate/hexanes = 1/1, v/v) gave the product **4d** as a colorless oil (30.0 mg, 21% yield over three steps). [α]_D²² = +37.8 (c = 0.5 Chloroform). ¹H NMR (500 MHz, CDCl₃) δ 4.07 (t, *J* = 6.7 Hz, 2H), 4.05–3.98 (m, 1H), 3.80–3.70 (m, 1H), 3.12 (t, *J* = 6.9 Hz, 2H), 2.77 (s, 1H), 2.74–2.56 (m, 4H), 1.67–1.54 (m, 3H), 1.52–1.25 (m, 12H), 1.15 (d, *J* = 6.2 Hz, 3H), 0.91 (t, *J* = 7.4 Hz, 3H). ¹³C NMR (125 MHz, CDCl₃) δ 199.1, 171.7, 68.6, 68.0, 64.8, 50.8, 39.2, 36.5, 34.3, 30.6, 29.4, 25.6, 25.3, 24.1, 23.5, 19.1, 13.7. HRMS (ESI-TOF) calcd for C₁₇H₃₂NaO₅S [M+Na]⁺: 371.1863, Found: 371.1862.

Synthesis of 4e



Diploidalide-B **2a** (220.9 mg, 1.2 mmol, 1.0 equiv.) was added to a reaction tube containing a Teflon-coated magnetic stir bar. Methanol (4 mL) and Pd/C (128.2 mg, 10% on activated carbon) were added successively. The resulting mixture was stirred at room temperature under 1 atm H₂ atmosphere until full conversion (as monitored by LC-MS). The reaction mixture was filtered through a pad of celite, and concentrated under reduced pressure. Purification using flash silica gel column chromatography (ethyl acetate/hexanes = 1/2, v/v) gave the product **2c** as a colorless oil (115.0 mg, 51% yield).

To a reaction tube containing a Teflon-coated magnetic stir bar were added **2c** (115.0 mg, 0.62 mmol, 1.0 equiv.), CH₂Cl₂/PhMe (2:1, 4.5 mL) and cooled to 4 °C under N₂ atmosphere. 2,6-Di-*t*-butylpyridine (166.4 mg, 0.87 mmol, 1.4 equiv.) was added followed by methyl trifluoromethanesulfonate (142.0 mg, 0.87 mmol, 1.4 equiv.) and stirred for 72h at 4 °C. The reaction was quenched with saturated NH₄Cl solution and extracted with CH₂Cl₂ three times. The combined organic extracts were washed with brine, then filtered through a pad of celite and concentrated under reduced pressure. The crude residue was used directly in the next step without further purification.

1.0 mL THF was added to a vial containing the crude mixture obtained above followed by addition of NaOH solution (282 mg, dissolved in 1.62 mL water, 15 equiv.). Methanol and THF (1:1) were added dropwise until a

homogeneous solution was obtained. The reaction mixture was refluxed at 75 °C for 12 hours and then allowed to room temperature. The reaction was quenched by the addition of 1M HCl to a pH of 2 and extracted with EtOAc three times, the combined organic extracts were dried over Na₂SO₄ and concentrated under reduced pressure. The crude residue was used directly in the next step without further purification.

A reaction vial containing a Teflon-coated magnetic stir bar and the crude residue from the previous step (60.0 mg, 0.28 mmol, 1 equiv.) was charged with CH₂Cl₂ (10 mL) and cooled to 0 °C. Butyl 3-mercaptopropanoate (58.5 mg, 0.36 mmol, 1.3 equiv.) was added to the flask. EDCI (64.0 mg, 0.33 mmol, 1.2 equiv.), DMAP (37.4 mg, 0.31 mmol, 1.1 equiv.) and DIPEA (43.1 mg, 0.33 mmol, 1.2 equiv.) were then added to the reaction mixture in succession. The reaction mixture was stirred at room temperature overnight and then water (15 mL) was added. The aqueous layer was extracted with CH₂Cl₂ (3 x 15 mL). The combined organic layers were dried over Na₂SO₄, filtered and concentrated under reduced pressure. The crude residue was used directly in the next step without further purification.

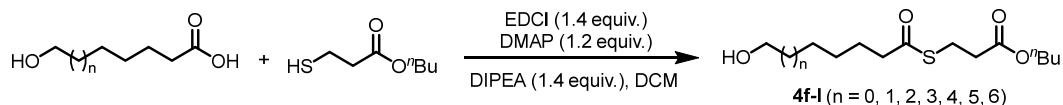
The above residue (64.0 mg, 0.18 mmol, 1.0 equiv.) was added to a reaction tube containing a Teflon-coated magnetic stir bar. Toluene (5 mL) and ClCH₂COOH (82.9 mg, 0.88 mmol, 5.0 equiv.) and PPh₃ (231.4 mg, 0.88 mmol, 5.0 equiv.) were added successively. The reaction mixture was cooled to 0 °C and DIAD (178.6 mg, 0.88 mmol, 5 equiv.) was added dropwise. Then allowed to room temperature and stir overnight. After 20 h, quenched with 8 mL water, extracted with EtOAc three times, the combined organic extracts were dried over Na₂SO₄ and concentrated under reduced pressure. The crude residue was used directly in the next step without further purification.

0.4 mL THF was added to a vial containing the crude mixture obtained above followed by addition of NaOH solution (108 mg, dissolved in 0.62 mL water, 15 equiv.). Methanol and THF (1:1) were added dropwise until a homogeneous solution was obtained. The reaction mixture was refluxed at 75 °C for 12 hours and then allowed to room temperature. The reaction was quenched by the addition of 1M HCl to a pH of 2 and extracted with EtOAc three times, the combined organic extracts were dried over Na₂SO₄ and concentrated under reduced pressure. The crude residue was used directly in the next step without further purification.

A reaction vial containing a Teflon-coated magnetic stir bar and the crude residue from the previous step (39.2 mg, 0.18 mmol, 1 equiv.) was charged with CH₂Cl₂ (10 mL) and cooled to 0 °C. Butyl

3-mercaptopropanoate (37.9 mg, 0.23 mmol, 1.3 equiv.) was added to the flask. EDCI (41.4 mg, 0.22 mmol, 1.2 equiv.), DMAP (24.2 mg, 0.20 mmol, 1.1 equiv.) and DIPEA (27.9 mg, 0.22 mmol, 1.2 equiv.) were then added to the reaction mixture in succession. The reaction mixture was stirred at room temperature overnight and then water (15 mL) was added. The aqueous layer was extracted with CH₂Cl₂ (3 x 15 mL). The combined organic layers were dried over Na₂SO₄, filtered and concentrated under reduced pressure. Purification using flash silica gel column chromatography (ethyl acetate/hexanes = 1/1, v/v) gave the product **4e** as a colorless oil (13.5 mg, 3% yield over seven steps). $[\alpha]_D^{22} = +2.7$ (c = 0.5 Chloroform). ¹H NMR (500 MHz, CDCl₃) δ 4.08 (t, *J* = 6.7 Hz, 2H), 3.83–3.72 (m, 1H), 3.68–3.59 (m, 1H), 3.32 (s, 3H), 3.12 (t, *J* = 7.0 Hz, 2H), 2.78 (dd, *J* = 14.9, 7.0 Hz, 1H), 2.64–2.55 (m, 3H), 1.68–1.55 (m, 3H), 1.53–1.26 (m, 12H), 1.17 (d, *J* = 6.1 Hz, 3H), 0.92 (t, *J* = 7.4 Hz, 3H). ¹³C NMR (125 MHz, CDCl₃) δ 197.3, 171.7, 77.8, 68.1, 64.7, 57.2, 48.6, 39.2, 34.4, 33.9, 30.6, 29.6, 25.7, 25.0, 24.1, 23.5, 19.1, 13.7. HRMS (ESI-TOF) calcd for C₁₈H₃₄NaO₅S [M+Na]⁺: 385.2019, Found: 385.2021.

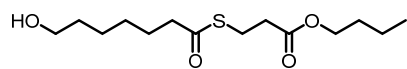
Synthesis of 4f-4l



To a reaction vial containing a Teflon-coated magnetic stir bar was charged with corresponding acid (1.0 equiv.) and CH₂Cl₂ (0.15 mM) and cooled to 0 °C. Butyl 3-mercaptopropanoate (1.4 equiv.) was added the flask. EDCI (1.4 equiv.), DMAP (1.2 equiv.) and DIPEA (1.4 equiv.) were then added to the reaction mixture in succession. The reaction mixture was stirred at room temperature overnight and then water was added. The aqueous layer was extracted with CH₂Cl₂ three times. The combined organic layers were dried over Na₂SO₄, filtered and concentrated under reduced pressure. Purification using flash silica gel column chromatography (ethyl acetate/hexanes = 1/2 to 1/1, v/v) gave the product **4f-1**.

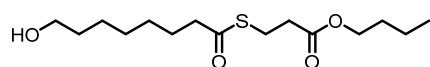
Butyl 3-[(6-hydroxyhexanoyl)thio]propanoate (**4f**): Purification using preparative TLC (ethyl acetate/hexanes = 1/1 to 3/1, v/v) gave the product as a colorless oil (31.0 mg, 14% yield). ¹H NMR (500 MHz, CDCl₃) δ 4.08 (t, *J* = 6.7 Hz, 2H), 3.63 (t, *J* = 6.5 Hz, 2H), 3.10 (t, *J* = 7.0 Hz, 2H), 2.60 (t, *J* = 7.0 Hz, 2H), 2.55 (t, *J* = 7.5 Hz, 2H), 1.68 (p, *J* = 7.5 Hz, 2H), 1.64–1.50 (m, 5H), 1.44–1.30 (m, 4H), 0.92 (t, *J* = 7.4 Hz, 3H). ¹³C NMR (125 MHz, CDCl₃) δ 199.2, 171.8, 64.7, 62.6,

43.9, 34.5, 32.3, 30.6, 25.3, 25.1, 24.0, 19.1, 13.7. **HRMS** (ESI-TOF) calcd for $C_{13}H_{24}NaO_4S$ $[M+Na]^+$: 299.1288, Found: 299.1292.



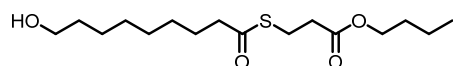
Butyl 3-((7-hydroxyheptanoyl)thio)propanoate (**4g**): Purification using preparative TLC (ethyl acetate/hexanes = 1/1 to 2/1, v/v) gave the product as

a colorless oil (46.5 mg, 26% yield). **1H NMR** (400 MHz, $CDCl_3$) δ 4.07 (t, J = 6.7 Hz, 2H), 3.60 (t, J = 6.6 Hz, 2H), 3.08 (t, J = 7.0 Hz, 2H), 2.59 (t, J = 7.0 Hz, 2H), 2.52 (t, J = 7.5 Hz, 2H), 1.71–1.44 (m, 6H), 1.42–1.25 (m, 6H), 0.91 (t, J = 7.4 Hz, 3H). **^{13}C NMR** (100 MHz, $CDCl_3$) δ 199.3, 171.8, 64.7, 62.7, 43.9, 34.5, 32.4, 30.6, 28.7, 25.5, 25.4, 24.0, 19.1, 13.7. **HRMS** (ESI-TOF) calcd for $C_{14}H_{26}NaO_4S$ $[M+Na]^+$: 313.1444, Found: 313.1442.



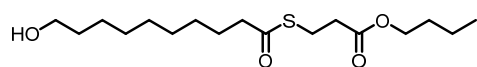
Butyl 3-((8-hydroxyoctanoyl)thio)propanoate (**4h**): Purification using preparative TLC (ethyl acetate/hexanes = 1/2 to 1/1, v/v) gave the product

as a colorless oil (5.0 mg, 20% yield). **1H NMR** (500 MHz, $CDCl_3$) δ 4.09 (t, J = 6.7 Hz, 2H), 3.63 (t, J = 6.6 Hz, 2H), 3.10 (t, J = 7.0 Hz, 2H), 2.61 (t, J = 7.0 Hz, 2H), 2.53 (t, J = 7.5 Hz, 2H), 1.72–1.49 (m, 6H), 1.47–1.28 (m, 9H), 0.92 (t, J = 7.4 Hz, 3H). **^{13}C NMR** (125 MHz, $CDCl_3$) δ 199.3, 171.8, 64.7, 63.0, 44.0, 34.5, 32.7, 30.6, 29.0, 28.8, 25.5, 25.5, 24.0, 19.1, 13.7. **HRMS** (ESI-TOF) calcd for $C_{15}H_{28}NaO_4S$ $[M+Na]^+$: 327.1601, Found: 327.1598.



Butyl 3-((9-hydroxynonanoyl)thio)propanoate (**4i**): Purification using preparative TLC (ethyl acetate/hexanes = 1/2 to 1/1, v/v) gave the product

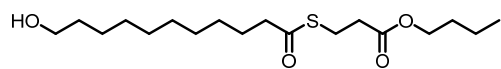
as a colorless oil (12.0 mg, 20% yield). **1H NMR** (500 MHz, $CDCl_3$) δ 4.09 (t, J = 6.7 Hz, 2H), 3.63 (t, J = 6.6 Hz, 2H), 3.11 (t, J = 7.0 Hz, 2H), 2.61 (t, J = 7.0 Hz, 2H), 2.57–2.49 (m, 2H), 1.71–1.47 (m, 7H), 1.44–1.27 (m, 10H), 0.93 (t, J = 7.4 Hz, 3H). **^{13}C NMR** (125 MHz, $CDCl_3$) δ 199.3, 171.8, 64.7, 63.0, 44.0, 34.5, 32.7, 30.6, 29.2, 29.2, 28.8, 25.6, 25.5, 24.0, 19.1, 13.7. **HRMS** (ESI-TOF) calcd for $C_{18}H_{32}NaO_5S$ $[M+Na]^+$: 341.1757, Found: 341.1756.



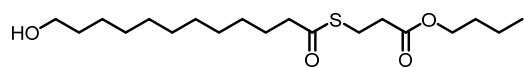
Butyl 3-((10-hydroxydecanoyl)thio)propanoate (**4j**): Purification using preparative TLC (ethyl acetate/hexanes = 1/2 to 1/1, v/v) gave the

product as a colorless oil (184 mg, 54% yield). **1H NMR** (500 MHz, $CDCl_3$) δ 4.09 (t, J = 6.7 Hz, 2H), 3.62 (t, J = 6.6 Hz, 2H), 3.10 (t, J = 7.0 Hz, 2H), 2.60 (t, J = 7.0 Hz, 2H), 2.52 (t, J = 7.5 Hz, 2H), 1.75–1.45 (m, 6H), 1.45–1.17 (m, 13H), 0.92 (t, J = 7.4 Hz, 3H). **^{13}C NMR** (125 MHz, $CDCl_3$) δ 199.3, 171.8, 64.7, 63.0, 44.0, 34.5,

32.8, 30.6, 29.3, 29.3, 29.1, 28.9, 25.7, 25.6, 23.9, 19.1, 13.7. **HRMS** (ESI-TOF) calcd for C₁₇H₃₂NaO₄S [M+Na]⁺: 355.1914, Found: 355.1933.



Butyl 3-[(11-hydroxyundecanoyl)thio]propanoate (**4k**): Purification using preparative TLC (ethyl acetate/hexanes = 1/3 to 1/2, v/v) gave the product as a colorless oil (190 mg, 55% yield). **¹H NMR** (500 MHz, CDCl₃) δ 4.09 (t, *J* = 6.7 Hz, 2H), 3.63 (t, *J* = 6.7 Hz, 2H), 3.11 (t, *J* = 7.0 Hz, 2H), 2.61 (t, *J* = 7.0 Hz, 2H), 2.53 (t, *J* = 7.5 Hz, 2H), 1.69–1.49 (m, 6H), 1.43–1.21 (m, 15H), 0.93 (t, *J* = 7.4 Hz, 3H). **¹³C NMR** (125 MHz, CDCl₃) δ 199.3, 171.8, 64.7, 63.1, 44.1, 34.5, 32.8, 30.6, 29.5, 29.4, 29.3, 29.2, 28.9, 25.7, 25.6, 23.9, 19.1, 13.7. **HRMS** (ESI-TOF) calcd for C₁₈H₃₄NaO₄S [M+Na]⁺: 369.2070, Found: 369.2075.

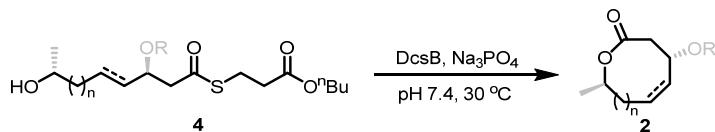


Butyl 3-[(12-hydroxydodecanoyl)thio]propanoate (**4l**): Purification using preparative TLC (ethyl acetate/hexanes = 1/3 to 1/2, v/v) gave the product as a colorless oil (150 mg, 42% yield). **¹H NMR** (500 MHz, CDCl₃) δ 4.09 (t, *J* = 6.7 Hz, 2H), 3.64 (t, *J* = 6.6 Hz, 2H), 3.11 (t, *J* = 7.0 Hz, 2H), 2.61 (t, *J* = 7.0 Hz, 2H), 2.53 (t, 2H), 1.70–1.51 (m, 6H), 1.44–1.21 (m, 17H), 0.93 (t, *J* = 7.4 Hz, 3H). **¹³C NMR** (125 MHz, CDCl₃) δ 199.4, 171.8, 64.7, 63.1, 44.1, 34.5, 32.8, 30.6, 29.5, 29.5, 29.4, 29.4, 29.2, 28.9, 25.7, 25.6, 23.9, 19.1, 13.7. **HRMS** (ESI-TOF) calcd for C₁₉H₃₆NaO₄S [M+Na]⁺: 383.2227, Found: 383.2233.

13.2 Small-scale *in vitro* characterization and kinetics study of DcsB

Assay of DcsB activity and time-course was performed in 400 μL-scale assay containing Na₃PO₄ buffer (100 mM Na₃PO₄, 300 mM NaCl, 5% glycerol, pH 7.4), 1 mM compound **4**, and 0.49 μM DcsB. The reaction was incubated at 30 °C for 0.5-6 h monitored by LC or GC-MS analysis (various time points for time course) and quenched with equal volume of ethyl acetate solution (90% ethyl acetate, 9% methanol and 1% formic acid). The organic layer was evaporated to dryness under vacuum. The residue was dissolved in 400 μL methanol. The sample was analyzed by LC or GC-MS (yield was determined by using the desired product as the internal standard). To determine the kinetics of DcsB towards compound **4a**, the assays were performed at 400 μL-scale with 0.49 μM Dcs B and 1 mM **4a** in Na₃PO₄ buffer (100 mM Na₃PO₄, 300 mM NaCl, 5% glycerol, pH 7.4) at 30 °C for 30 min. Data fitting was performed using GraphPad Prism 5.

13.3 Preparative scale *in vitro* reactions



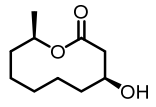
A 50 ml Teflon tube was charged with SMBP-derived ketide **4** (1 mM), Na₃PO₄ buffer (100 mM Na₃PO₄, 300 mM NaCl, 5% glycerol, pH 7.4) and DcsB (0.49 μM). The reaction was incubated at 30 °C for 1-6 h. After the reaction was complete, the reaction mixture was quenched with equal volume of ethyl acetate solution (90% ethyl acetate, 9% methanol and 1% formic acid) and extracted with EtOAc three times. The combined organic layers were washed with brine, then dried over anhydrous Na₂SO₄ and filtered. After the solvent was removed under reduced pressure, the residue was purified by preparative silica gel column purification to afford the desired product **2**.

(4*S*,10*R*,*E*)-4-methoxy-10-methyl-3,4,7,8,9,10-hexahydro-2H-oxecin-2-one (**2b**): $[\alpha]_D^{22} = -38.8$ (c = 1.0 Chloroform). ¹H NMR (500 MHz, CDCl₃) δ 5.74–5.58 (m, 2H), 5.45 (dt, *J* = 16.0, 2.4 Hz, 1.3H), 5.30 (dd, *J* = 15.8, 8.5 Hz, 1H), 5.08–4.96 (m, 1H), 4.80 (p, *J* = 6.7 Hz, 1.4H), 4.15–4.05 (m, 2H), 3.36 (s, 3H), 3.30 (s, 1.7H), 2.95 (dd, *J* = 13.9, 8.0 Hz, 1H), 2.71 (dd, *J* = 12.0, 3.1 Hz, 1.3H), 2.50–2.39 (m, 2H), 2.39–2.30 (m, 1.3H), 2.27–2.19 (m, 1.2H), 2.02–1.90 (m, 1.5H), 1.89–1.78 (m, 2H), 1.78–1.68 (m, 2H), 1.66–1.58 (m, 2H), 1.56–1.38 (m, 3H), 1.21–1.14 (m, 5H). ¹³C NMR (125 MHz, CDCl₃) δ 170.7, 169.8, 137.8, 129.9, 129.2, 128.5, 79.2, 72.4, 71.0, 57.1, 56.3, 42.8, 42.7, 35.9, 33.1, 32.3, 31.7, 29.7, 28.3, 22.5, 22.1, 18.5. HRMS (ESI-TOF) calcd for C₁₁H₁₈NaO₃ [M+Na]⁺: 221.1148, Found: 221.1148.

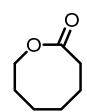
Note: Compound **2b** contains one pair of conformational isomer. The *in vitro* reaction was scaled to 35.2 mL.

(4*R*,10*R*)-4-hydroxy-10-methyl-3,4,7,8,9,10-hexahydro-2H-oxecin-2-one (**2c**): $[\alpha]_D^{22} = -20.4$ (c = 1.0 Chloroform). ¹H NMR (500 MHz, CDCl₃) δ 5.07–4.96 (m, 1H), 4.43–4.31 (m, 1H), 2.89–2.77 (m, 1H), 2.36 (dd, *J* = 15.4, 10.0 Hz, 1H), 2.00–1.90 (m, 1H), 1.82–1.67 (m, 2H), 1.67–1.47 (m, 5H), 1.47–1.35 (m, 1H), 1.26 (d, *J* = 6.5 Hz, 4H), 1.16–1.01 (m, 1H). ¹³C NMR (125 MHz, CDCl₃) δ 170.7, 73.2, 66.5, 43.6, 37.0, 31.5, 25.5, 23.4, 22.9, 19.4. HRMS (ESI-TOF) calcd for C₁₀H₁₈NaO₃ [M+Na]⁺: 209.1148, Found: 209.1145.

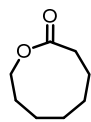
The *in vitro* reaction was scaled to 49.8 mL.

 (4*S*,10*R*)-4-hydroxy-10-methyloxecan-2-one (**2d**): $[\alpha]_D^{22} = -16.3$ ($c = 0.3$ Chloroform). **¹H NMR** (500 MHz, CDCl₃) δ 5.03–4.93 (m, 1H), 4.13–4.02 (m, 1H), 2.66 (ddd, $J = 11.9, 4.2, 0.9$ Hz, 1H), 2.47 (dd, $J = 11.8, 9.7$ Hz, 1H), 1.85–1.59 (m, 5H), 1.52–1.32 (m, 3H), 1.30–1.19 (m, 5H), 1.16–1.03 (m, 1H). **¹³C NMR** (125 MHz, CDCl₃) δ 171.1, 72.4, 69.8, 44.1, 35.4, 31.2, 26.7, 21.6, 20.9, 20.3. **HRMS** (ESI-TOF) calcd for C₁₀H₁₈NaO₃ [M+Na]⁺: 209.1148, Found: 209.1149.

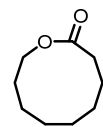
The in vitro reaction was scaled to 40.0 mL-scale assay.

 Oxocan-2-one (**2g**): **¹H NMR** (500 MHz, CDCl₃) δ 4.39–4.28 (m, 2H), 2.55 (t, 2H), 1.91–1.84 (m, 2H), 1.80 (p, $J = 5.9$ Hz, 2H), 1.67–1.59 (m, 2H), 1.59–1.52 (m, 2H). **¹³C NMR** (125 MHz, CDCl₃) δ 176.8, 67.9, 31.3, 30.9, 28.4, 25.8, 23.9. **HRMS** (ESI-TOF) calcd for C₇H₁₃O₂ [M+H]⁺: 129.0910, Found: 129.0909.

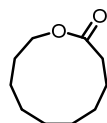
The in vitro reaction was scaled to 24.7 mL-scale assay.

 Oxonan-2-one (**2h**): **¹H NMR** (500 MHz, CDCl₃) δ 4.29 (t, $J = 5.8$ Hz, 2H), 2.28 (t, 2H), 1.77–1.67 (m, 4H), 1.66–1.60 (m, 2H), 1.51–1.40 (m, 4H). **¹³C NMR** (125 MHz, CDCl₃) δ 175.7, 64.4, 35.5, 29.4, 27.7, 25.0, 24.1, 22.9. **HRMS** (ESI-TOF) calcd for C₈H₁₅O₂ [M+H]⁺: 143.1067, Found: 143.1070.

The in vitro reaction was scaled to 35.6 mL

 Oxecan-2-one (**2i**): **¹H NMR** (500 MHz, CDCl₃) δ 4.30–4.25 (m, 1H), 4.11 (t, $J = 6.7$ Hz, 1H), 2.80–2.75 (m, 1H), 2.65 (td, $J = 6.8, 0.7$ Hz, 1H), 2.36–2.32 (m, 1H), 1.83–1.73 (m, 2H), 1.66–1.59 (m, 2H), 1.56–1.51 (m, 2H), 1.50–1.44 (m, 1H), 1.43–1.34 (m, 2H), 0.94 (t, $J = 7.4$ Hz, 2H). **¹³C NMR** (125 MHz, CDCl₃) δ 174.1, 171.7, 66.2, 64.6, 38.5, 35.0, 30.6, 29.7, 27.3, 25.8, 24.5, 24.2, 23.0, 22.7, 20.7, 19.8, 19.1, 13.7. **HRMS** (ESI-TOF) calcd for C₉H₁₇O₂ [M+H]⁺: 157.1223, Found: 157.1227.

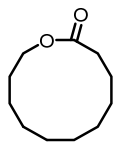
The in vitro reaction was scaled to 35.0 mL.

 Oxacycloundecan-2-one (**2j**): Purification using preparative TLC (ethyl acetate/hexanes = 1/20 to 1/1, v/v) gave the product as a colorless oil (8.1 mg, 77% yield). **¹H NMR** (500 MHz, CDCl₃) δ 4.22–4.15

(m, 2H), 4.11 (t, $J = 6.7$ Hz, 2H), 2.78 (q, $J = 7.0$ Hz, 2H), 2.65 (t, $J = 6.8$ Hz, 2H), 2.41–2.29 (m, 3H), 1.83–1.68 (m, 5H), 1.67–1.59 (m, 3H), 1.58–1.49 (m, 3H), 1.49–1.28 (m, 11H), 0.94 (t, $J = 7.4$ Hz, 3H). ^{13}C NMR (125 MHz, CDCl_3) δ 174.3, 171.7, 64.8, 64.6, 38.5, 35.3, 30.6, 26.2, 25.4, 25.3, 24.7, 24.1, 22.4, 21.3, 19.8, 19.1, 13.7.

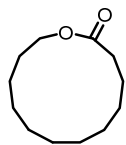
HRMS (ESI-TOF) calcd for $\text{C}_{10}\text{H}_{19}\text{O}_2$ $[\text{M}+\text{H}]^+$: 171.1380, Found: 171.1383.

Note: The compound has conformational isomer. The in vitro reaction was scaled to 61.8 mL.



Oxacyclododecan-2-one (**2k**): Purification using preparative TLC (ethyl acetate/hexanes = 1/20 to 1/1, v/v) gave the product as a colorless oil (1.0 mg, 10% yield). ^1H NMR (500 MHz, CDCl_3) δ 4.28–4.15 (m, 2H), 2.45–2.29 (m, 2H), 1.76–1.61 (m, 4H), 1.60–1.48 (m, 3H), 1.45–1.28 (m, 9H). ^{13}C NMR (125 MHz, CDCl_3) δ 174.0, 64.6, 34.4, 26.1, 24.9, 24.8, 24.5, 24.0, 23.8, 23.5, 23.3. **HRMS** (ESI-TOF) calcd for $\text{C}_{11}\text{H}_{21}\text{O}_2$ $[\text{M}+\text{H}]^+$: 185.1536, Found: 185.1555.

Note: The in vitro reaction was scaled to 54.3 mL.



Oxacyclotridecan-2-one (**2l**): Purification using preparative TLC (ethyl acetate/hexanes = 1/20 to 1/1, v/v) gave the product as a colorless oil (5.0 mg, 72% yield). ^1H NMR (500 MHz, CDCl_3) δ 4.17–4.13 (m, 2H), 2.37–2.31 (m, 2H), 1.72–1.52 (m, 5H), 1.48–1.26 (m, 13H). ^{13}C NMR (125 MHz, CDCl_3) δ 174.2, 64.6, 34.7, 27.4, 26.6, 26.4, 26.4, 25.4, 25.4, 24.9, 24.5, 24.2. **HRMS** (ESI-TOF) calcd for $\text{C}_{12}\text{H}_{23}\text{O}_2$ $[\text{M}+\text{H}]^+$: 199.1693, Found: 199.1707.

Note: The in vitro reaction was scaled to 35.0 mL.

14. Computational Methods

14.1 Molecular docking methodology

Structures of interest were covalently and non-covalently docked into the thioesterase DscB using Autodock4 and Autodock vina.^{15,16} First, the thioesterase structure was ‘cleaned;’ the substrate analogue ligand and water molecules were stripped from the file. The ligand geometries were optimized using Grimme’s program xtb.¹⁷ Covalent docking parameters were generated using MGLTools supplied with Autodock4 and AutodockTools. Covalent Autodock4 simulations used 10 Lamarckian genetic algorithm docking runs that were centered on a grid of (65,61,61) cartesian x,y,z points spaced at 0.375 Å centered on the nucleophilic serine 114 (Ser114). Autodock vina simulations were exhaustively (22) ran in a 30 Å box centered on the Ser114.

In order to validate non-covalent docking results, we initially re-docked the crystallographic ligand. This yielded good results, and we then used these parameter settings for all ligands. Below is an example config file for non-covalent docking with AutoDock Vina:

```
receptor = protein/TE_clean.pdbqt
ligand = ligand/TE_substrate_flexible.pdbqt
center_x = 66
center_y = 78
center_z = 95
size_x = 30.0
size_y = 30.0
size_z = 30.0
exhaustiveness = 22
out = output-1-flexible.pdbqt
log = output-1-flexible.log
```

The validity of the covalent docking was more difficult to verify, and so we resorted to using the manual recommendations. Below is an example input docking parameter file:

```
autodock_parameter_version 4.2      # used by autodock to validate parameter set
outlev 1                            # diagnostic output level
intelec                             # calculate internal electrostatics
seed pid time                       # seeds for random generator
ligand_types C HD OA               # atoms types in ligand
fld TE-clean_rigid.maps.fld        # grid_data_file
map TE-clean_rigid.C.map           # atom-specific affinity map
```



```

map TE-clean_rigid.HD.map      # atom-specific affinity map
map TE-clean_rigid.OA.map      # atom-specific affinity map
elecmap TE-clean_rigid.e.map    # electrostatics map
desolvmap TE-clean_rigid.d.map  # desolvation map
move empty                      # small molecule
flexres ligcovalent-fix_flex.pdbqt # file containing flexible residues
about 65.805 69.992 98.8294     # small molecule center
tran0 random                    # initial coordinates/A or random
quaternion0 random              # initial orientation
dihe0 random                    # initial dihedrals (relative) or random
torsdof 12                      # torsional degrees of freedom
rmstol 2.0                      # cluster_tolerance/A
extrng 1000.0                   # external grid energy
e0max 0.0 10000                 # max initial energy; max number of retries
ga_pop_size 150                 # number of individuals in population
ga_num_evals 2500000            # maximum number of energy evaluations
ga_num_generations 27000        # maximum number of generations
ga_elitism 1                    # number of top individuals to survive to next
                                # generation
ga_mutation_rate 0.02           # rate of gene mutation
ga_crossover_rate 0.8           # rate of crossover
ga_window_size 10               #
ga_cauchy_alpha 0.0             # Alpha parameter of Cauchy distribution
ga_cauchy_beta 1.0             # Beta parameter Cauchy distribution
set_ga                          # set the above parameters for GA or LGA
sw_max_its 300                  # iterations of Solis & Wets local search
sw_max_succ 4                   # consecutive successes before changing rho
sw_max_fail 4                   # consecutive failures before changing rho
sw_rho 1.0                      # size of local search space to sample
sw_lb_rho 0.01                  # lower bound on rho
ls_search_freq 0.06             # probability of performing local search on
                                # individual
set_pswl                        # set the above pseudo-Solis & Wets parameters
unbound_energy 0.0              # state of unbound ligand
ga_run 10                       # do this many hybrid GA-LS runs
analysis                        # perform a ranked cluster analysis
rmsatoms all                    # rms atoms

```

14.2 Density functional theory calculation methodology

The cyclization transition state was located at the B3LYP-D3(BJ)/6-31G(d,p)¹⁸⁻²² level of theory as implemented in Gaussian 16 Rev. A.03 (sse4).²³ In order to construct the theozyme model, the side chains of His276 and Asp247 and the covalently docked Ser114-bound acyl-intermediate were cut from the structure (**Figure 3c**) and protons were added to the amino acid side chains. Then, a scan calculation of the forming C–O bond was set up from 3.5 to 1.7 Å. The highest energy point along the scan coordinate was then used as a guess geometry for a Berny transition state optimization. The coordinates of the optimized geometry have been supplied to the publisher as an xyz file and are pasted below.

Theozyme transition state

E	-1265.637547
H	-1265.124732
G	-1265.220420
Imag. Freq.	-150.003

Cartesian coordinates

C	-0.182208	-2.401703	-1.491813
C	-1.220461	-3.384656	-0.959944
H	-0.564144	-1.913905	-2.402428
H	0.752630	-2.906758	-1.757078
H	-2.149323	-2.876795	-0.682447
H	-0.835441	-3.900834	-0.073626
O	1.528225	0.502388	-0.386301
C	1.931064	1.027062	-1.638696
C	3.465977	1.064578	-1.758034
C	4.117858	1.949649	-0.672735
C	5.234751	1.244017	0.128419
C	4.707177	-0.047212	0.702675
C	3.777466	-0.103118	1.654118
C	2.980457	-1.333099	1.940397
C	1.562164	-1.233481	1.363245
C	1.509059	-1.189130	-0.181364
C	1.281694	0.329910	-2.839855
O	2.924073	-1.515405	3.371498
O	2.373870	-1.791549	-0.850543
H	2.189472	-2.122213	3.533148

H	0.194902	0.312770	-2.722959
H	1.639593	-0.697808	-2.913039
H	1.524426	0.864992	-3.766764
H	1.576702	2.075911	-1.641236
H	3.739088	1.426004	-2.758925
H	3.806222	0.030087	-1.680238
H	4.506892	2.880210	-1.109516
H	3.341074	2.232743	0.045160
H	5.582966	1.915228	0.925702
H	6.099375	1.048930	-0.519146
H	4.951039	-0.967465	0.177274
H	3.449409	0.801507	2.167091
H	3.469781	-2.193575	1.464306
H	1.030042	-0.383653	1.799288
H	1.016388	-2.143316	1.652683
C	-2.032709	0.681175	0.119926
H	-2.067216	-0.384274	-0.033412
C	-1.228880	2.707600	0.345157
H	-0.486616	3.490263	0.385141
C	-2.596008	2.745615	0.497801
N	-0.890326	1.394039	0.106919
N	-3.086765	1.461523	0.354143
H	0.090440	0.998711	-0.079345
C	-3.493276	3.908915	0.772241
H	-4.235781	4.040102	-0.024152
H	-2.915060	4.834478	0.850780
H	-4.048306	3.776128	1.708739
H	-1.459381	-4.140450	-1.719597
O	0.092309	-1.423769	-0.506019
C	-5.367530	-0.896234	0.139661
O	-4.334761	-1.516154	-0.072589
O	-5.450613	0.396748	0.392876
H	-4.492365	0.839075	0.383344
C	-6.732512	-1.567302	0.137612
H	-7.217806	-1.426207	1.108462
H	-7.375122	-1.100995	-0.615781
H	-6.623549	-2.631403	-0.073083

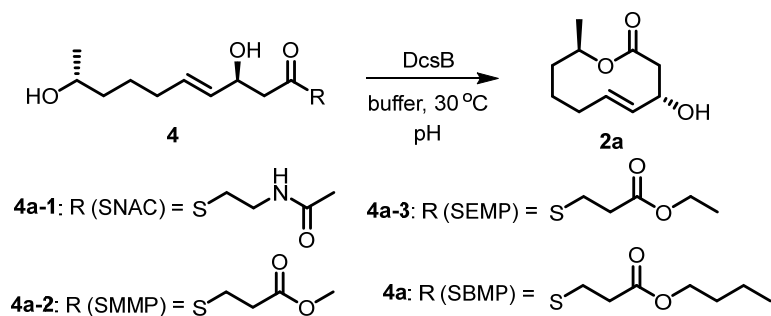
SUPPLEMENTARY TABLES

Table S1. Bioinformatics analysis of *dcs* gene cluster

Protein	Size (aa)	Proposed function	Homologs (ident/pos)	Source Strain
DcsA	2414	HRPKS with domains: KS_AT_KR_DH_ER_ACP	XP_018702120.1(83%/87%)	<i>Cordyceps fumosorosea</i>
DcsB	319	Thioesterase	TQV91950.1 (72%/77%)	<i>Cordyceps javanica</i>
DcsC	545	Cytochrome P450	OAA48824.1 (80%/82%)	<i>Beauveria brongniartii</i>
DcsD	252	Short-chain Dehydrogenase/ Reductase (SDR)	ATY63300.1 (84%/92%)	<i>Cordyceps militaris</i>

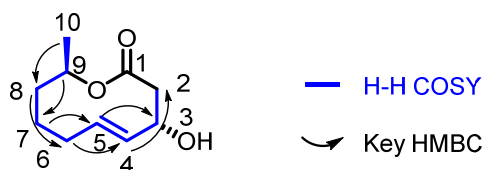
Table S2. Primers used in this project

Primers	Sequence (5'-3')
pDWG1001-F1	CTCCCTTCTCTGAACAATAAACCCACAGAAAGGCATTTATGTCTGGGCCAAGAACCTATTG
pDWG1001-R1	AGCAATGTACGCGACATCG
pDWG1001-F2	TTGAAATCGGACCATCTGGTGC
pDWG1001-R2	ACAACACCTGCAGCTTCATAGC
pDWG1001-F3	ATCGAGGTCGAGGTTGTCTG
pDWG1001-R3	CTTGGGTCTCTCCCCTCACCCAAATCAATTCACCGGAGTTTTTGGTGCAGGGTACGTGTG
pDWG1001-F4	ACTCCGGTGAATTGATTTGGG
pDWG1001-R4	TGTTTAGATGTGTCTATGTGGCGG
pDWG1001-F5	GACTAACCATTACCCCGCCACATAGACACATCTAAACAATGGCACCTCTTTCATCGTTCC
pDWG1001-R5	GTAGGAGTGATGAGACCCAACAACCATGATACCAGGGGCCGATTGGGATGAACCATTAC
pDWG1002-F1	CCTGAGCTTCATCCCCAGCATCATTACACCTCAGCAATGGCTTCTCCTACTATTGTCCTC
pDWG1002-R1	TGGGTCTCTCCCCTCACCCAAATCAATTCACCGGAGTCATCGAAGAGGTGTACAAGGAGG
pDWG1002-F2	ACTCCGGTGAATTGATTTGGG
pDWG1002-R2	TGTTTAGATGTGTCTATGTGGCGG
pDWG1002-F3	GCTTGACTAACCATTACCCCGCCACATAGACACATCTAAACAATGGCCGCGAGCAATTTCC
pDWG1002-R3	GACTTCAACACAGTGGAGGACATACCCGTAATTTTCTGTGTGCTTCAGGCATATCTCGGC
pDWG1003-F1	TGAGAGCCTGAGCTTCATCCCCAGCATCATTACACCTCAGCAATGGCCGCGAGCAATTTCC
pDWG1003-R1	GACTTCAACACAGTGGAGGACATACCCGTAATTTTCTGTGTGCTTCAGGCATATCTCGGC
pDWG1004-F1	CTAACCATTACCCCGCCACATAGACACATCTAAACAATGGCTTCTCCTACTATTGTCCTC

Table S4. Optimization of thioesterase-catalyzed lactonization

entry ^a	substrate	buffer	pH	yield (%)
1	4a-1	Tris	7.4	3
2	4a-2	Tris	7.4	11
3	4a-2	Na ₃ PO ₄	7.4	43
4	4a-2	Na ₃ PO ₄	7.0	42
5	4a-2	Na ₃ PO ₄	8.0	40
6 ^b	4a-2	Na ₃ PO ₄	7.4	31
7 ^c	4a-2	Na ₃ PO ₄	7.4	38
8 ^{d,e}	4a-3	Na ₃ PO ₄	7.4	60
9 ^{d,f}	4a	Na ₃ PO ₄	7.4	73
10 ^g	4a	Na ₃ PO ₄	7.4	61

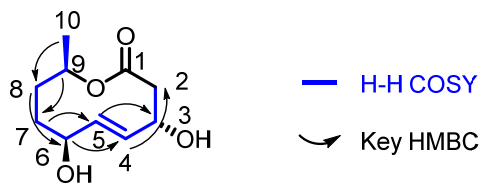
^aReaction condition: 1.0 mM substrate **4**, 23.4 μM dcsB, reaction buffer, pH as shown in Table at 30 $^\circ\text{C}$. ^bat 37 $^\circ\text{C}$. ^c5.9 μM DcsB. ^d1.9 μM DcsB. ^eTTN (total turnover number) up to 309. ^fTTN up to 376. ^g0.5 μM DcsB with TTN up to 1258.

Table S5. Spectroscopic data of **2a**

position	δ_{H} (mult., $J_{\text{H-H}}$ in Hz) (one major conformational isomer)	δ_{C} (one major conformational isomer)
1		170.9
2	2.54 (AB, $J_{\text{AB}} = 11.8, 3.5$ Hz, 1H), 2.47 (BA, $J_{\text{BA}} = 11.8, 3.7$ Hz, 1H)	44.7
3	4.59 (br, 1H)	68.0
4	5.55–5.48 (m, 1H)	132.7
5	5.65–5.55 (m, 1H)	128.1
6	2.29–2.11 (m, 1H), 1.97–1.84 (m, 1H)	32.5
7	1.83–1.65 (m, 1H), 1.58–1.31 (m, 1H)	27.9
8	1.83–1.65 (m, 1H), 1.58–1.31 (m, 1H)	35.2
9	4.85–4.72 (m, 1H)	72.7
10	1.11 (d, $J = 6.5$ Hz, 3H) 2.94 (s, OH)	21.9

In CDCl_3 : 500 MHz for ^1H NMR and 125 MHz for ^{13}C NMR; Chemical shifts are reported in ppm. All signals are determined by ^1H - ^1H COSY, HMBC and HSQC correlation. The absolute stereochemistry was determined by X-ray crystal analysis. $[\alpha]_{\text{D}}^{22} = -29.3$ ($c = 1.0$ Chloroform). **HRMS** (ESI-TOF) calcd for $\text{C}_{10}\text{H}_{16}\text{NaO}_3$ $[\text{M}+\text{Na}]^+$: 207.0992, Found: 207.0988.

Note: Compound **2a** contains one pair of conformational isomer, one is the major isomer and the other one is minor one.

Table S6. Spectroscopic data of **1**

position	δ_{H} (mult., $J_{\text{H-H}}$ in Hz)	δ_{C}
1		171.1, 170.6
2	2.92 (dd, $J = 13.5, 7.7$ Hz, 1H), 2.52 (td, 2H), 2.31 (dd, $J = 13.5, 5.7$ Hz, 1H)	44.4, 44.0
3	4.77–4.66 (m, 1H), 4.60–4.53 (m, 1H)	69.0, 67.3
4	5.90 (ddd, $J = 16.0, 3.3, 1.7$ Hz, 1H), 5.41 (dd, $J = 16.2, 7.5$ Hz, 1H)	129.3
5	5.80 (d, $J = 16.1$ Hz, 1H), 5.56 (dd, $J = 16.2, 8.8$ Hz, 1H)	136.8, 130.5
6	4.39 (s, 1H), 3.95 (td, $J = 8.6, 2.9$ Hz, 1H)	72.8, 67.7
7	2.06–1.86 (m, 2H), 1.81–1.59 (m, 2H)	31.3
8	1.81–1.59 (m, 3H), 1.44 (dd, $J = 15.8, 7.1$ Hz, 1H)	27.2
9	5.05–4.94 (m, 1H), 4.77–4.66 (m, 1H)	72.8, 71.0
10	1.22 (d, $J = 6.7$ Hz, 3H), 1.17 (d, $J = 6.4$ Hz, 3H)	17.5

In CD₃OD: 500 MHz for ¹H NMR and 125 MHz for ¹³C NMR; Chemical shifts are reported in ppm. All signals are determined by ¹H-¹H COSY, HMBC and HSQC correlation. The absolute stereochemistry was determined by X-ray crystal analysis. $[\alpha]_{\text{D}}^{22} = -12.2$ ($c = 1.0$ Methanol). **HRMS** (ESI-TOF) calcd for C₁₀H₁₆NaO₄ [M+Na]⁺: 223.0941, Found: 223.0941.

Note: This compound **1** contains one pair of conformational isomers at 1:1 ratio.

Table S7. Data collection and refinement statistics

Name	DcsB	DcsB- 4a-2' complex
PDB ID	7D78	7D79
Data collection		
Space group	<i>C121</i>	<i>P1</i>
Cell dimensions		
a, b, c (Å)	178.71, 47.57, 71.70	47.26, 59.01, 113.99
α , β , γ (°)	90.00, 93.19, 90.00	84.85, 78.55, 84.01
Resolution (Å)	50.00-1.97 (2.00 - 1.97)	50.00 - 2.11 (2.15 - 2.11)
R_{merge}	0.072 (0.256)	0.124 (0.544)
$I/\sigma I$	26.44 (6.56)	9.56 (1.88)
Redundancy	6.1 (5.5)	3.5 (3.0)
Completeness (%)	99.6 (98.2)	92.6 (90.1)
CC1/2	0.956 (0.958)	0.732 (0.734)
Refinement		
Resolution (Å)	38.84-1.97	39.00 - 2.10
No. reflections	42956	59724
$R_{\text{work}} / R_{\text{free}}$	0.146/0.183	0.182/0.227
No. non-H atoms		
Protein	4582	9012
Ligand	25	68
Water	524	573
B factor(Å ²)		
Protein	25.3	28.0
Ligand	36.1	34.2
R.m.s. deviations		
Bond lengths (Å)	0.007	0.002
Bond angles (°)	0.81	0.49
Ramachandran (%)		
Favored	96.43	96.35
Outliers	0.34	0.00
Rotamer outliers	0.00	0.2

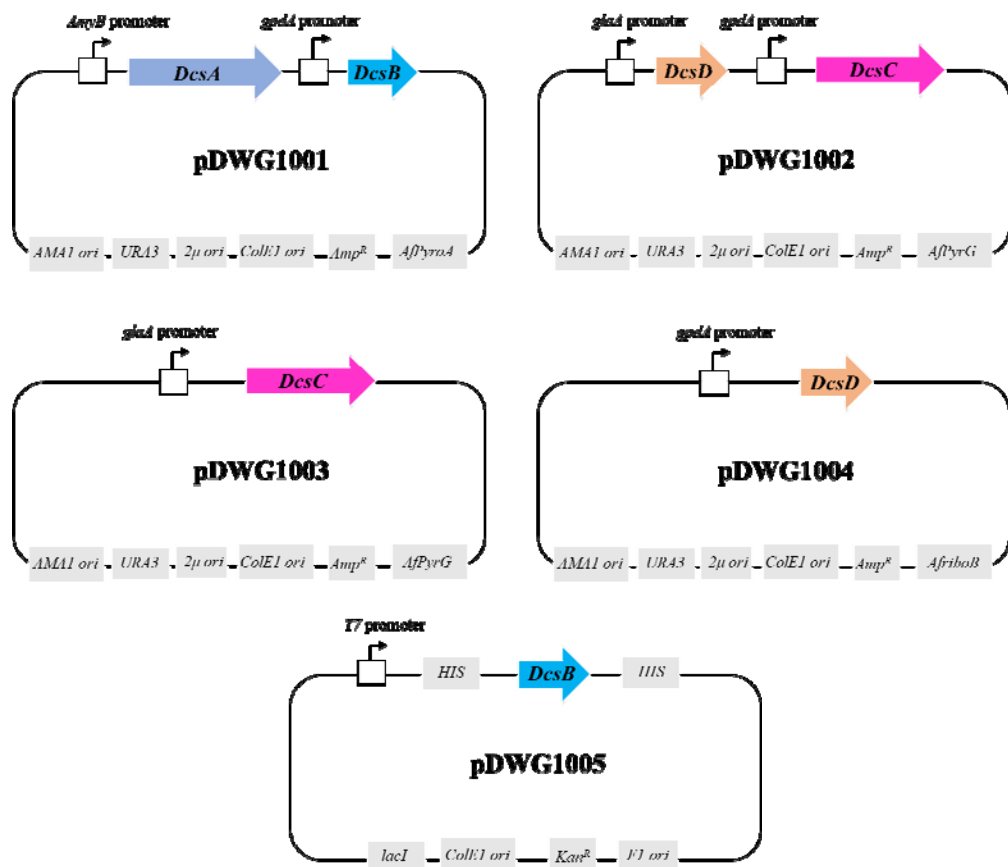


Figure S1. Plasmids used for heterologous expression of *dcs* gene cluster in *A. nidulans* and protein expressions in *E. coli*.

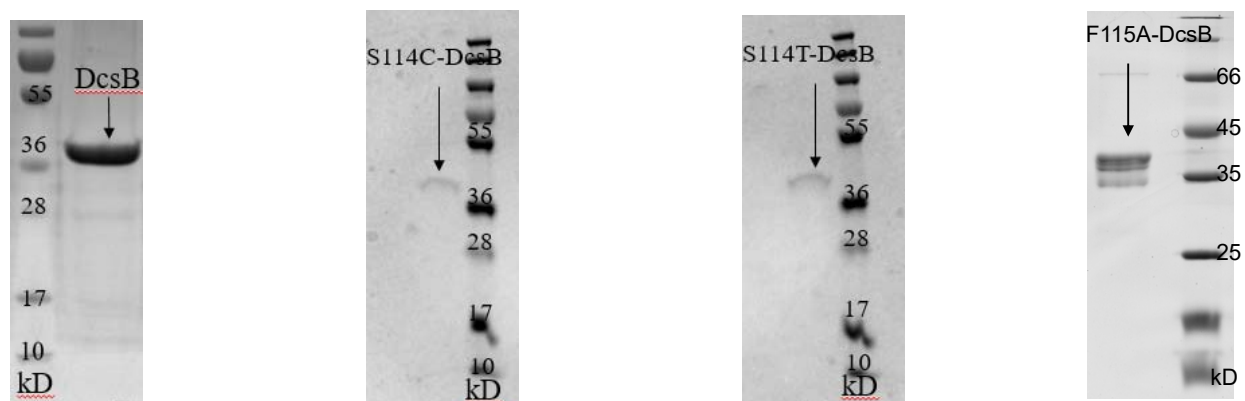


Figure S2. SDS-PAGE (6%) analysis of DcsB and mutants expressed and purified from *E. coli*.

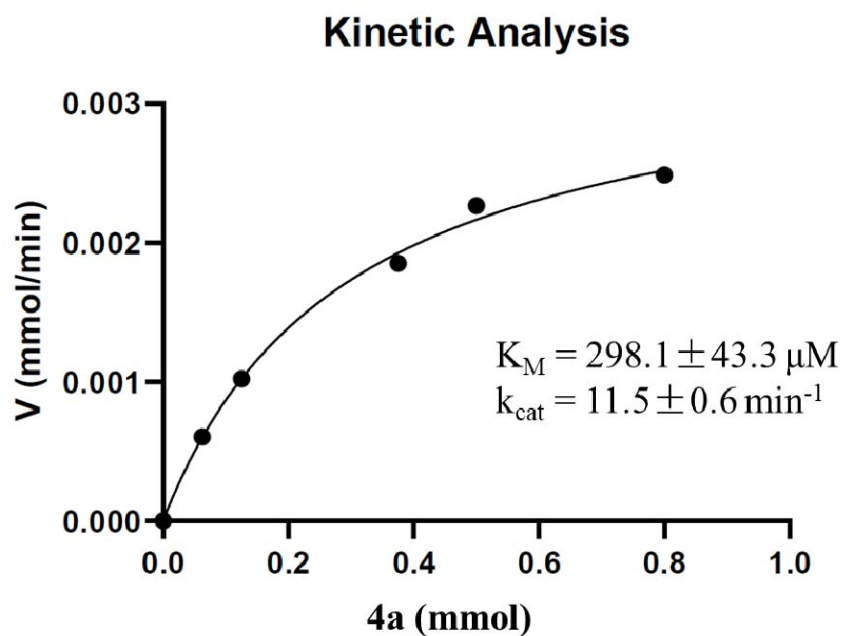


Figure S3. Kinetics study of DcsB-catalyzed conversion of **4a** to **2a**. For kinetics study, the assays were performed at 400 μL -scale with 0.49 μM DcsB and 62.5-800 μM **4a** in Na_3PO_4 buffer (100 mM Na_3PO_4 , 300 mM NaCl, 5% glycerol, pH 7.4,) incubated at 30°C for 30 min. Data fitting was performed using GraphPad Prism 5.

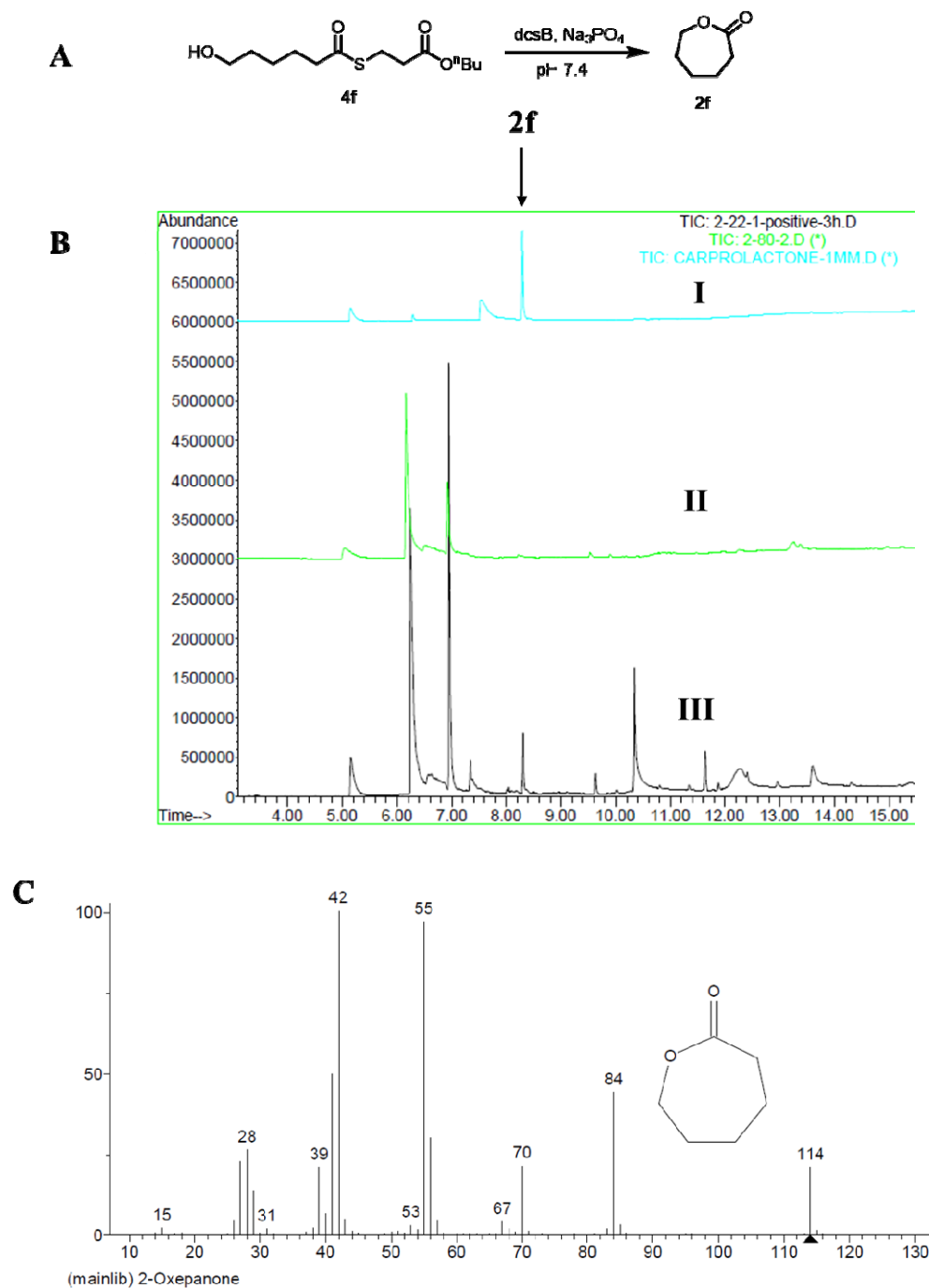


Figure S4. DcsB-catalyzed lactonization of **4f** for the formation of **2f**. (A) In vitro reaction of substrate **4f**. (B) (I) standard compound **2f** by GC-MS analysis; (II) Control reaction with denatured DcsB did not show the desired peak; (III) DcsB in vitro assay of **4f**, showing the desired peak. (C) MS data show the molecular weight of **2f**.

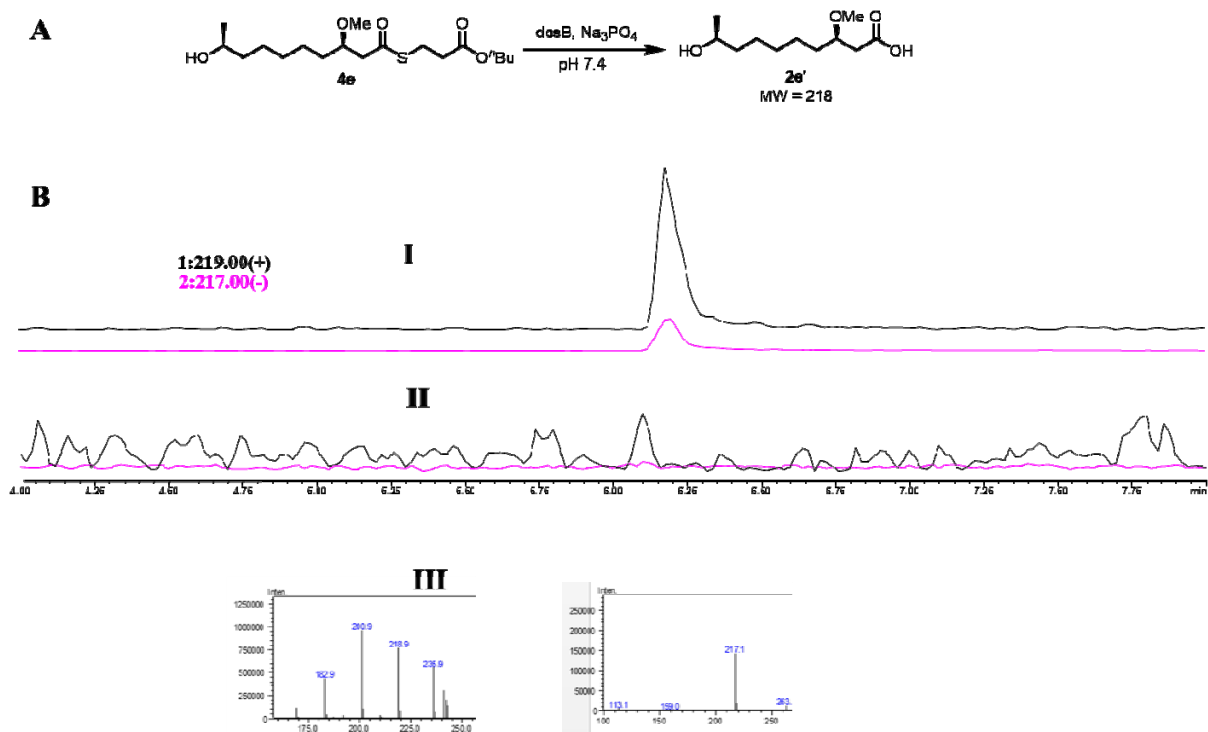


Figure S5. DcsB-catalyzed hydrolysis of **4e** for the formation of **2e'**. (A) In vitro reaction of substrate **4e**. (B) (I) LC-MS data for compound **2e'** from DcsB in vitro assay, showing the desired peak; (II) Control reaction with denatured DcsB did not show the desired peak; (III) MS show the molecular weight of **2e'**.

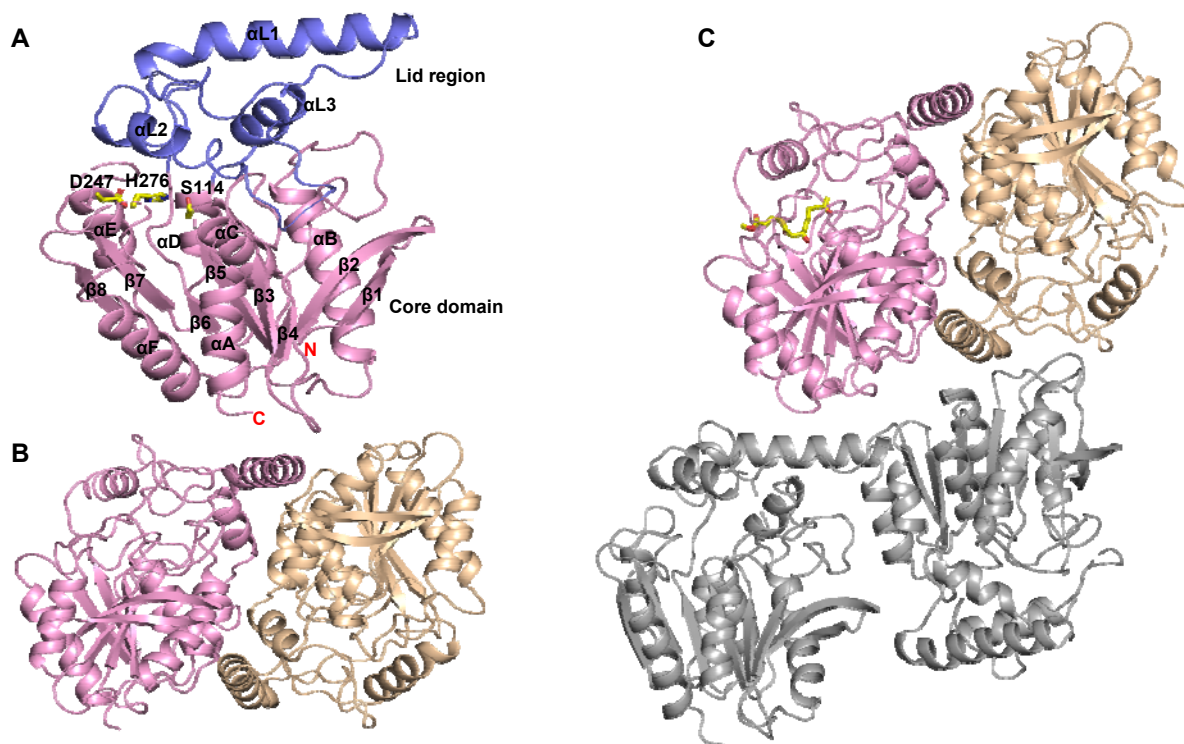


Figure S6. Structures of *apo* DcsB and its complex with substrate analog. (A) The cartoon model of the DcsB monomer contains a lid region (colored in blue) and a core domain (colored in pink). The catalytic triad is labeled as indicated with yellow sticks. (B) The homodimer structure of DcsB in the asymmetric unit. (C) The tetramer structure of DcsB-4a-2' (enzyme-substrate complex) in the asymmetric unit.

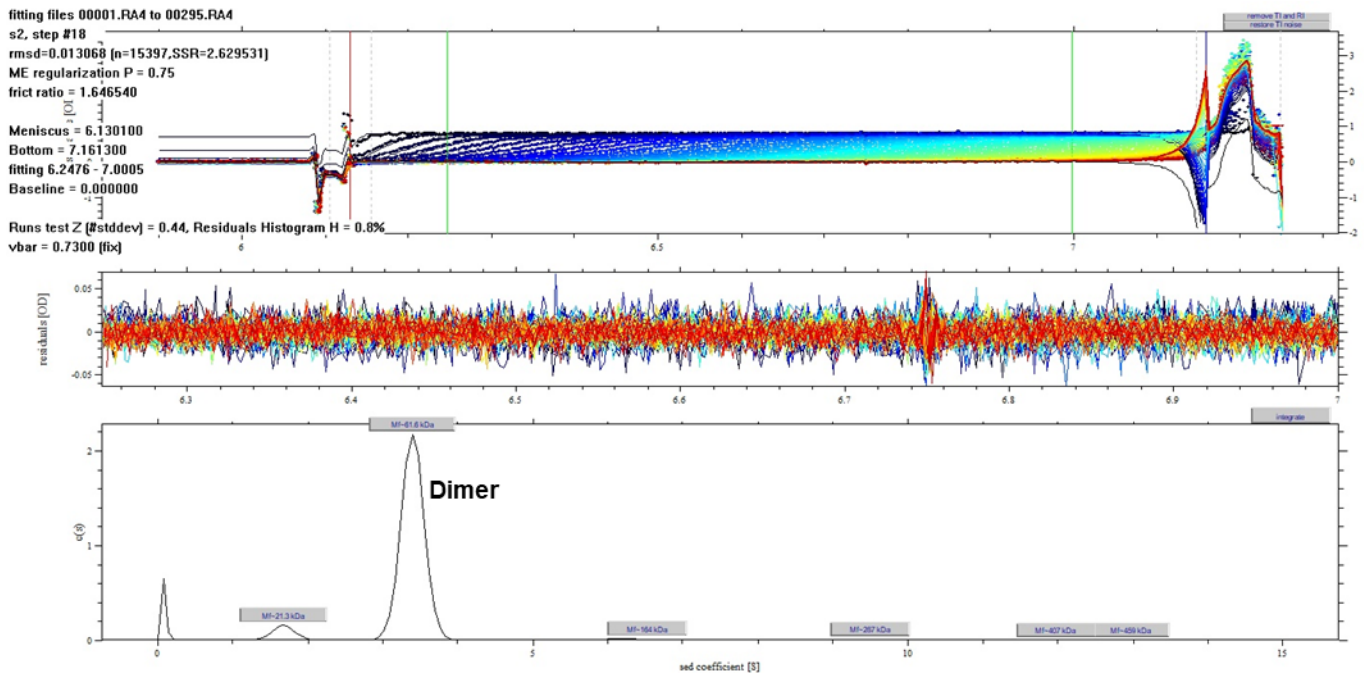


Figure S7. Solution oligomerization state of DcsB. Wild type DcsB exists as a dimer in solution as characterized by ultracentrifugation velocity. The major peak has a sedimentation coefficient consistent with a DcsB dimer.

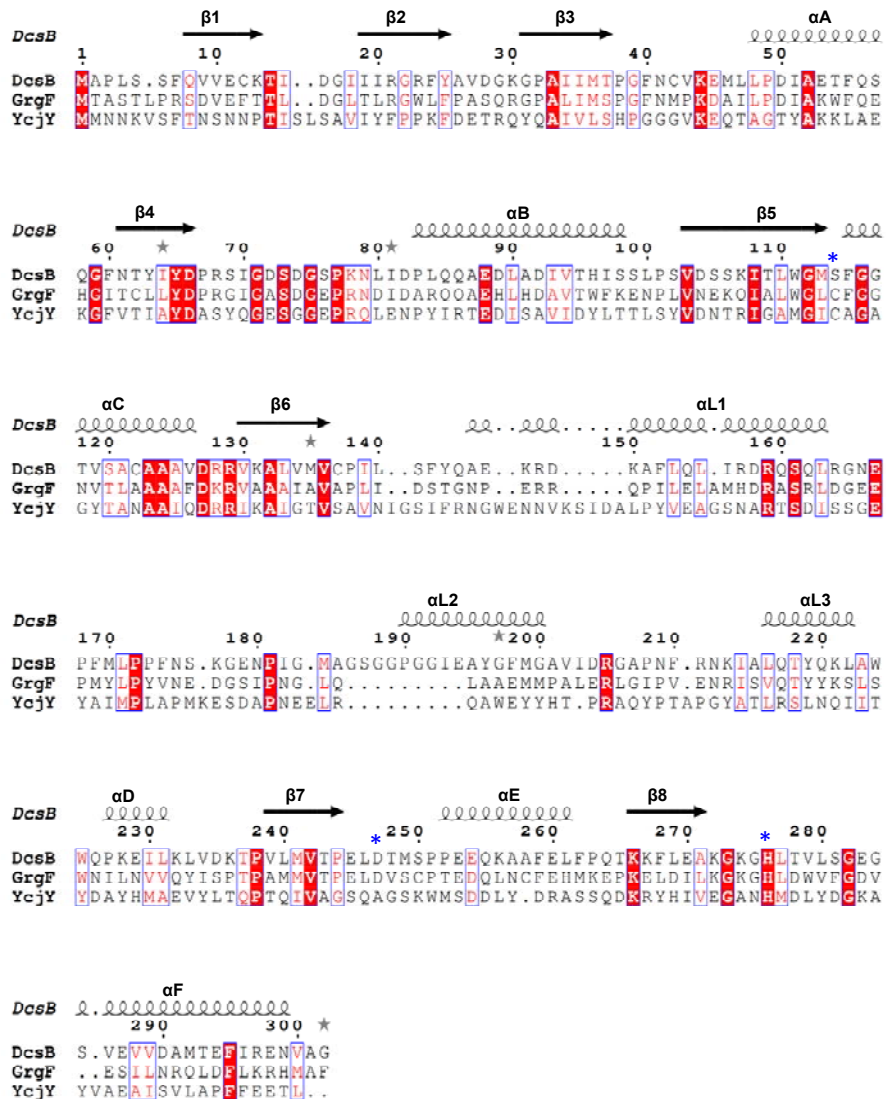


Figure S8. Sequence alignment of DcsB with the closest structural homologs identified by DALI search: α/β chain hydrolase GrgF (PDB ID: 6LZH, identity 38%) and uncharacterized protein YcjY (PDB ID: 5XB6, identity 19%). The catalytic triad residues are marked with an asterisk. Residues with strict identity are in white on a red background and those with identity above 70% are colored in red and framed in blue. The alignment was generated by T-coffee web-server using default parameters. The figure was generated by ESPrnt 3.0.

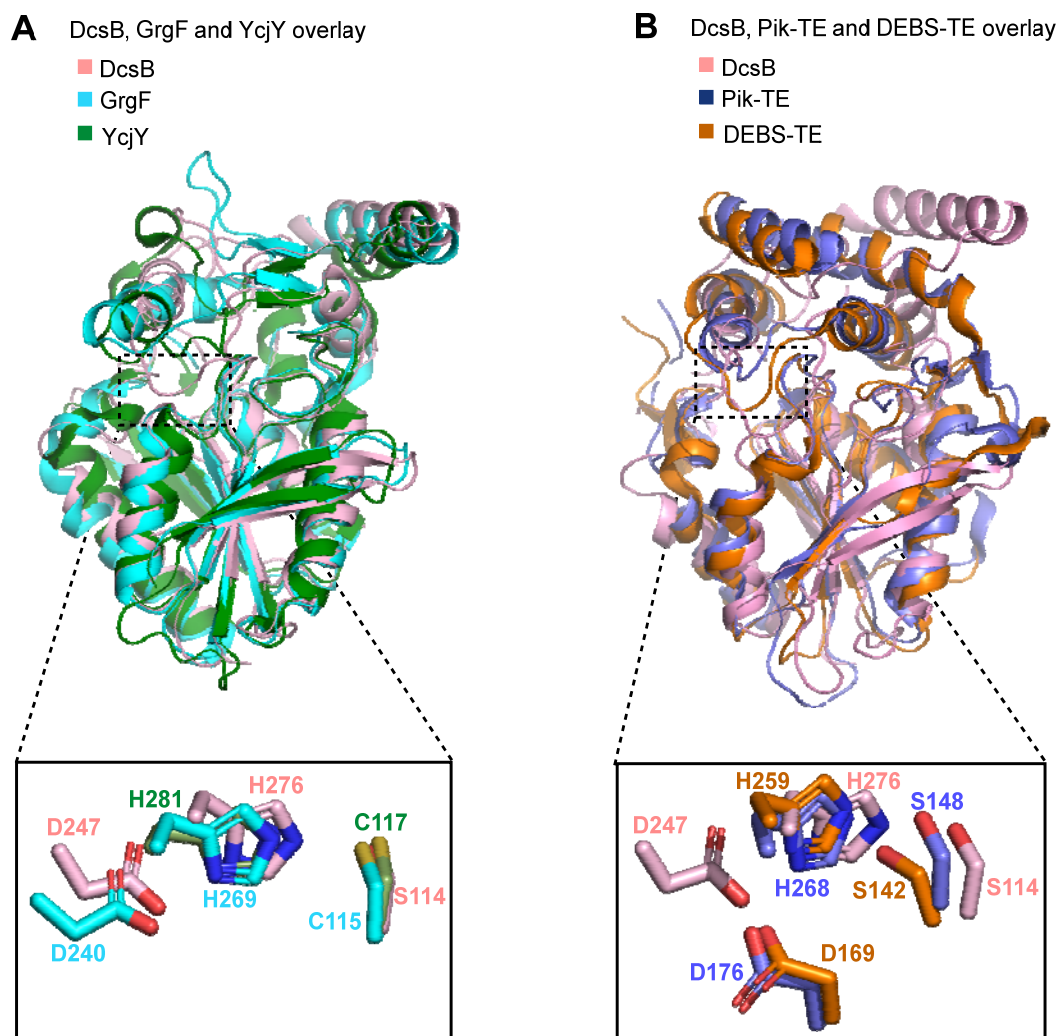


Figure S9. Structural comparison of DcsB with other homologs. (A) Superposition of DcsB (pink) with GrgF (cyan, PDB ID: 6LZH, RMSD 1.8 Å) and YcjY (dark green, PDB ID: 5XB6, RMSD 2.2 Å) identified by DALI search. (B) Superposition of DcsB (pink) with Pik-TE (blue, PDB ID: 2HFJ, RMSD 2.7 Å in core region) and DEBS-TE (orange, PDB ID: 1KEZ, RMSD 2.5 Å in core region).

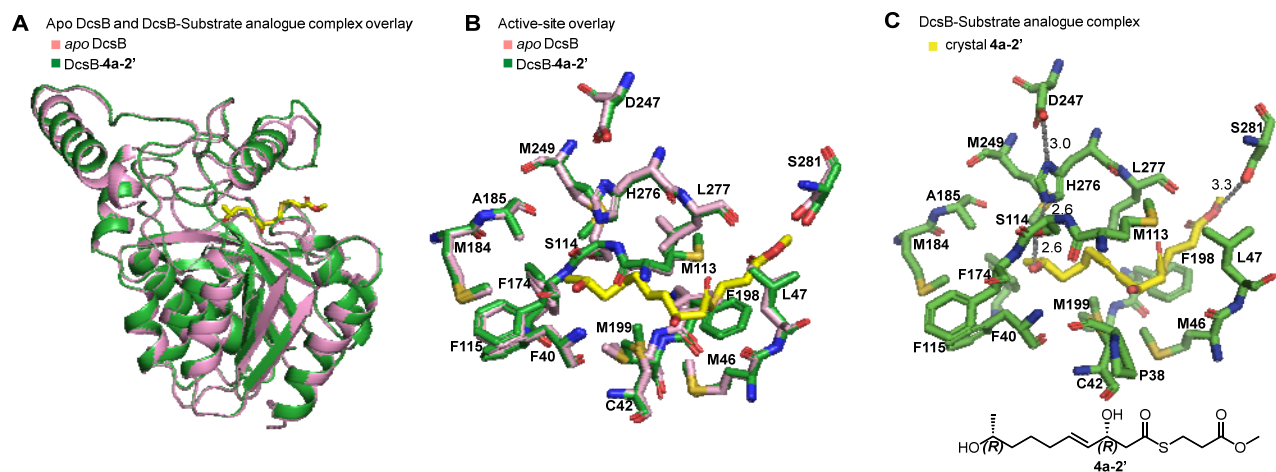


Figure S10. Comparison of the *apo* DcsB and its substrate analog **4a-2'** complex. (A) Overlay of the *apo* DcsB (residues, pink) and the DcsB-**4a-2'** complex (residues, green; **4a-2'**, yellow) with RMSD 0.146 Å for 257 C α atoms. (B) Active site overlay of the *apo* DcsB and the DcsB-**4a-2'** complex (colored as in A). Substantial conformational changes are observed for F198 and M199. (C) Active site view of DcsB cocrystal structure with substrate analogue **4a-2'**.

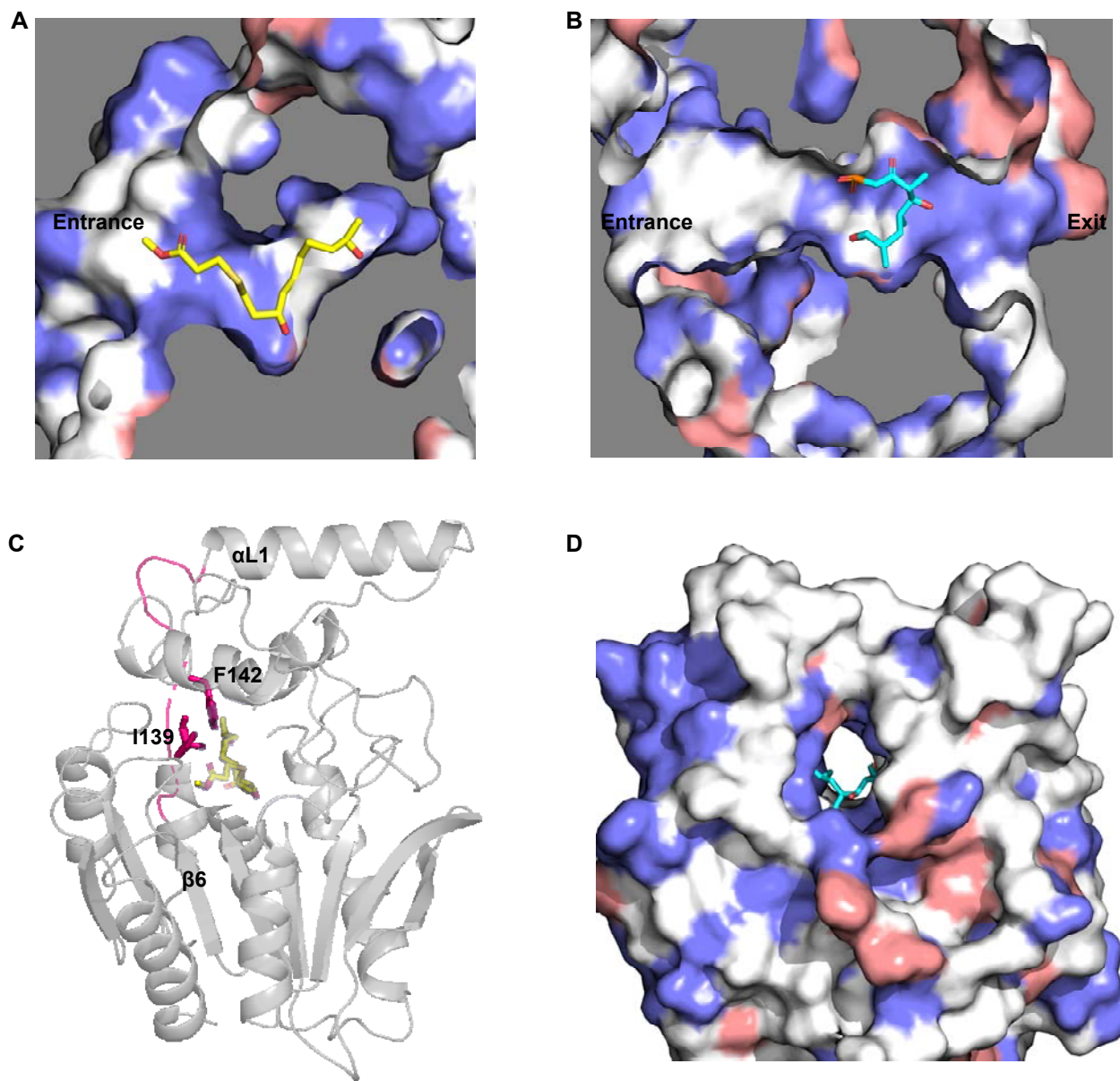


Figure S11. Clip view of the active site cavity of DcsB and Pik-TE. (A) Cut-away view of linear substrate analogue **4a-2'** in the active site of DcsB. (B) Cut-away view of linear substrate phosphopentaketide in the active site of Pik-TE (PDB ID: 2HFJ). The hydrophobic surface is shown in blue, whereas the hydrophilic surface is shown in white. (C) The active site cavity of DcsB shown in lightblue surface and the loop between $\beta 6$ and $\alpha L1$ shown in white. (D) The open channel of Pik-TE, substrate phosphopentaketide (cyan sticks) is viewed from the exit channel.

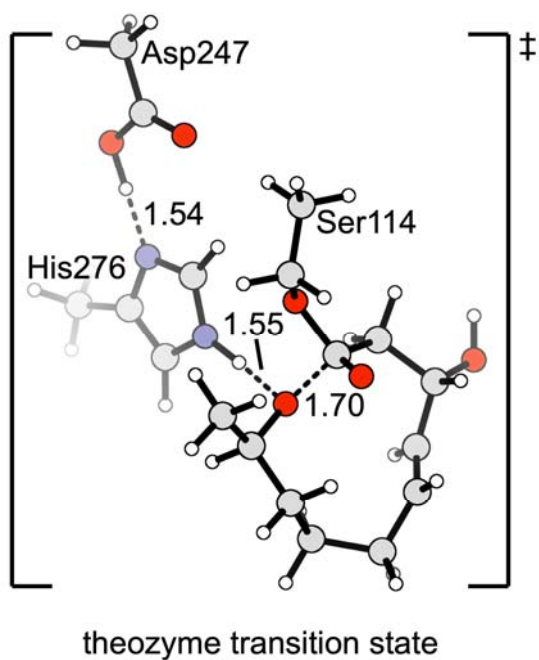


Figure S12. Calculated theozyme model for cyclization. Distances for forming bonds and hydrogen bonding are labeled in Angstrom. The structure was calculated at the B3LYP-D3(BJ)/6-31G(d,p) level of theory.

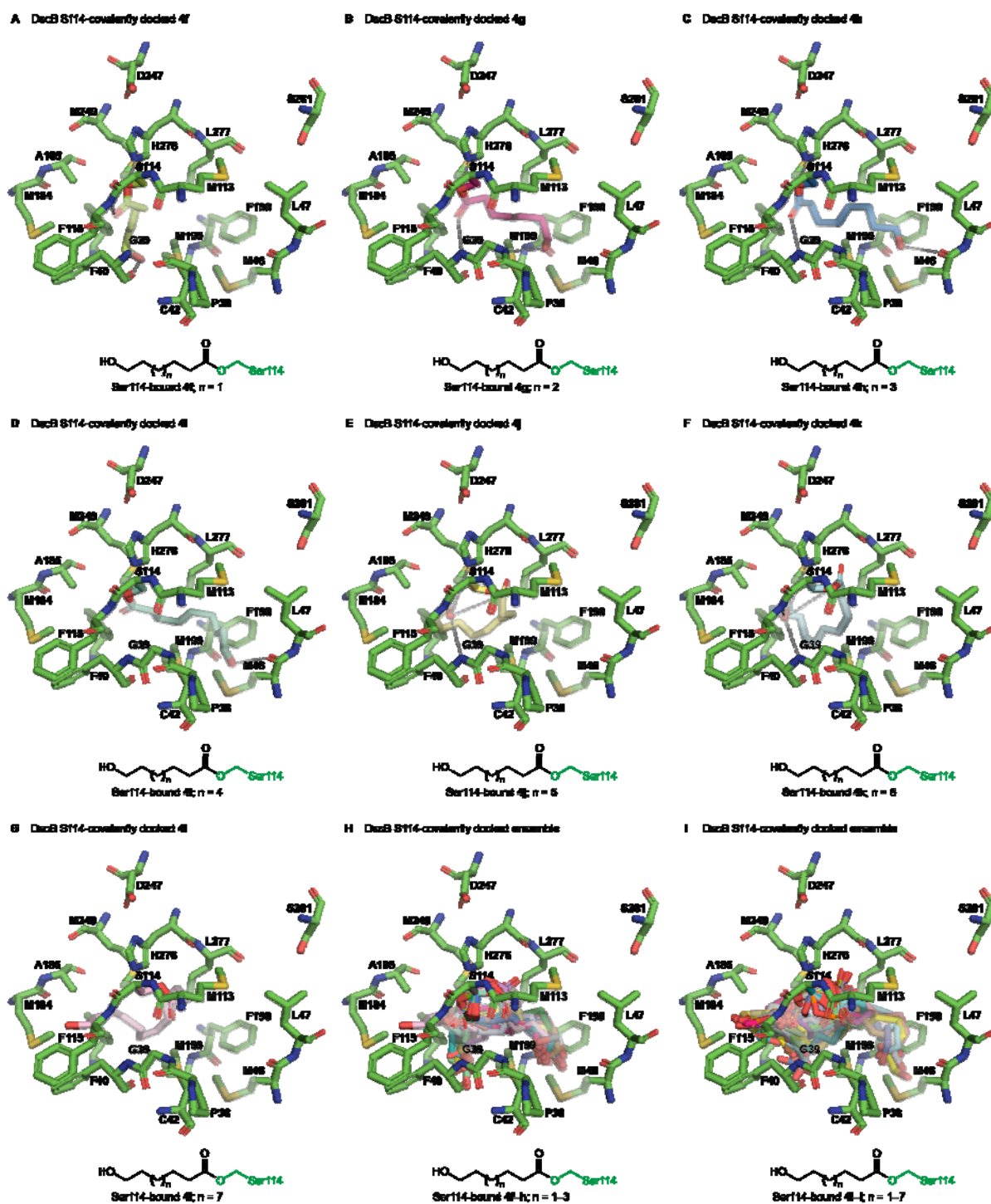


Figure S13. Covalent docking of 4f–l Ser114-bound acyl-intermediates. (A–G) Predicted lowest energy conformation shown. (H, I) ensembles of docked structures overlaid in active site. 4f–i adopt extended conformations whereas 4j–l adopt folded conformations.

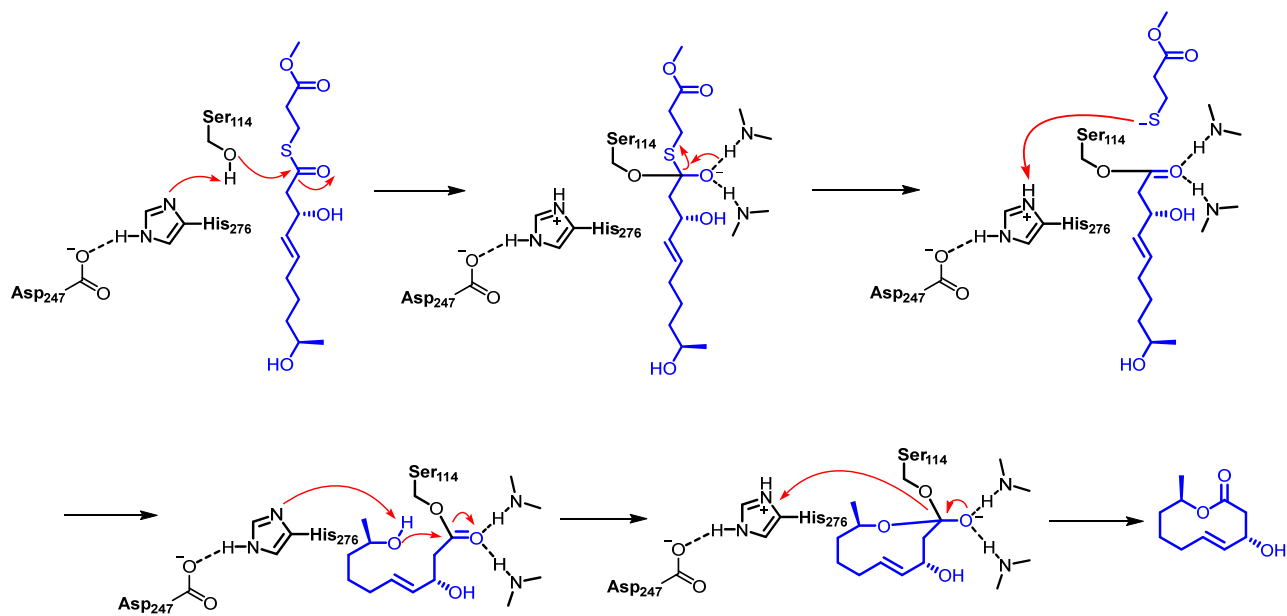


Figure S14. Proposed catalytic mechanism of DcsB

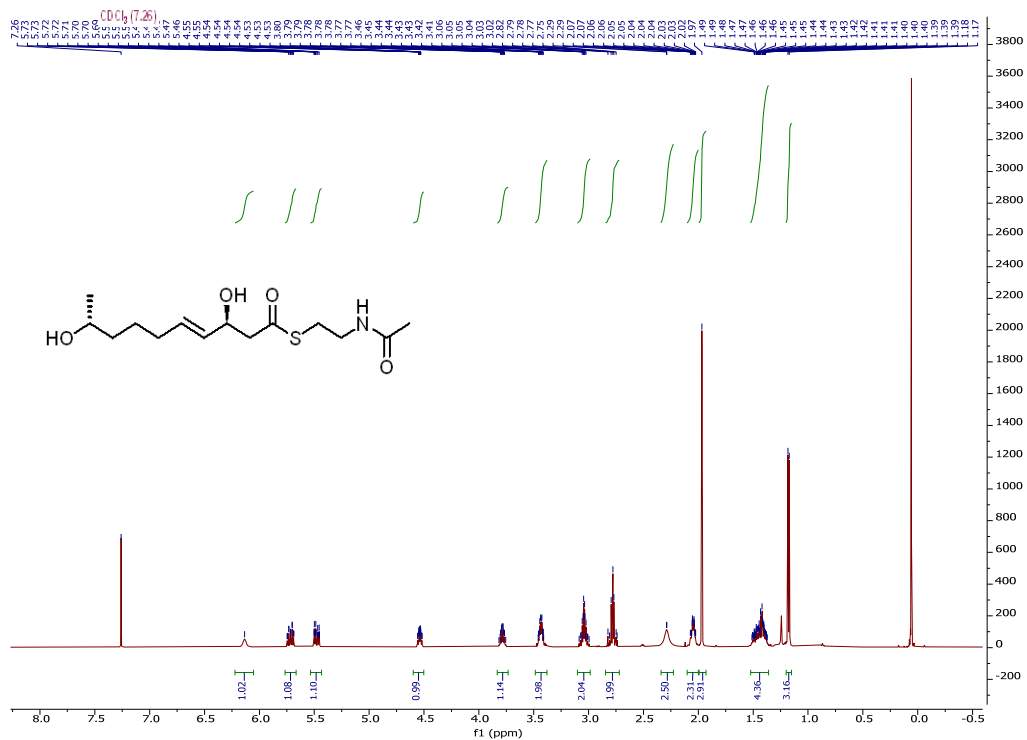


Figure S15. ¹H NMR Spectra of compound 4a-1. Chloroform-*d*1, 500 MHz for ¹H NMR

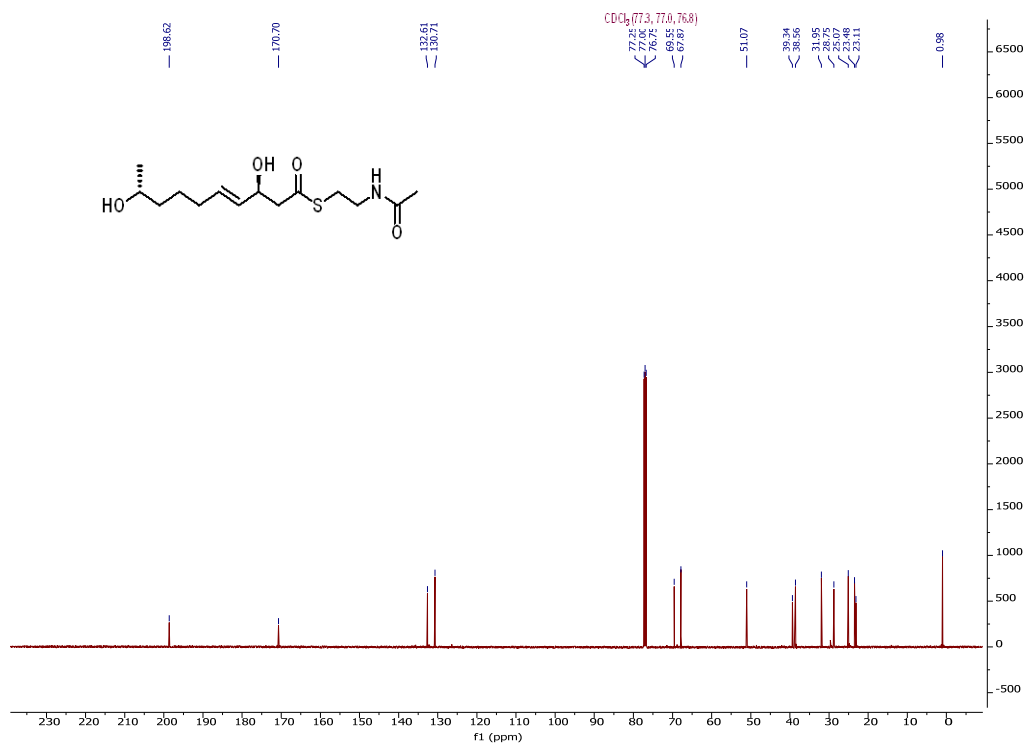


Figure S18. ^{13}C NMR Spectra of compound **4a-2**. Chloroform-*d*1, 125 MHz for ^{13}C NMR.

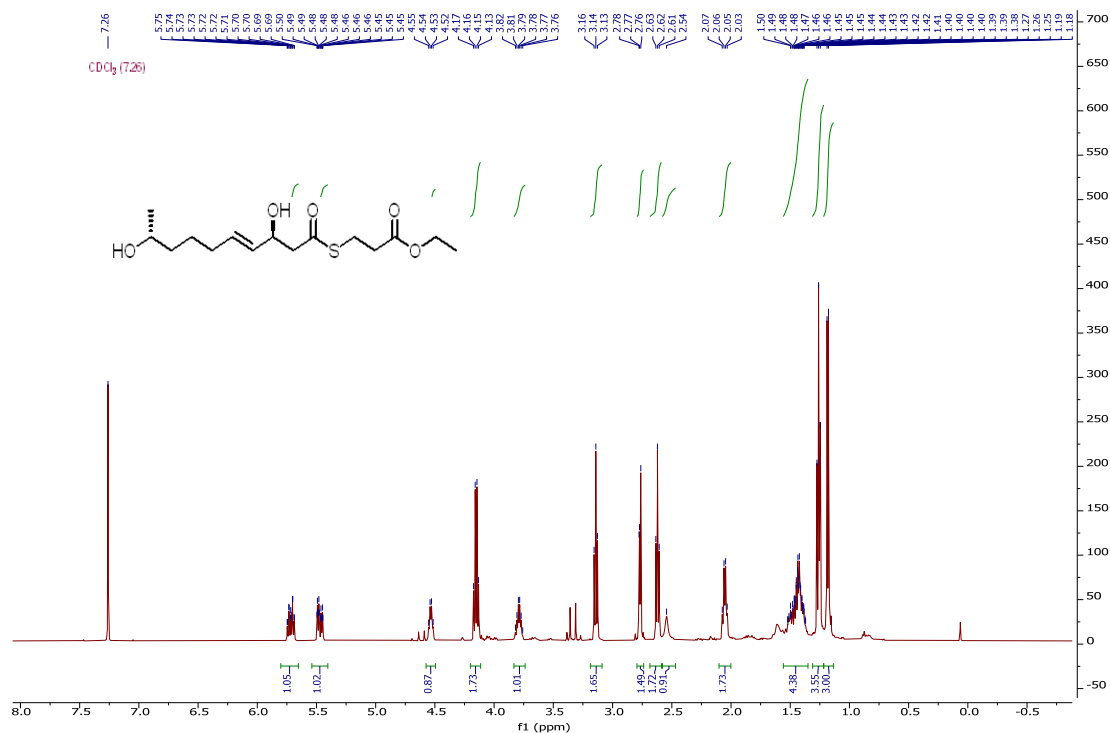


Figure S19. ^1H NMR Spectra of compound **4a-3**. Chloroform-*d*1, 500 MHz for ^1H NMR.

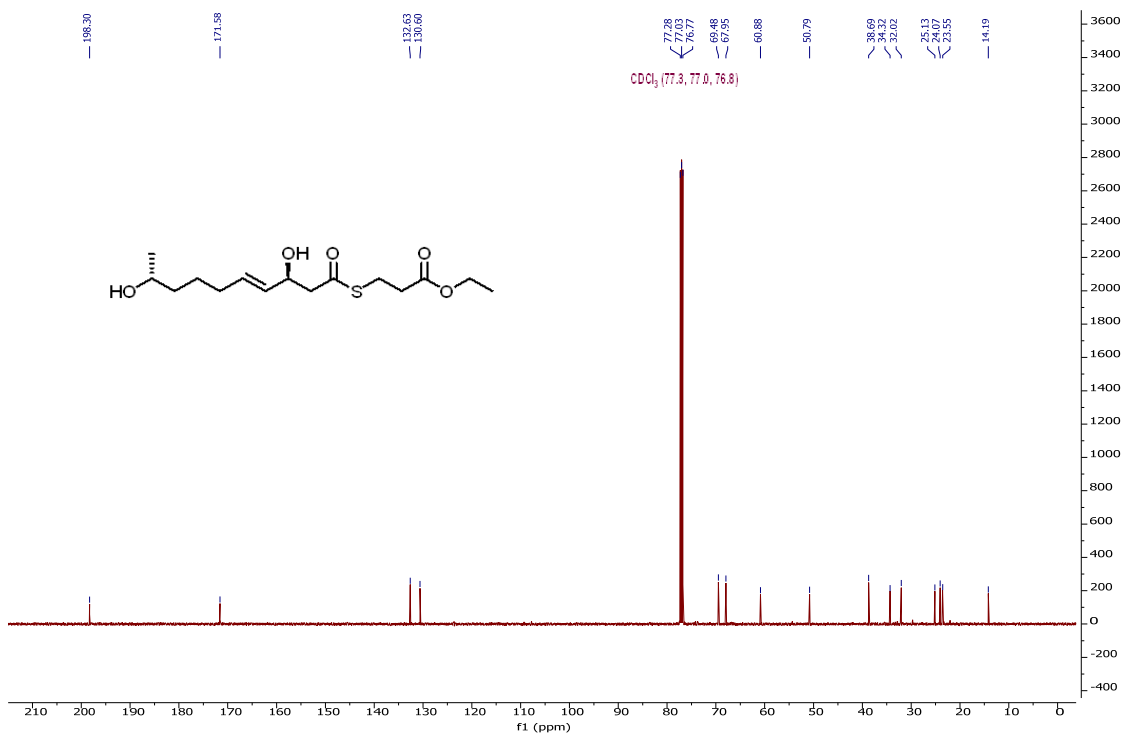


Figure S20. ^{13}C NMR Spectra of compound **4a-3**. Chloroform-*d*1, 125 MHz for ^{13}C NMR.

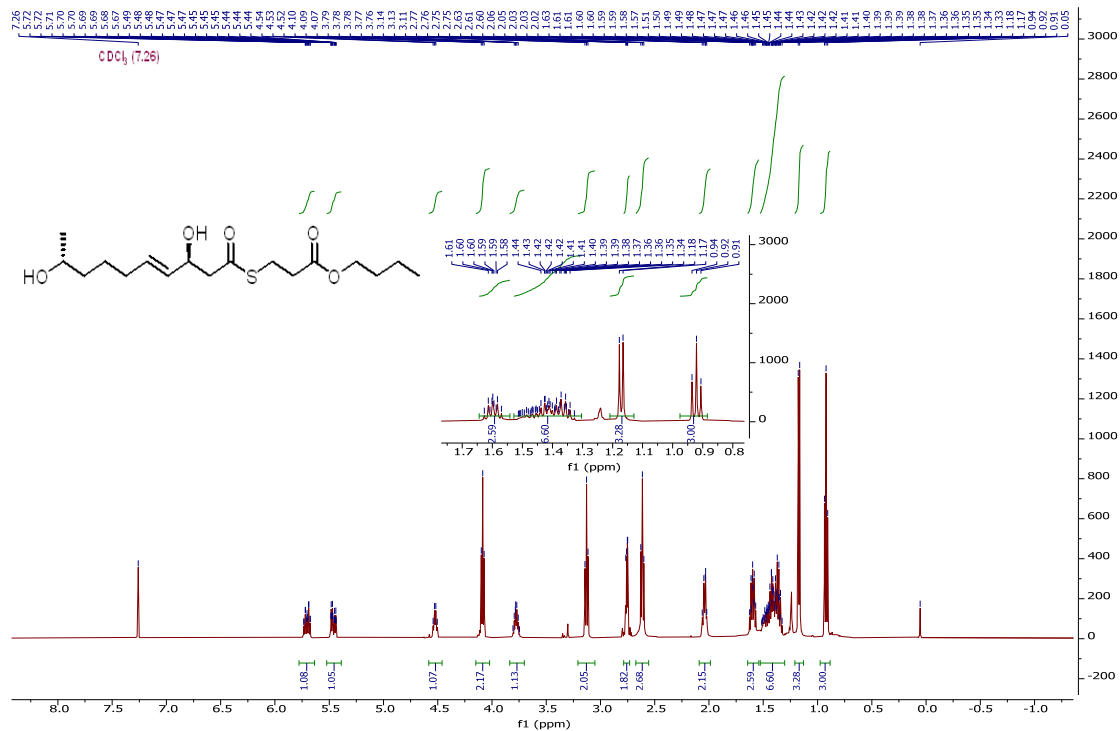


Figure S21. ¹H NMR Spectra of compound 4a. Chloroform-*d*1, 500 MHz for ¹H NMR.

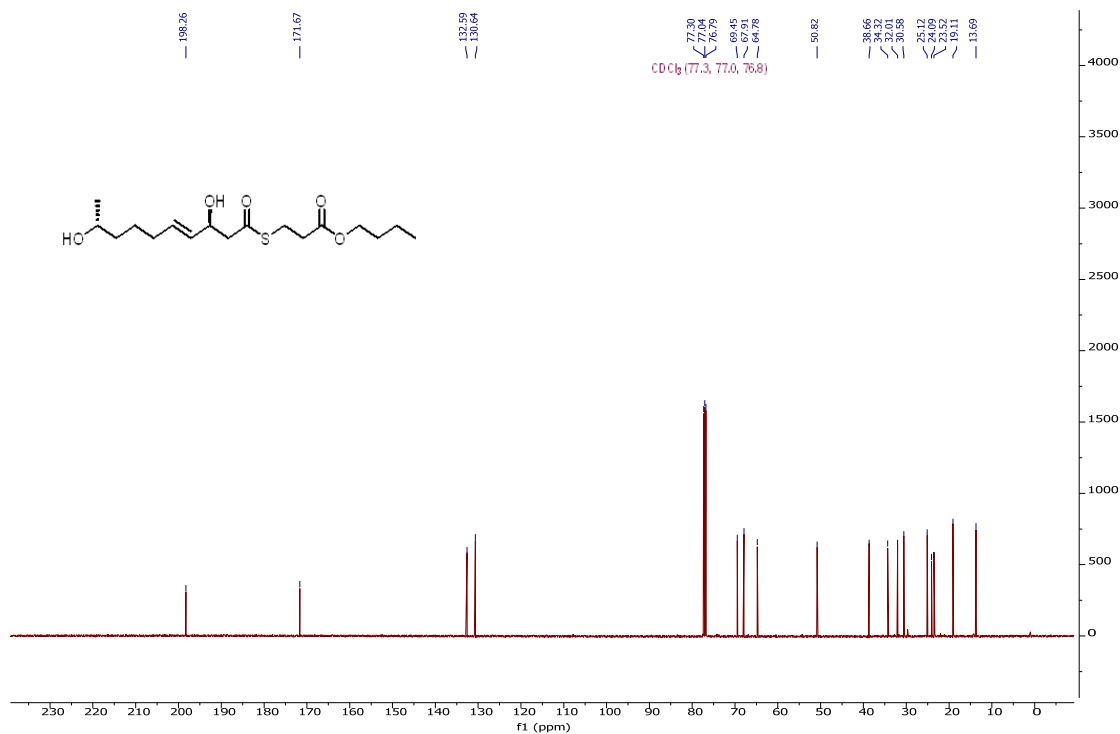


Figure S22. ¹³C NMR Spectra of compound 4a. Chloroform-*d*1, 125 MHz for ¹³C NMR.

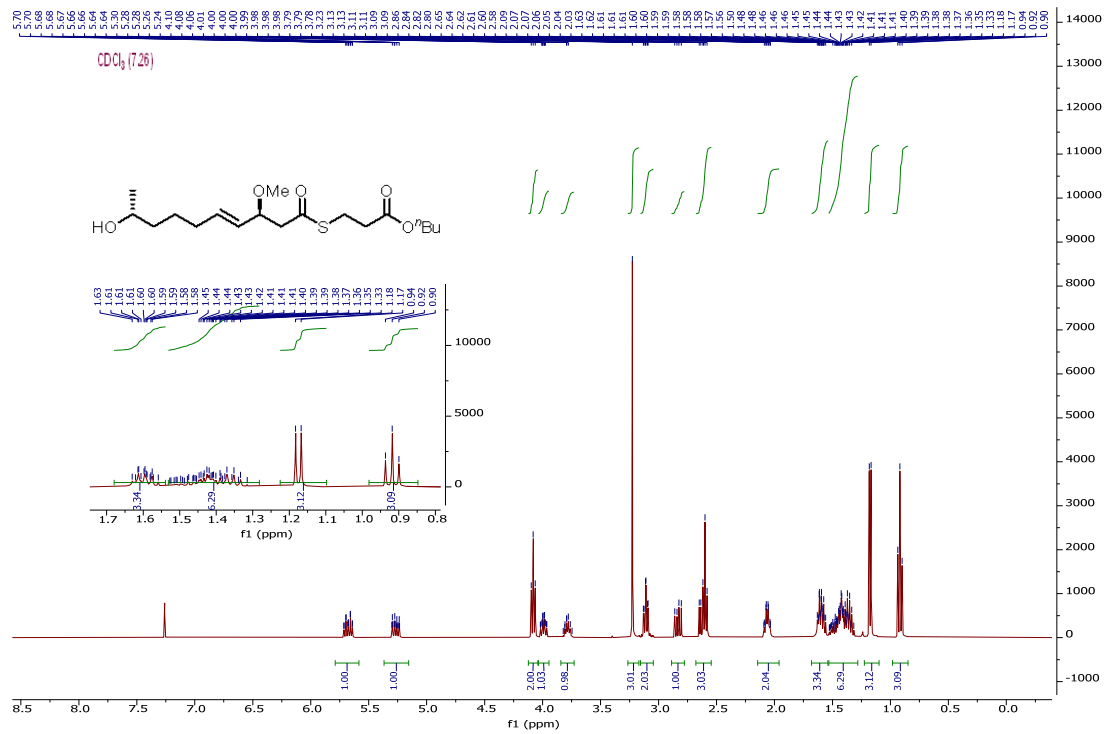


Figure S23. ^1H NMR Spectra of compound 4b. Chloroform-*d*1, 500 MHz for ^1H NMR.

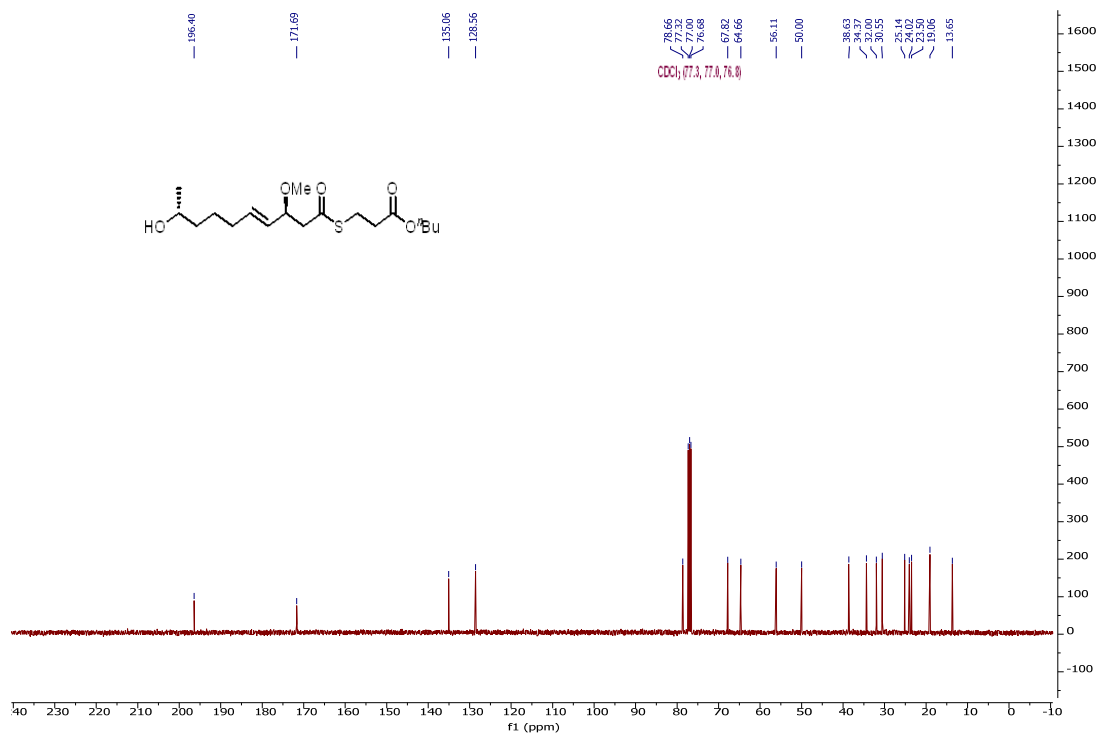
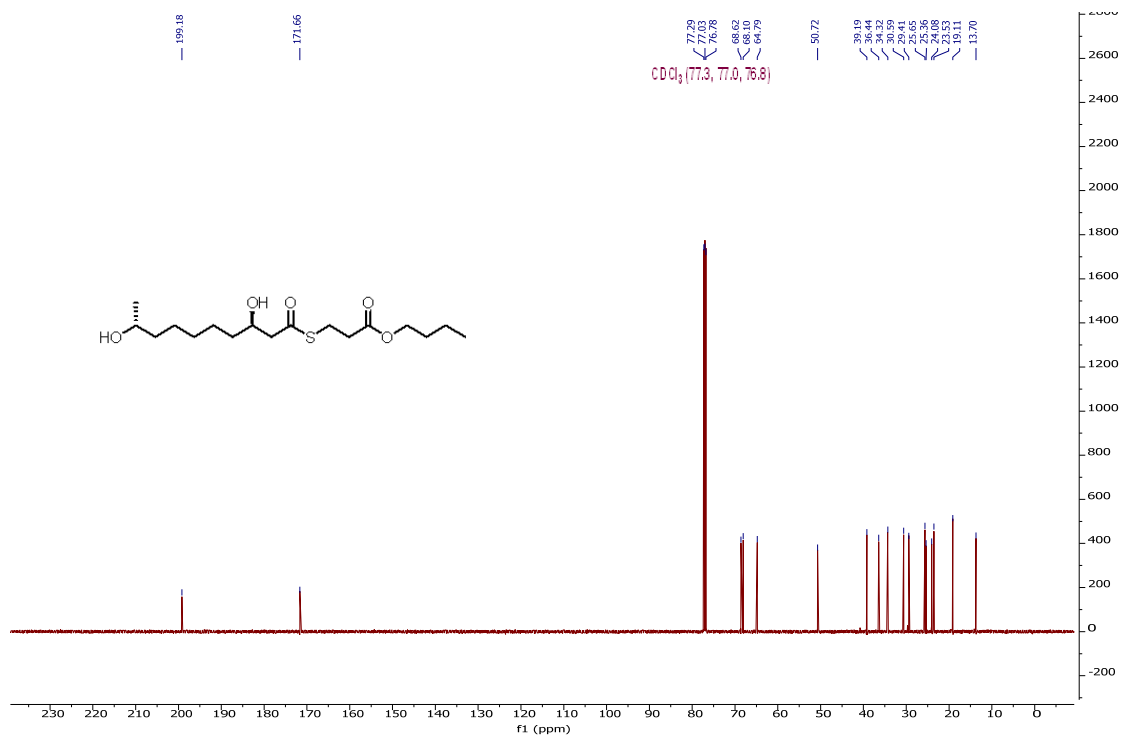
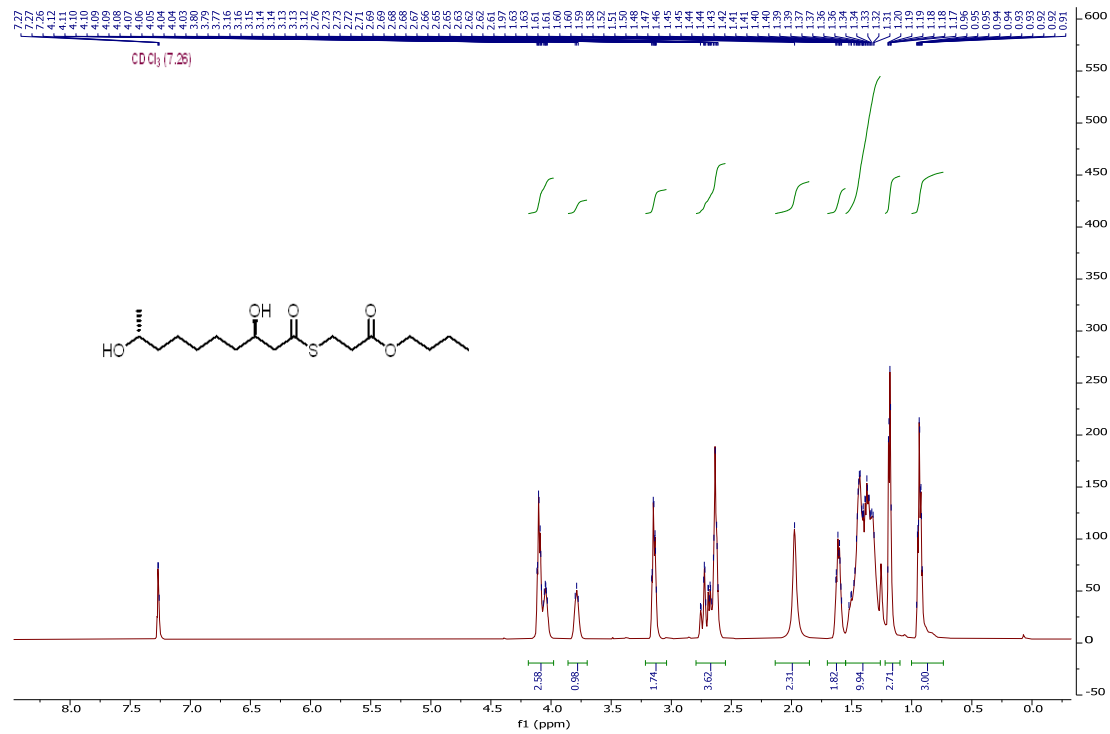


Figure S24. ^{13}C NMR Spectra of compound 4b. Chloroform-*d*1, 125 MHz for ^{13}C NMR.



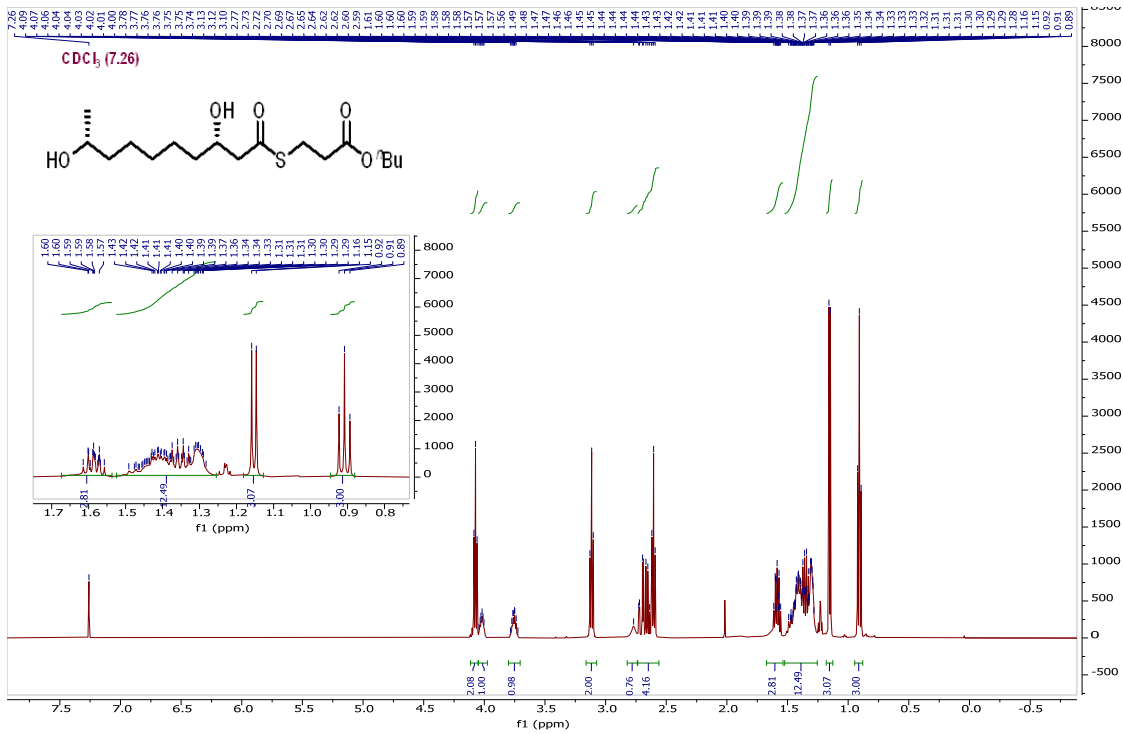


Figure S27. ¹H NMR Spectra of compound 4d. Chloroform-*d*₁, 500 MHz for ¹H NMR.

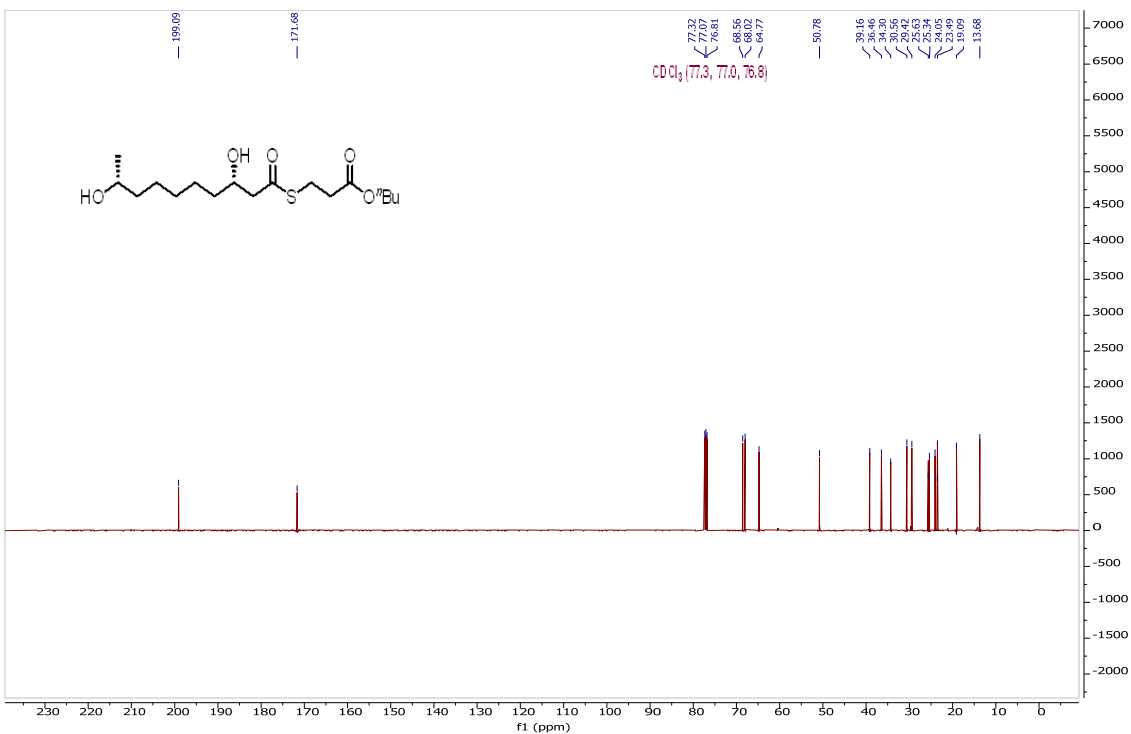


Figure S28. ¹³C NMR Spectra of compound 4d. Chloroform-*d*₁, 125 MHz for ¹³C NMR.

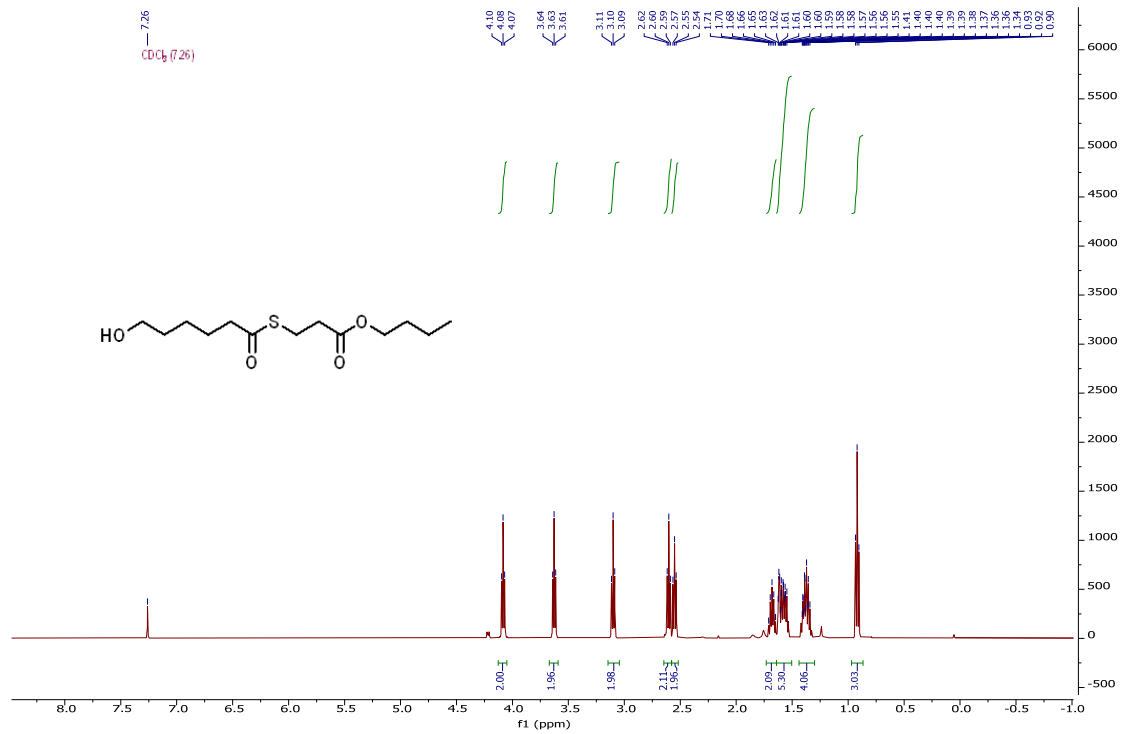


Figure S31. ¹H NMR Spectra of compound 4f. Chloroform-*d*1, 500 MHz for ¹H NMR.

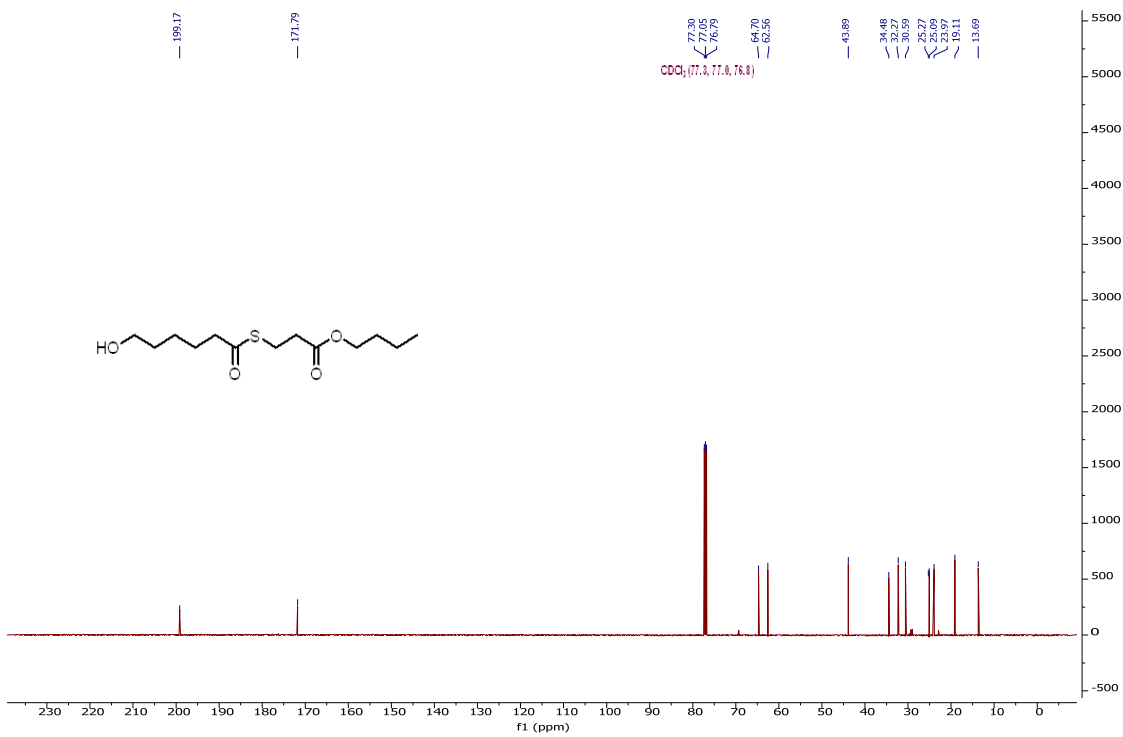


Figure S32. ¹³C NMR Spectra of compound 4f. Chloroform-*d*1, 125 MHz for ¹³C NMR.

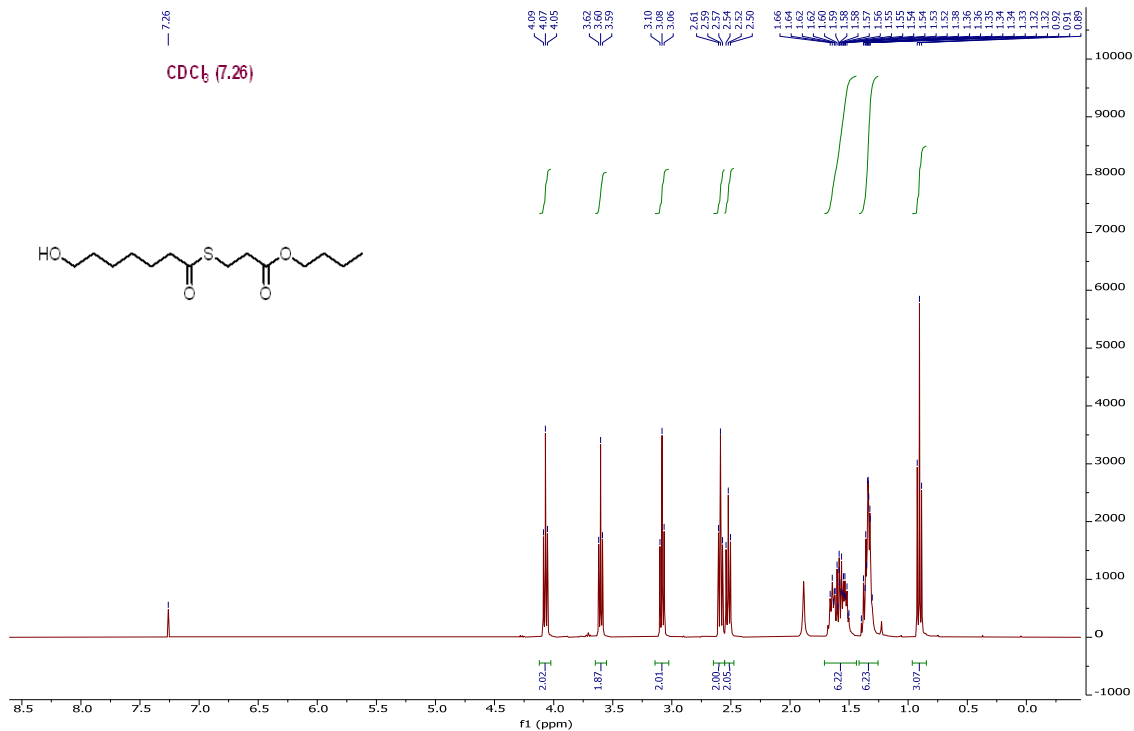


Figure S33. ^1H NMR Spectra of compound **4g**. Chloroform-*d*1, 500 MHz for ^1H NMR.

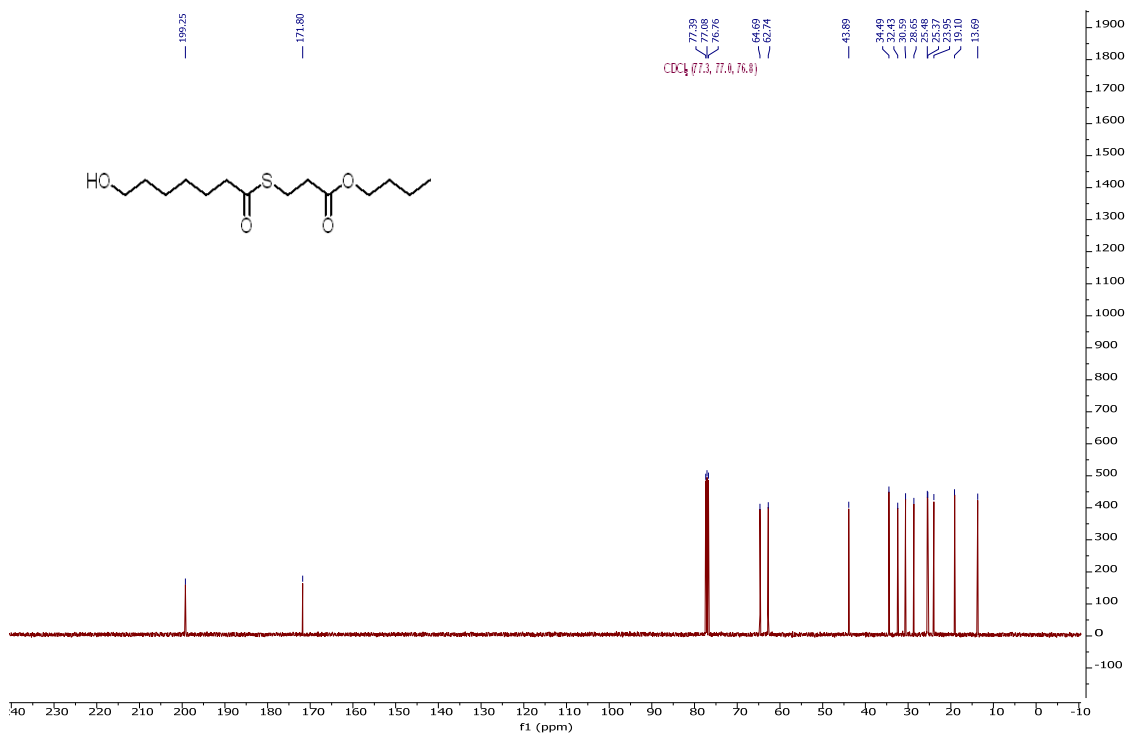


Figure S34. ^{13}C NMR Spectra of compound **4g**. Chloroform-*d*1, 125 MHz for ^{13}C NMR.

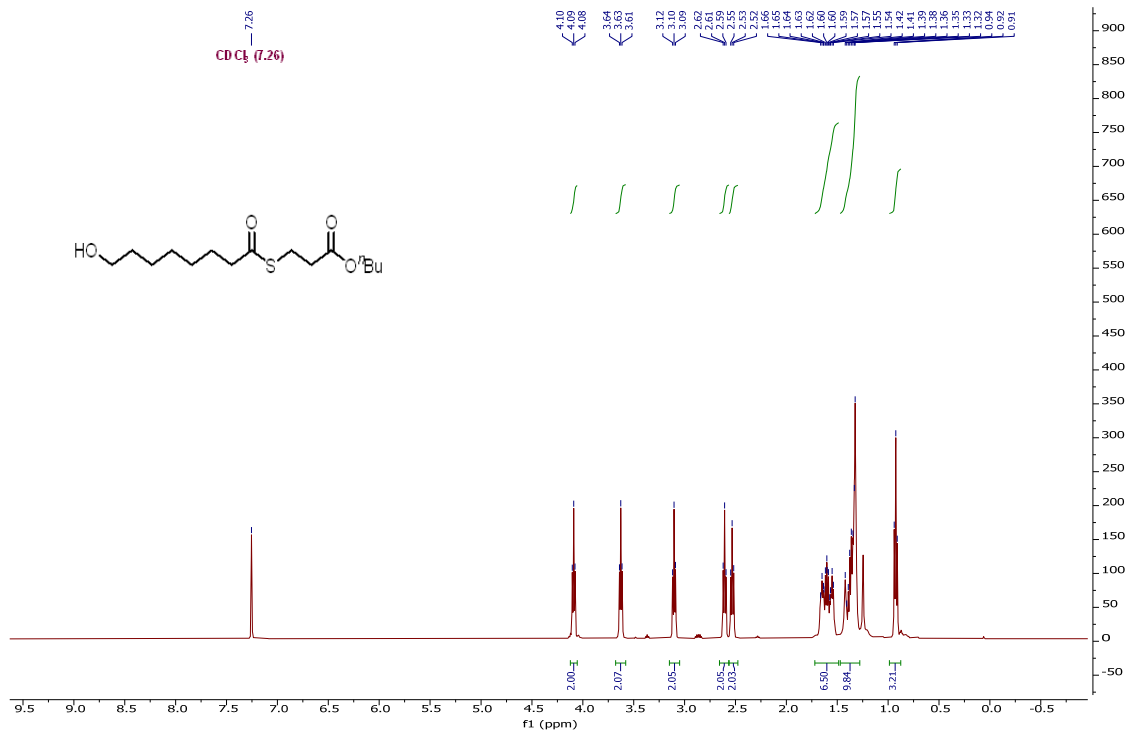


Figure S35. ^1H NMR Spectra of compound 4h. Chloroform-*d*1, 500 MHz for ^1H NMR.

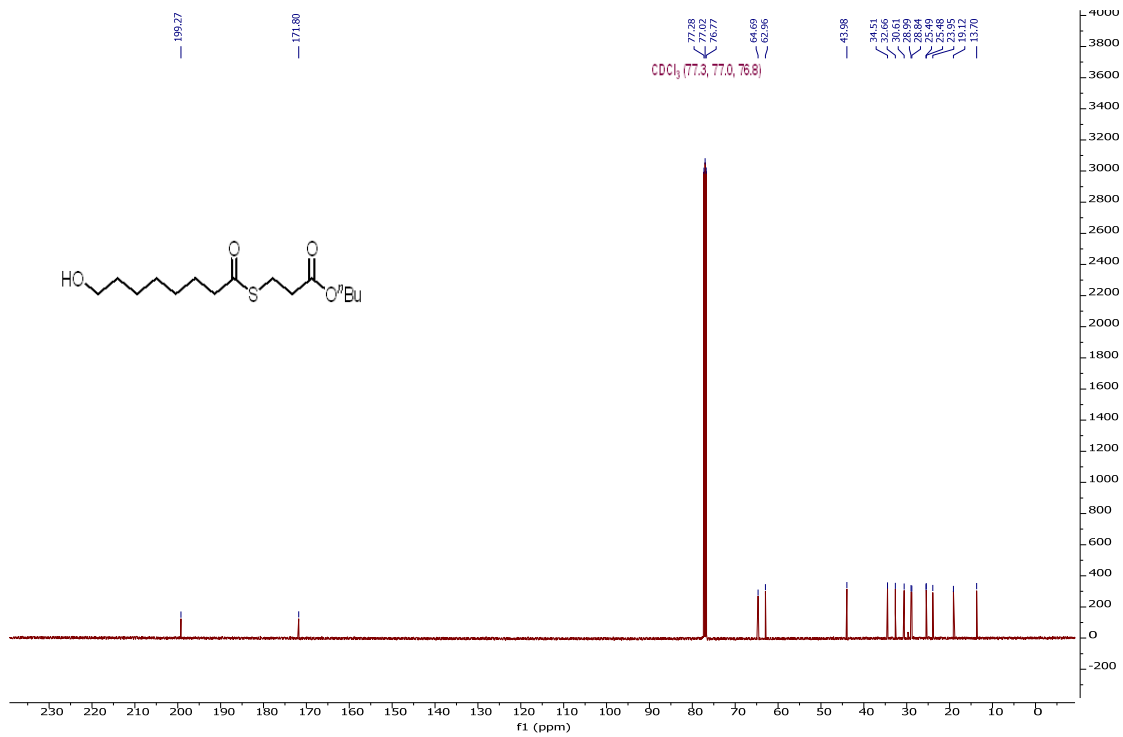


Figure S36. ^{13}C NMR Spectra of compound 4h. Chloroform-*d*1, 125 MHz for ^{13}C NMR.

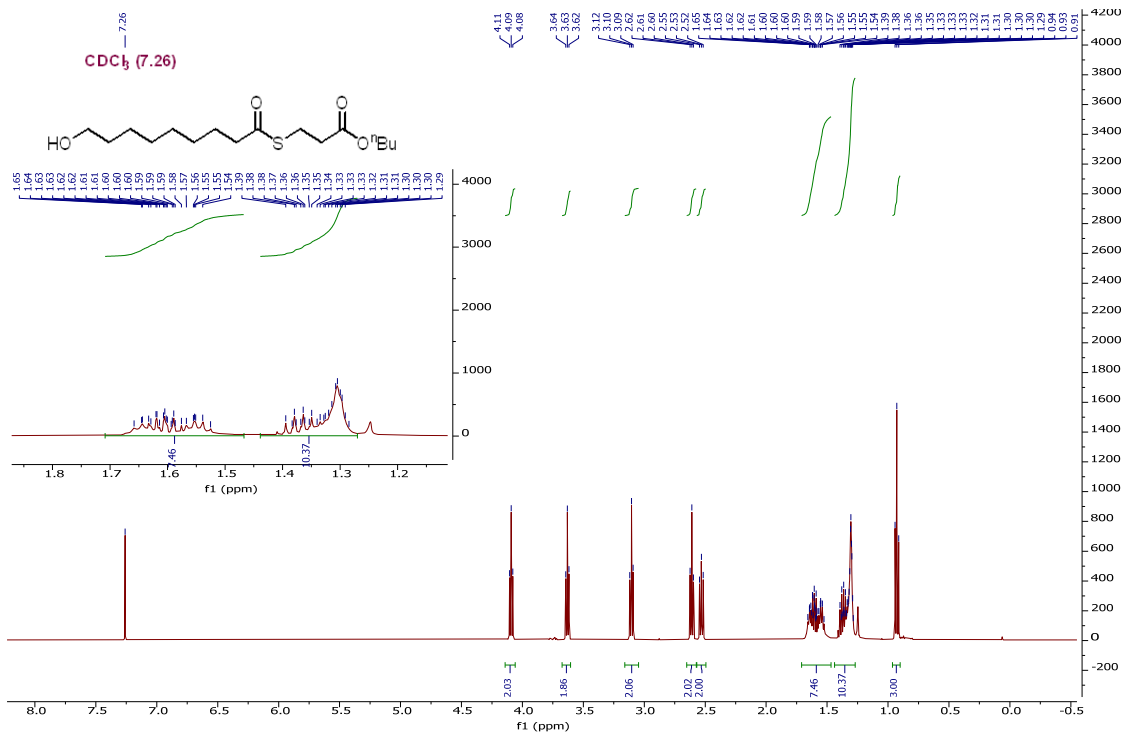


Figure S37. ^1H NMR Spectra of compound **4i**. Chloroform-*d*1, 500 MHz for ^1H NMR.

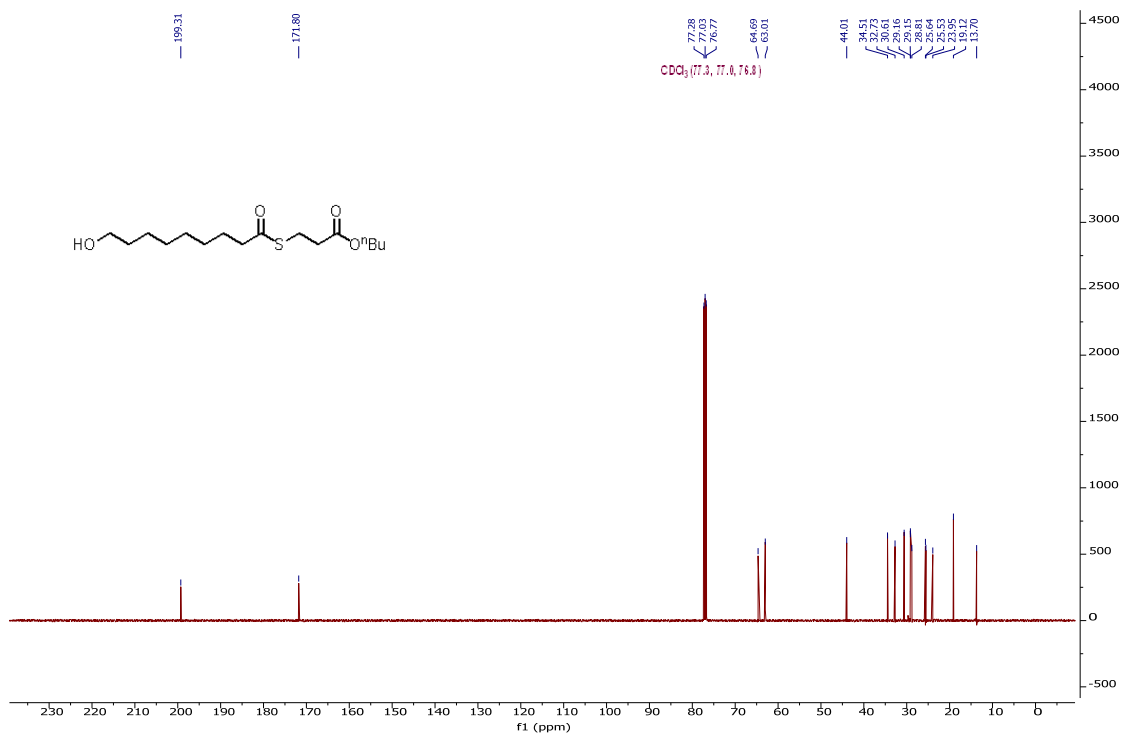


Figure S38. ^{13}C NMR Spectra of compound **4i**. Chloroform-*d*1, 125 MHz for ^{13}C NMR.

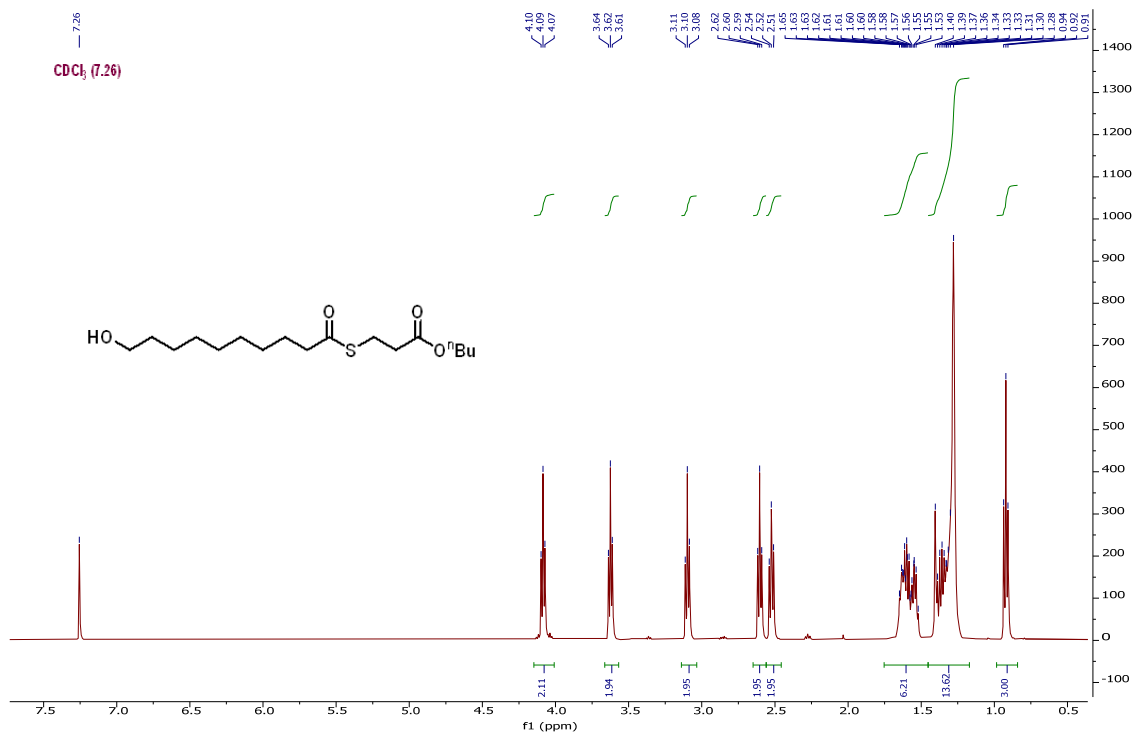


Figure S39. ^1H NMR Spectra of compound 4j. Chloroform-*d*1, 500 MHz for ^1H NMR.

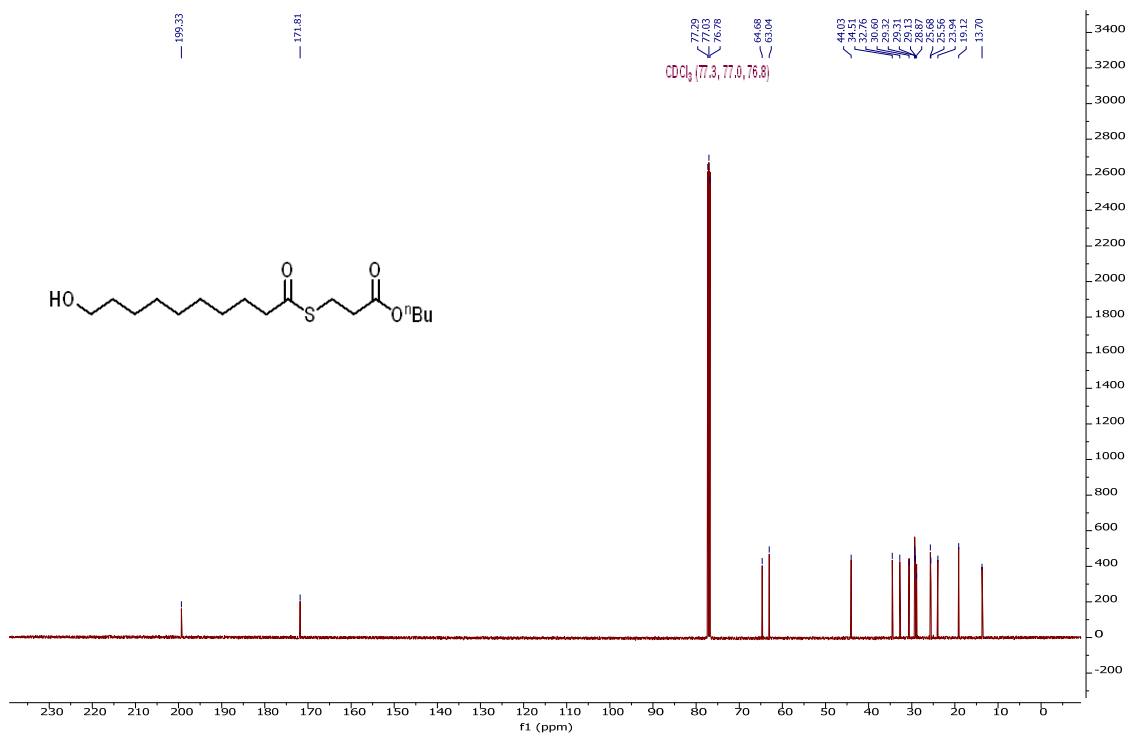


Figure S40. ^{13}C NMR Spectra of compound 4j. Chloroform-*d*1, 125 MHz for ^{13}C NMR.

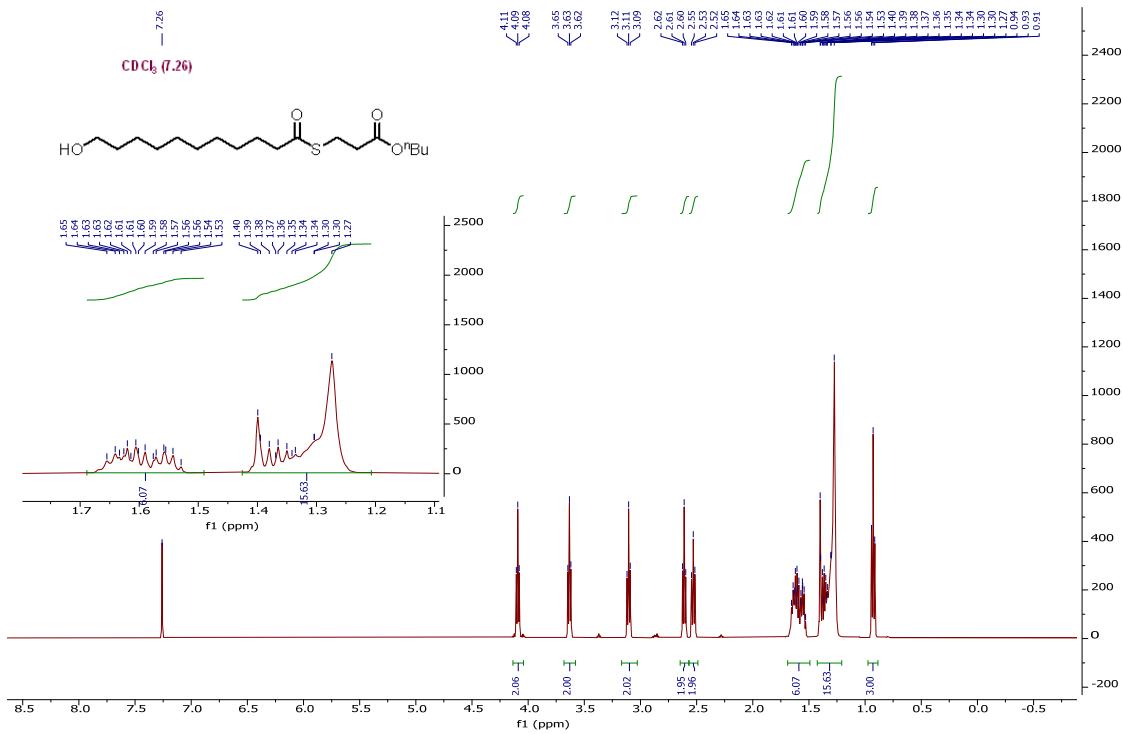


Figure S41. ^1H NMR Spectra of compound **4k**. Chloroform-*d*1, 500 MHz for ^1H NMR.

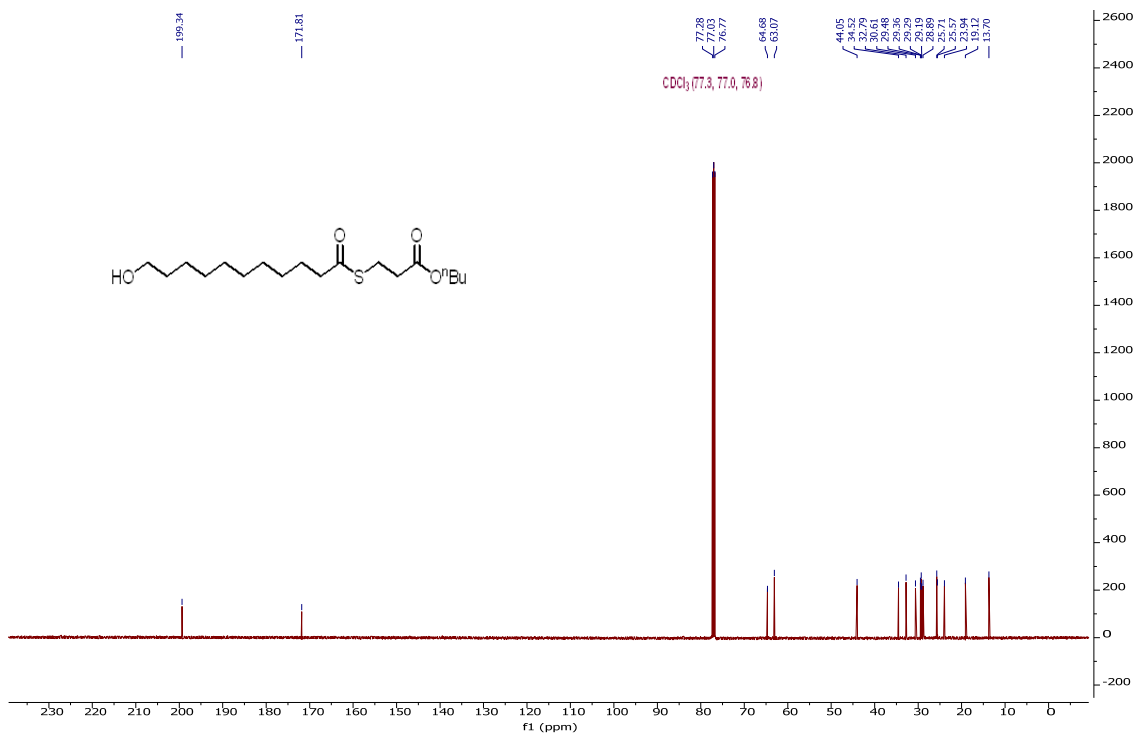


Figure S42. ^{13}C NMR Spectra of compound **4k**. Chloroform-*d*1, 125 MHz for ^{13}C NMR.

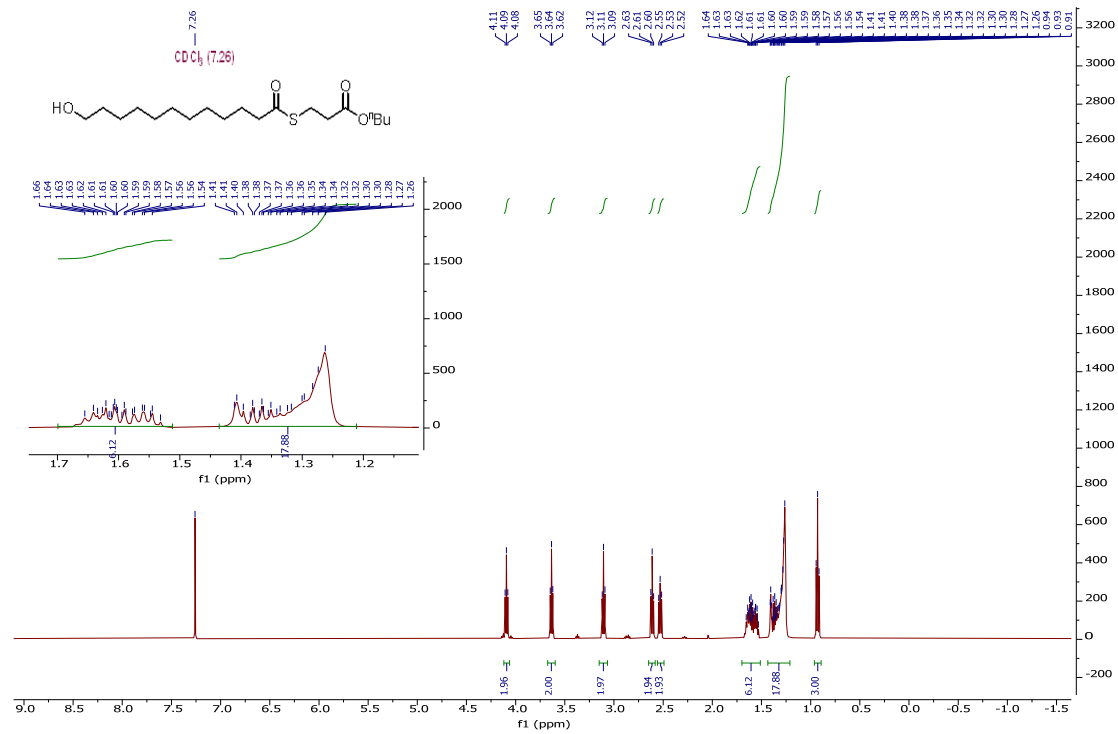


Figure S43. ^1H NMR Spectra of compound **4l**. Chloroform-*d*1, 500 MHz for ^1H NMR.

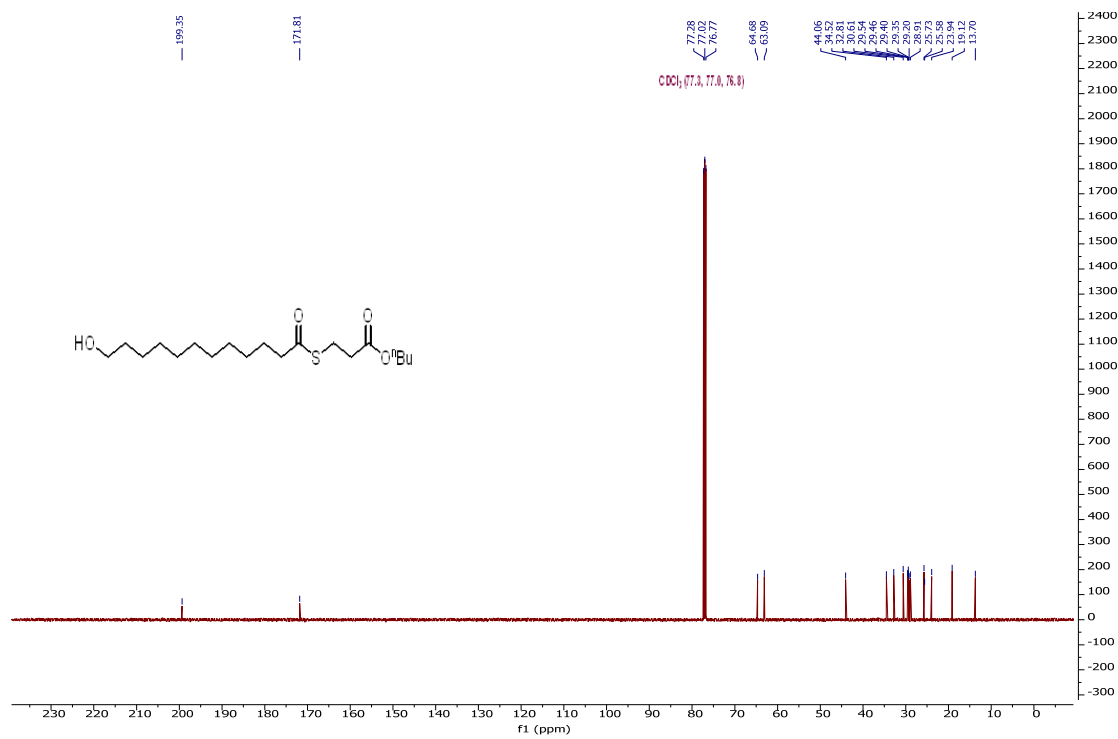


Figure S44. ^{13}C NMR Spectra of compound **4l**. Chloroform-*d*1, 125 MHz for ^{13}C NMR.

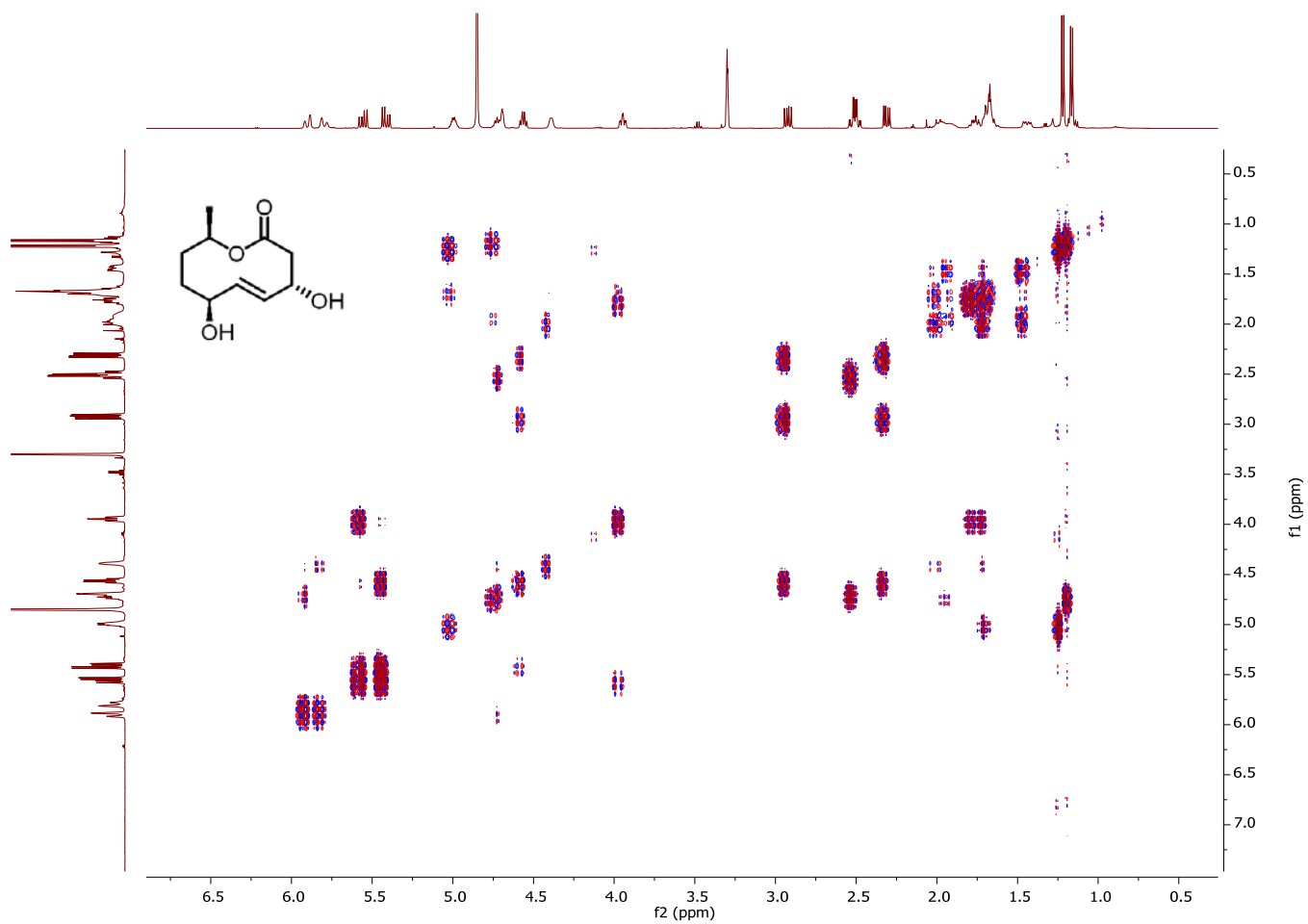


Figure S47. ^1H - ^1H COSY Spectra of compound **1**. Methanol- d_4 , 500 MHz for ^1H NMR

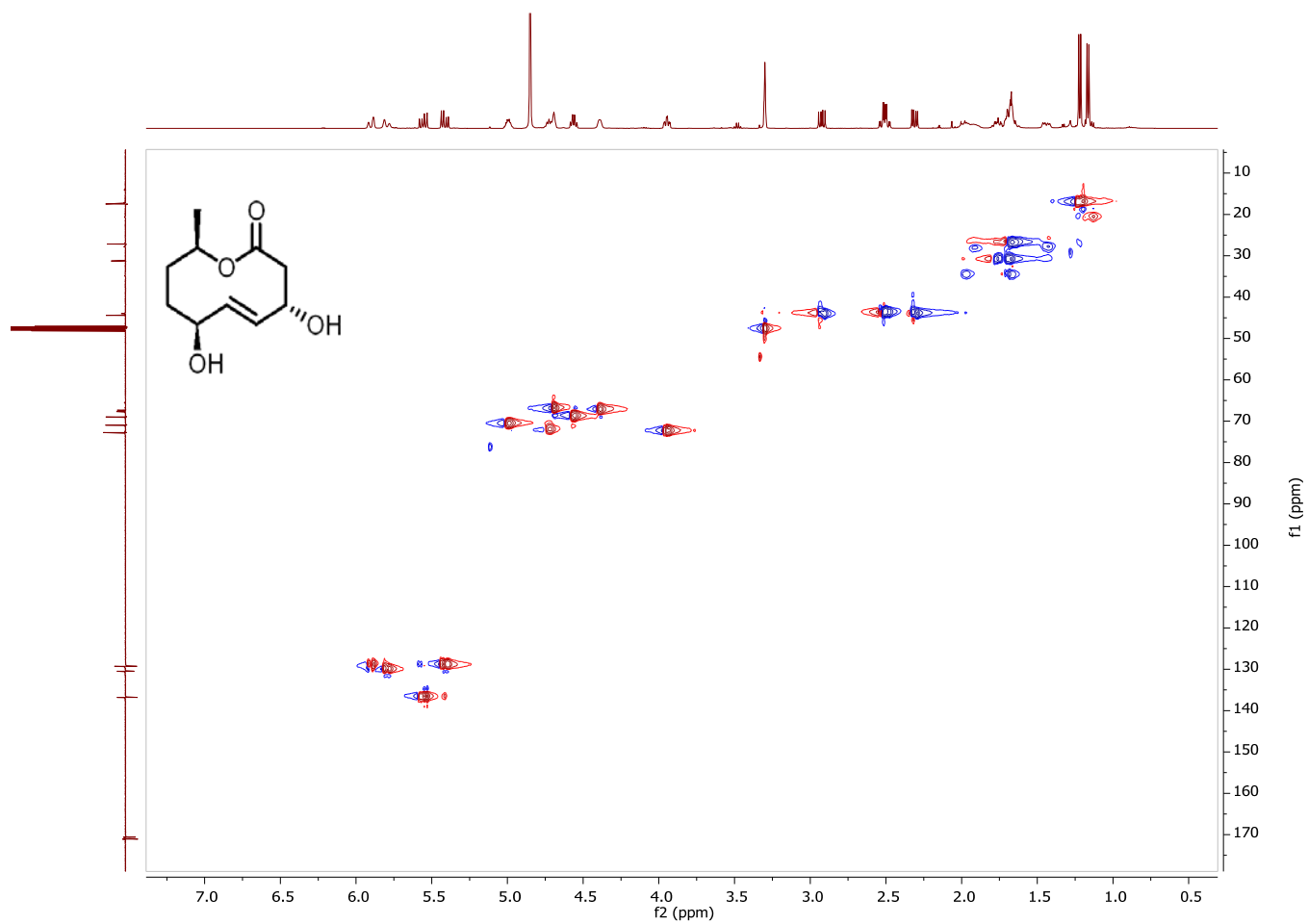


Figure S48. ^1H - ^{13}C HSQC Spectra of compound **1**. Methanol- d_4 , 500 MHz for ^1H NMR and 125 MHz for ^{13}C NMR.

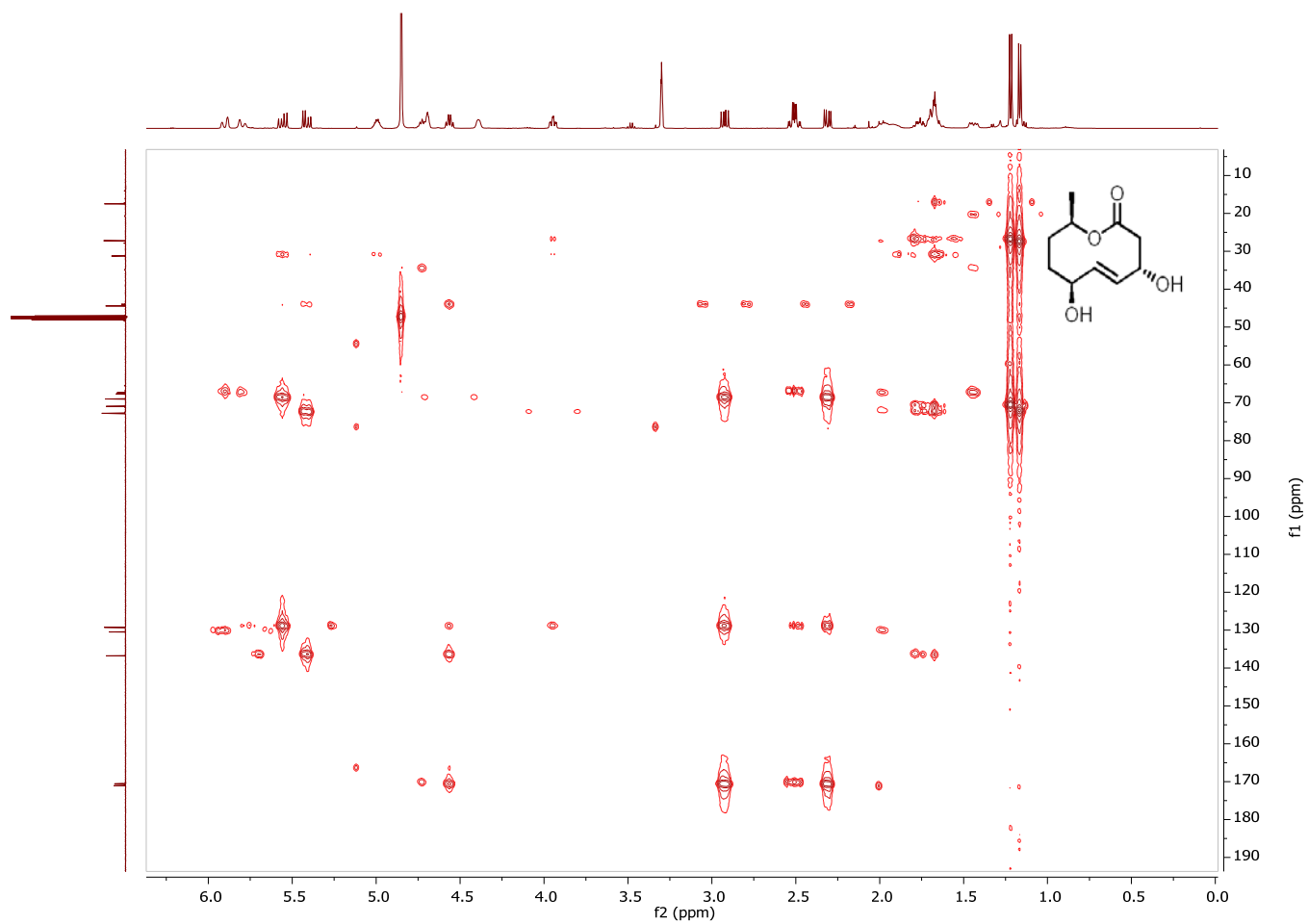


Figure S49. ^1H - ^{13}C HMBC Spectra of compound **1**. Methanol- d_4 , 500 MHz for ^1H NMR and 125 MHz for ^{13}C NMR.

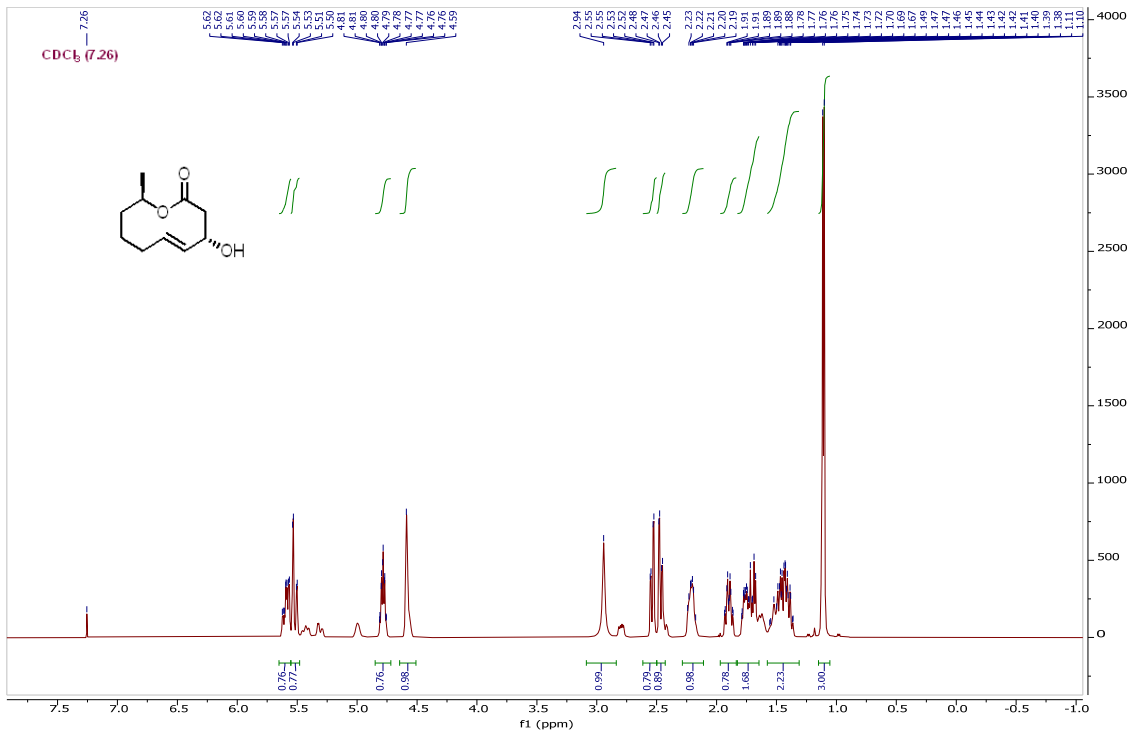


Figure S50. ¹H NMR Spectra of compound **2a**. Chloroform-*d*1, 500 MHz for ¹H NMR.

Note: Compound **2a** contains one pair of conformational isomer.

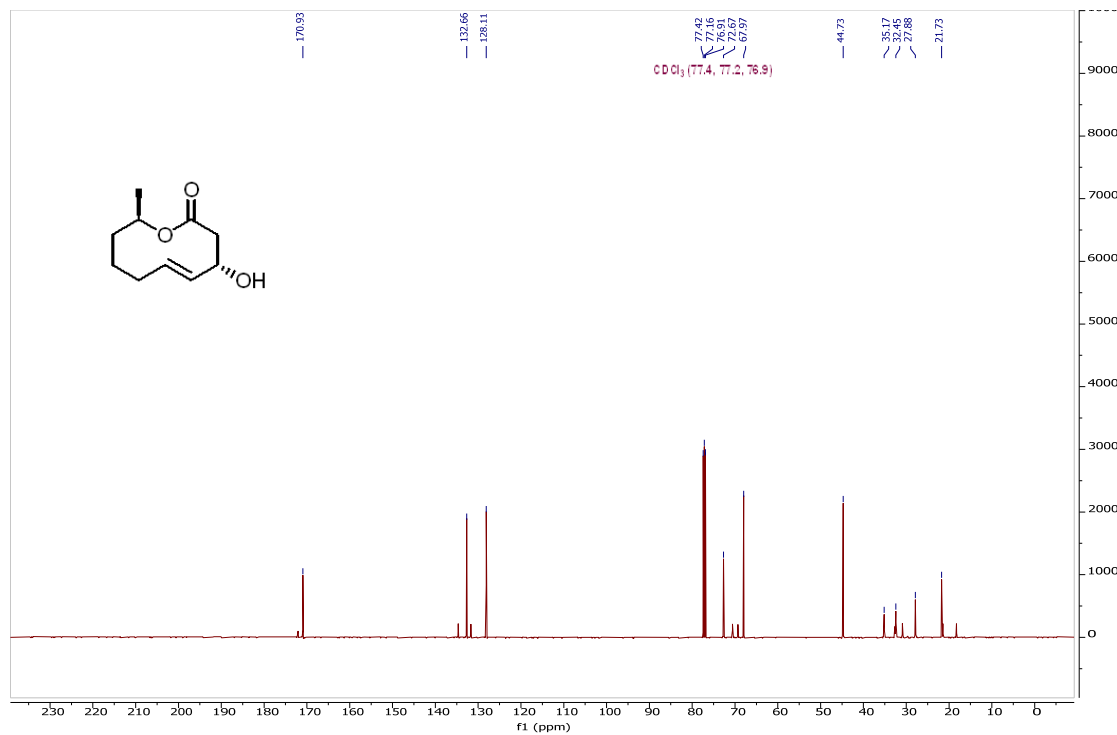


Figure S51. ¹³C NMR Spectra of compound **2a**. Chloroform-*d*1, 125 MHz for ¹³C NMR.

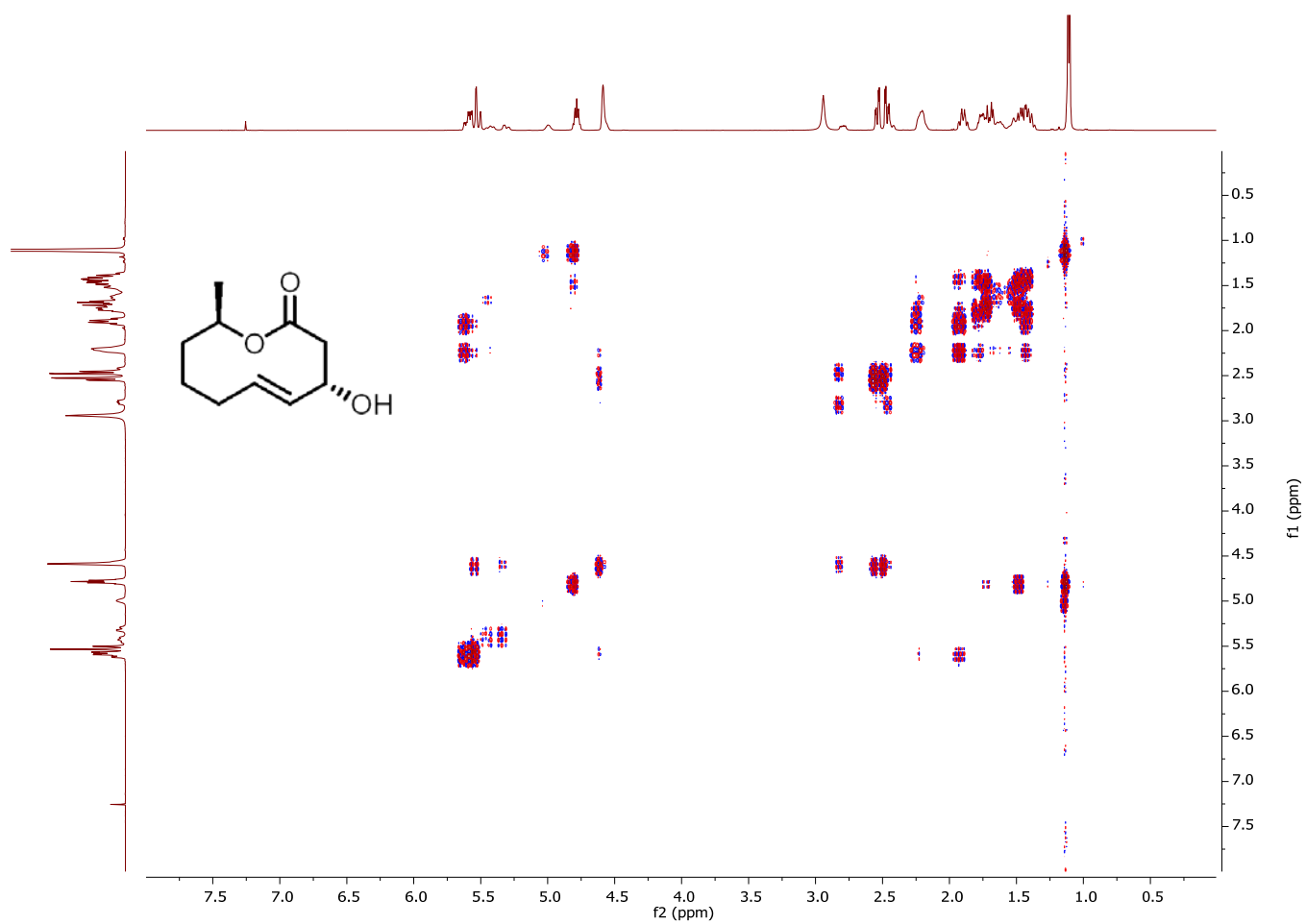


Figure S52. ^1H - ^1H COSY Spectra of compound **2a**, Methanol- d_4 , 500 MHz for ^1H NMR

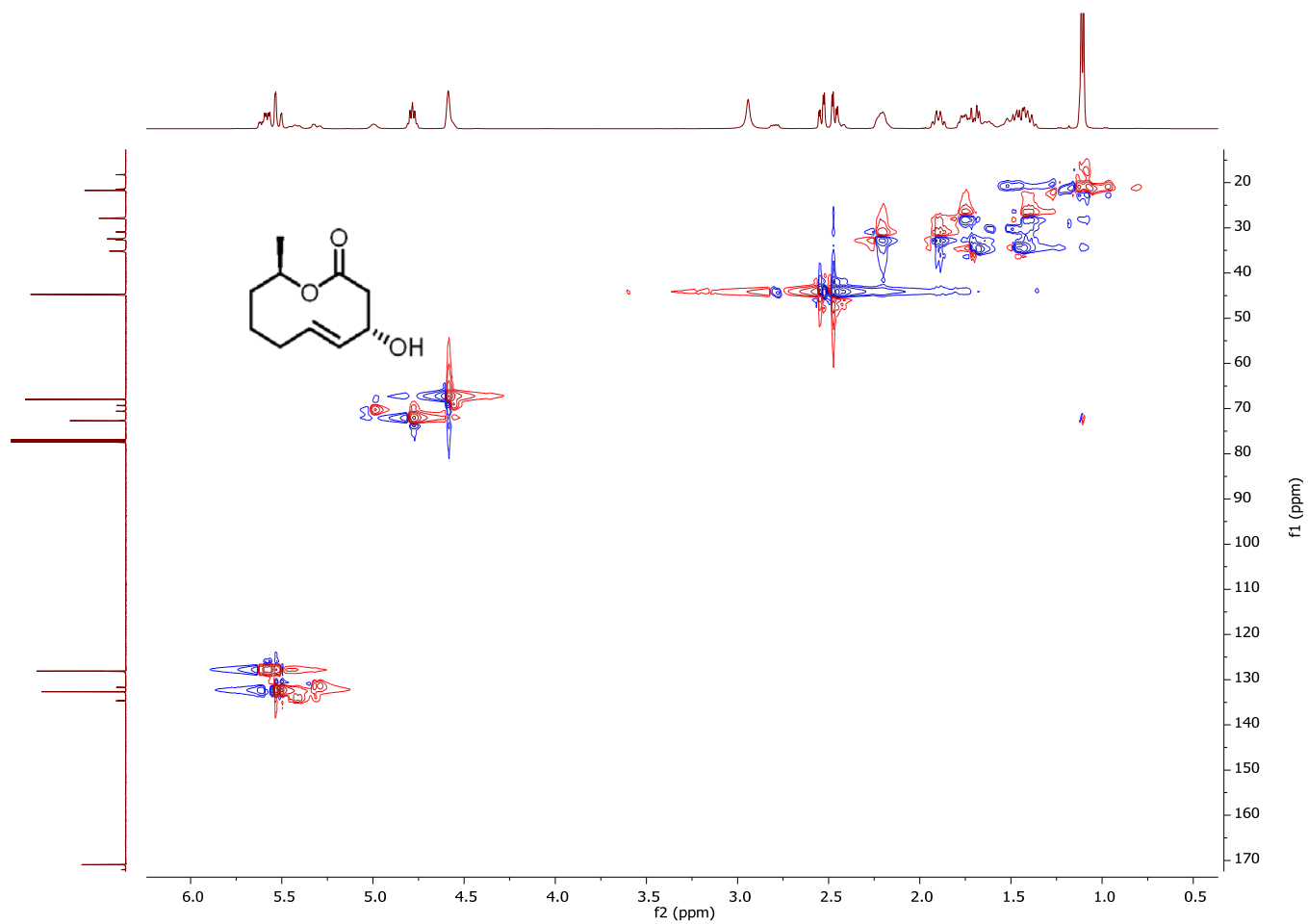


Figure S53. ^1H - ^{13}C HSQC Spectra of compound **2a**, Methanol- d_4 , 500 MHz for ^1H NMR and 125 MHz for ^{13}C NMR.

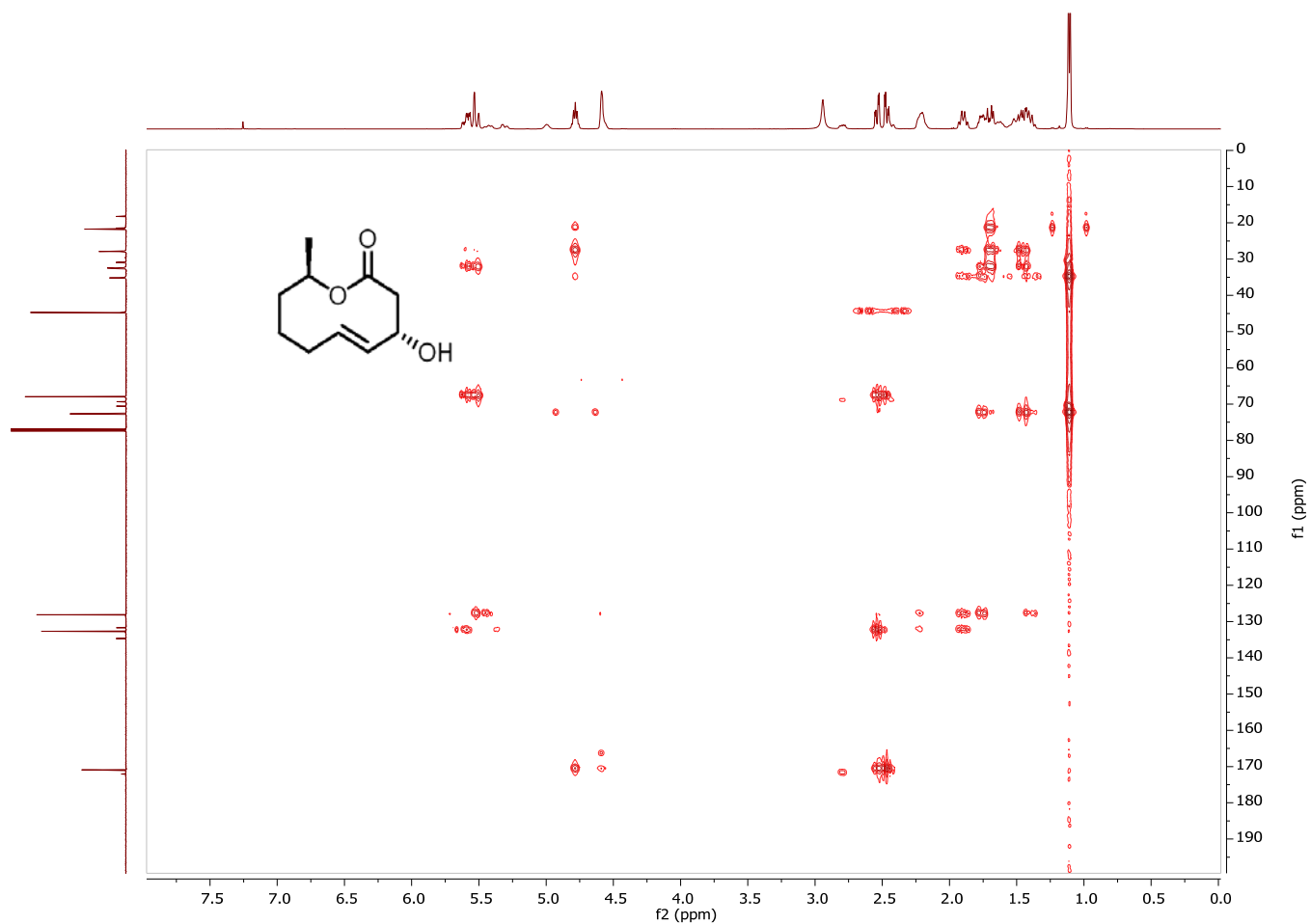


Figure S54. ^1H - ^{13}C HMBC Spectra of compound **2a**, $\text{Me}_2\text{SO}-d_6$, 500 MHz for ^1H NMR and 125 MHz for ^{13}C NMR.

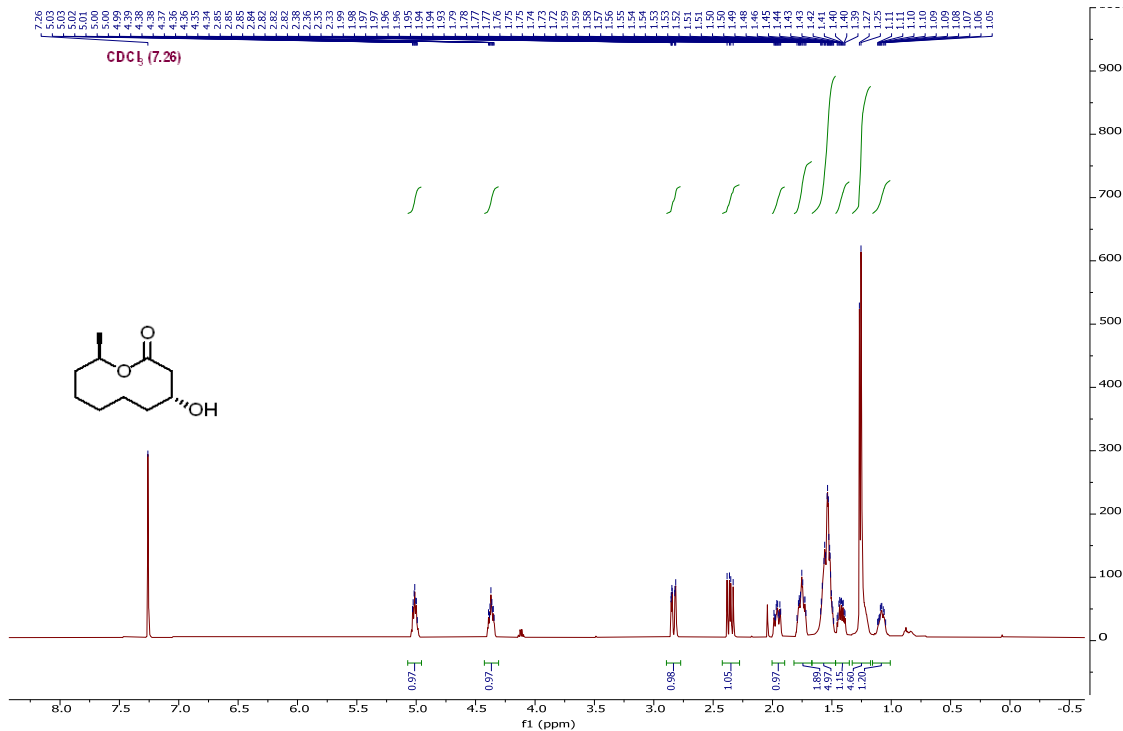


Figure S57. ^1H NMR Spectra of compound 2c. Chloroform-*d*1, 500 MHz for ^1H NMR.

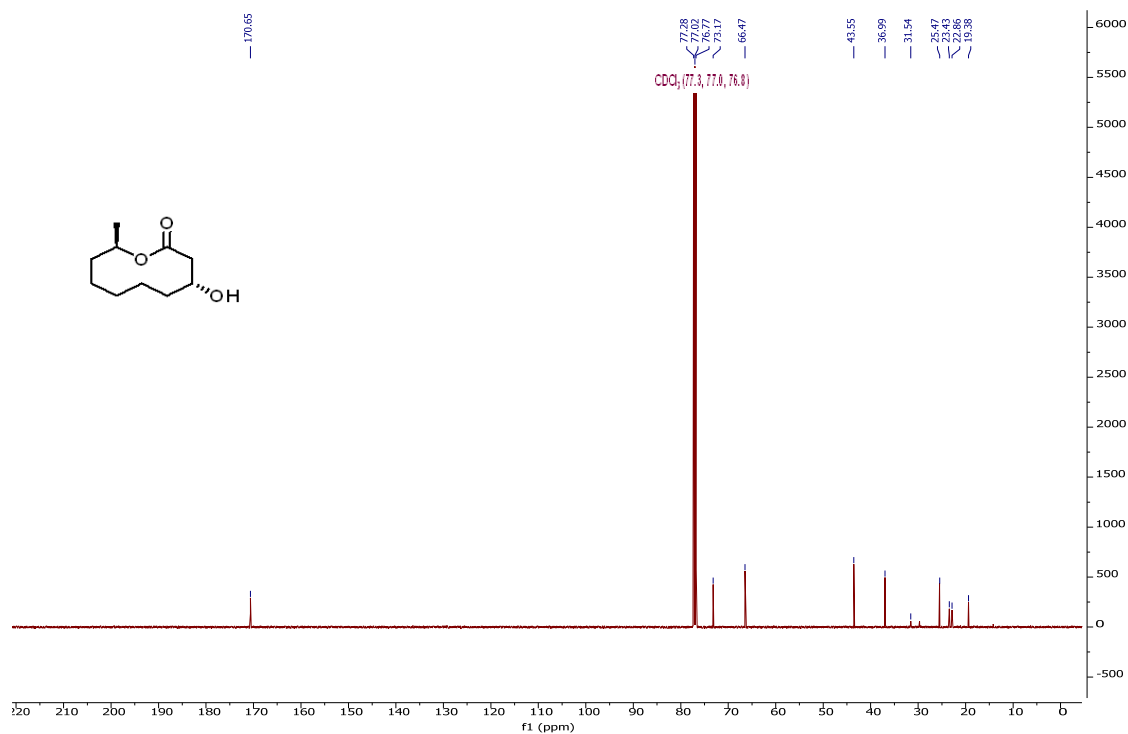


Figure S58. ^{13}C NMR Spectra of compound 2c. Chloroform-*d*1, 125 MHz for ^{13}C NMR.

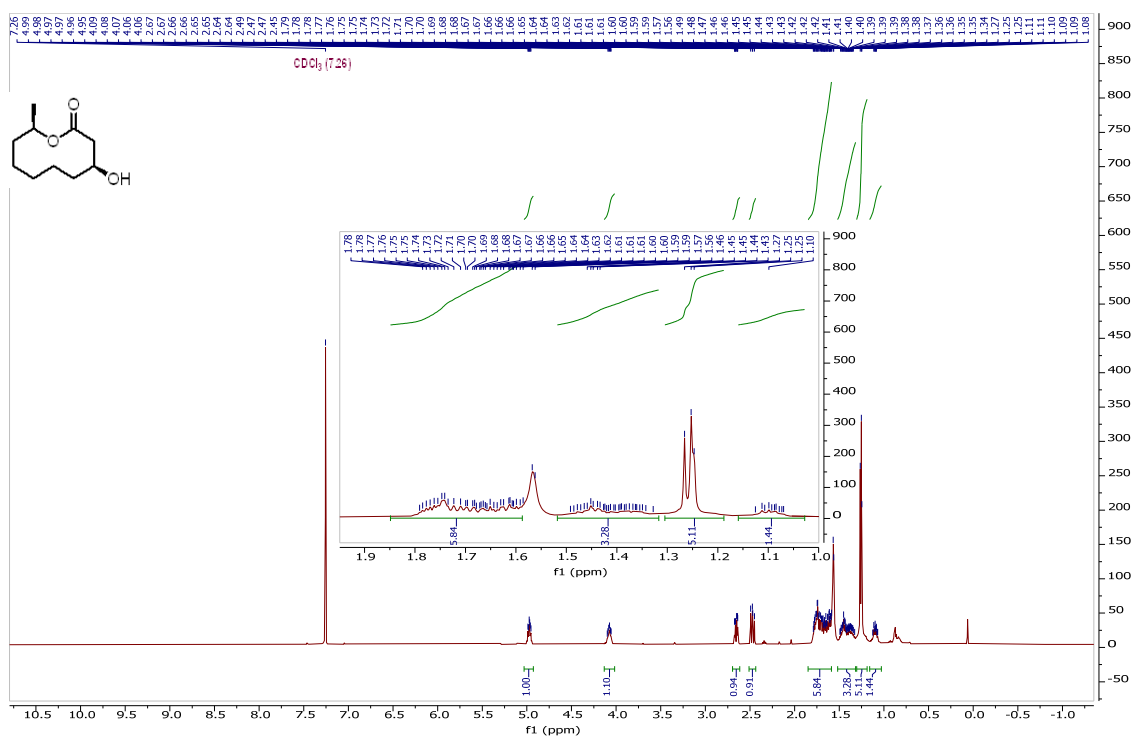


Figure S59. ¹H NMR Spectra of compound 2d. Chloroform-*d*1, 500 MHz for ¹H NMR.

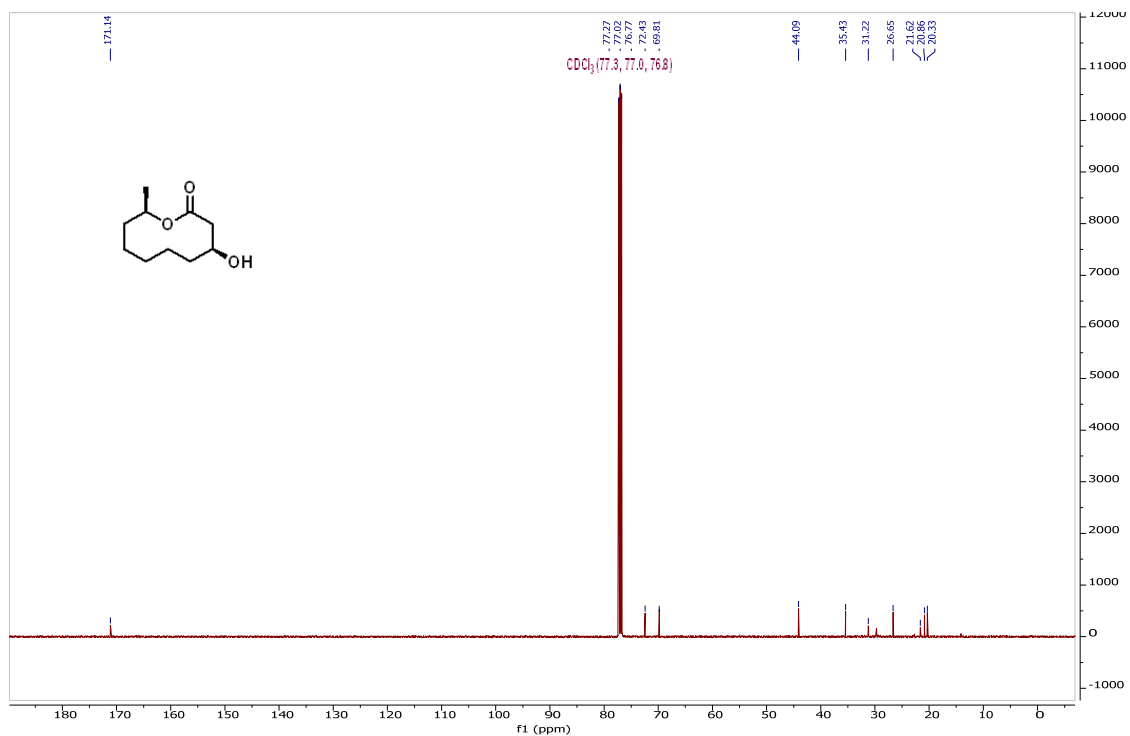


Figure S60. ¹³C NMR Spectra of compound 2d. Chloroform-*d*1, 125 MHz for ¹³C NMR.

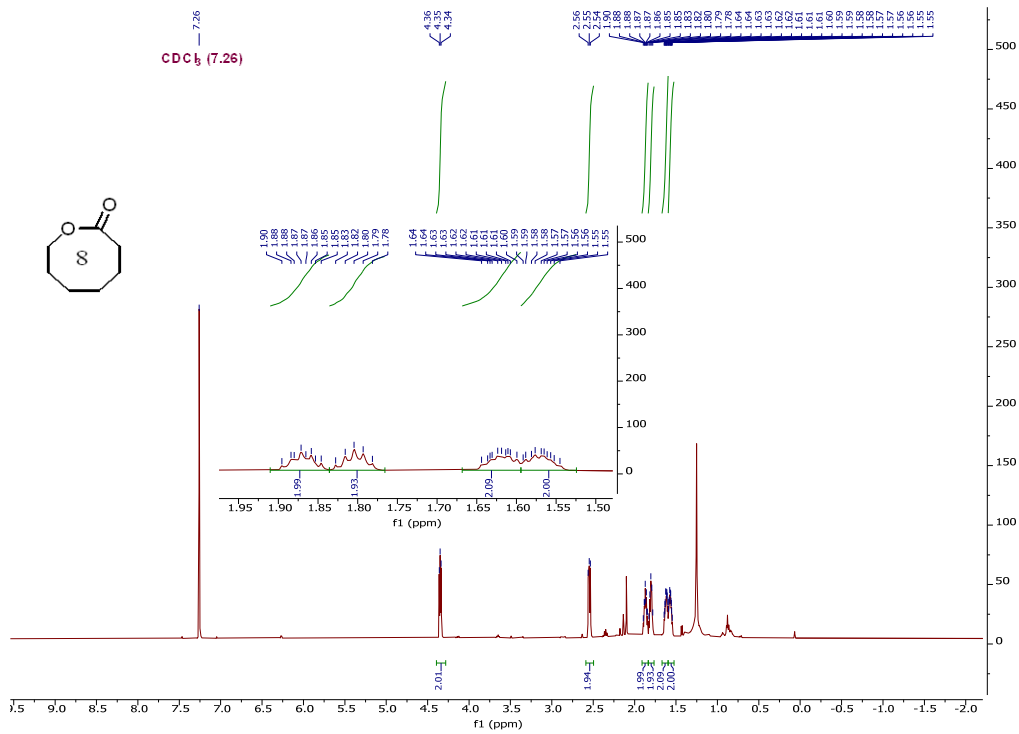


Figure S61. ¹H NMR Spectra of compound 2g. Chloroform-*d*1, 500 MHz for ¹H NMR.

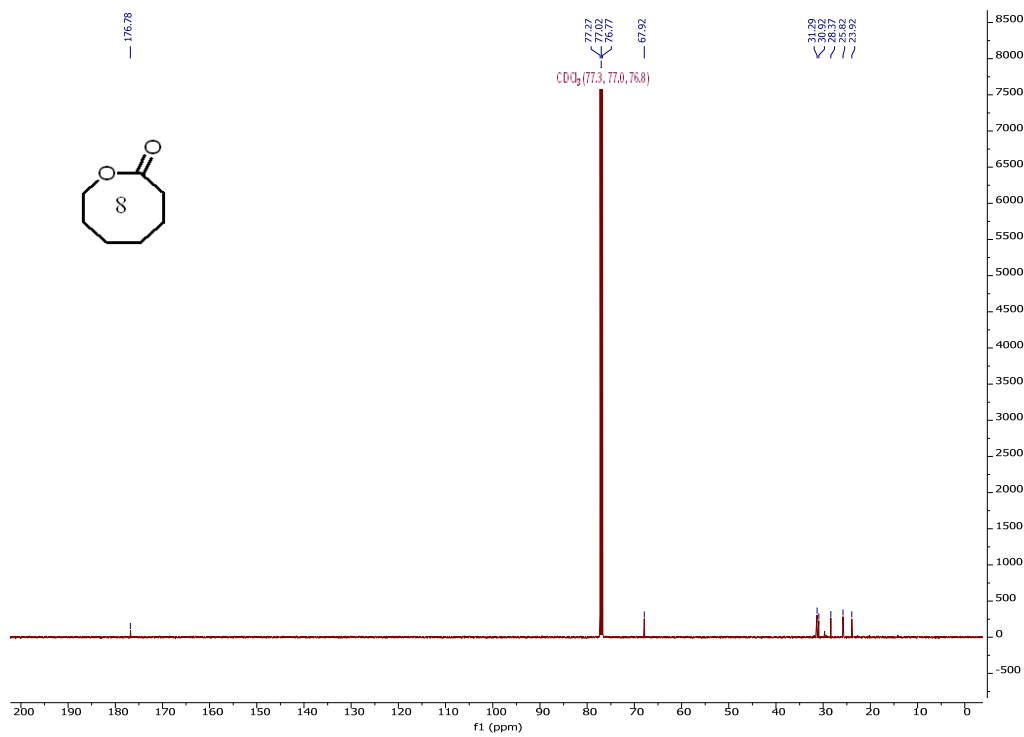


Figure S62. ¹³C NMR Spectra of compound 2g. Chloroform-*d*1, 125 MHz for ¹³C NMR.

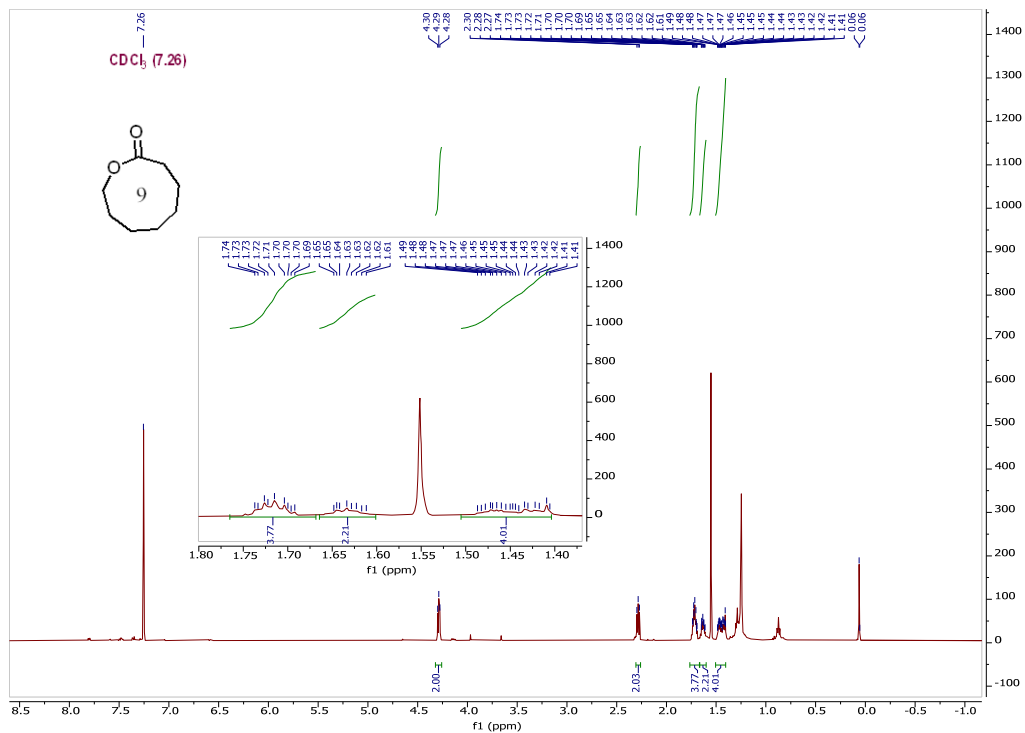


Figure S63. ¹H NMR Spectra of compound 2h. Chloroform-*d*1, 500 MHz for ¹H NMR.

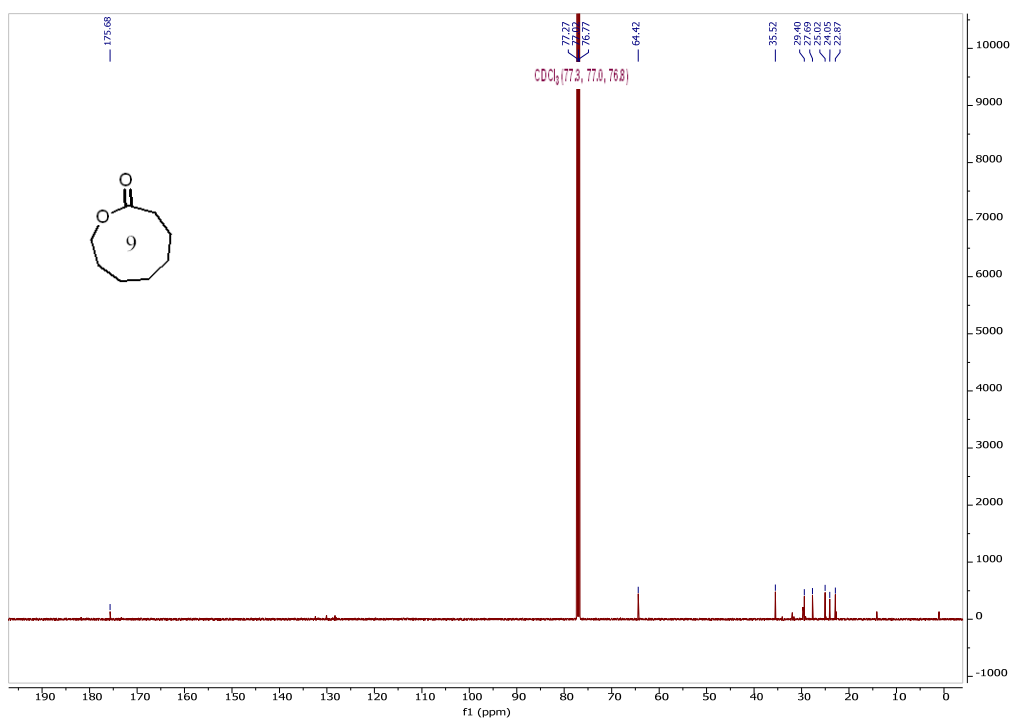


Figure S64. ¹³C NMR Spectra of compound 2h. Chloroform-*d*1, 125 MHz for ¹³C NMR.

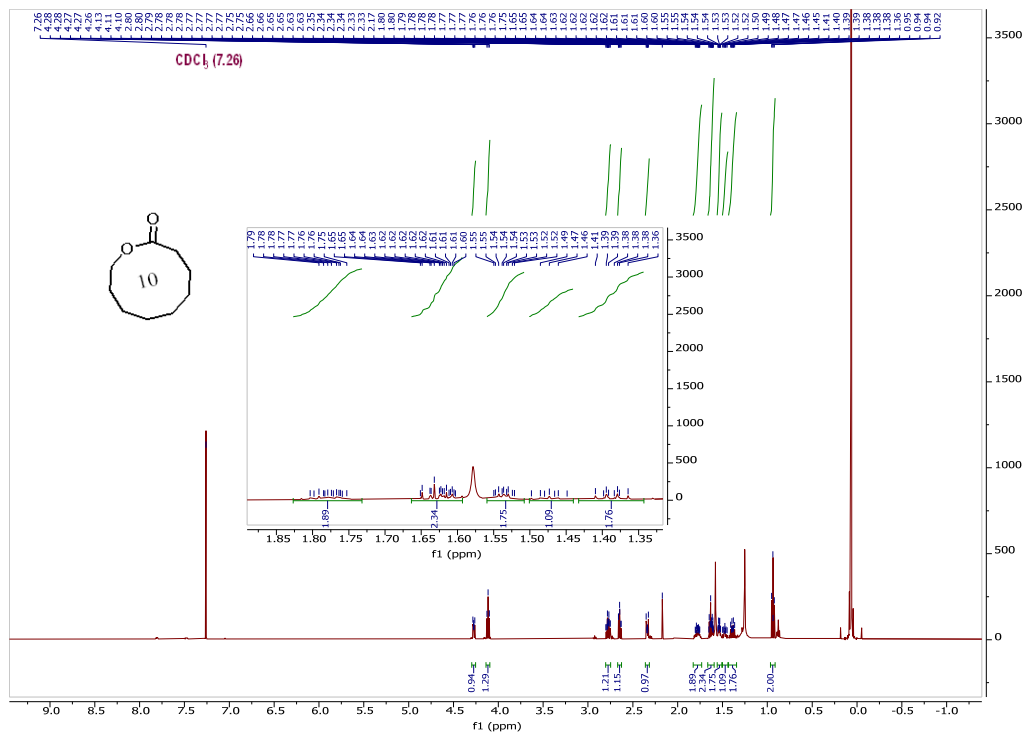


Figure S65. ^1H NMR Spectra of compound 2i. Chloroform-*d*1, 500 MHz for ^1H NMR.

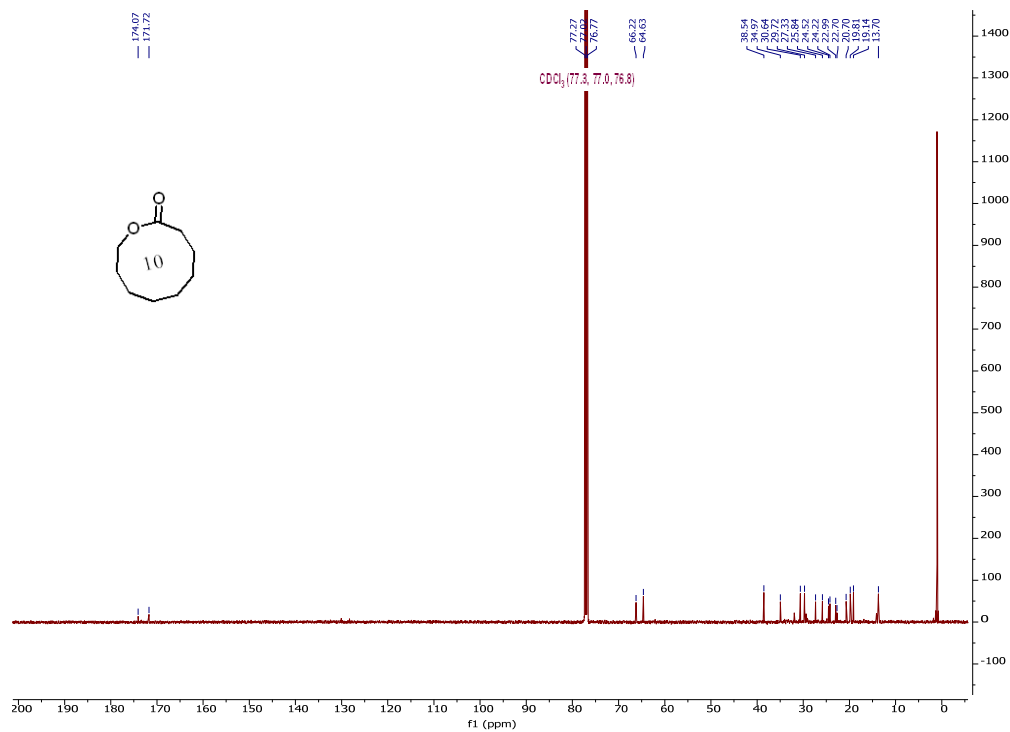


Figure S66. ^{13}C NMR Spectra of compound 2i. Chloroform-*d*1, 125 MHz for ^{13}C NMR.

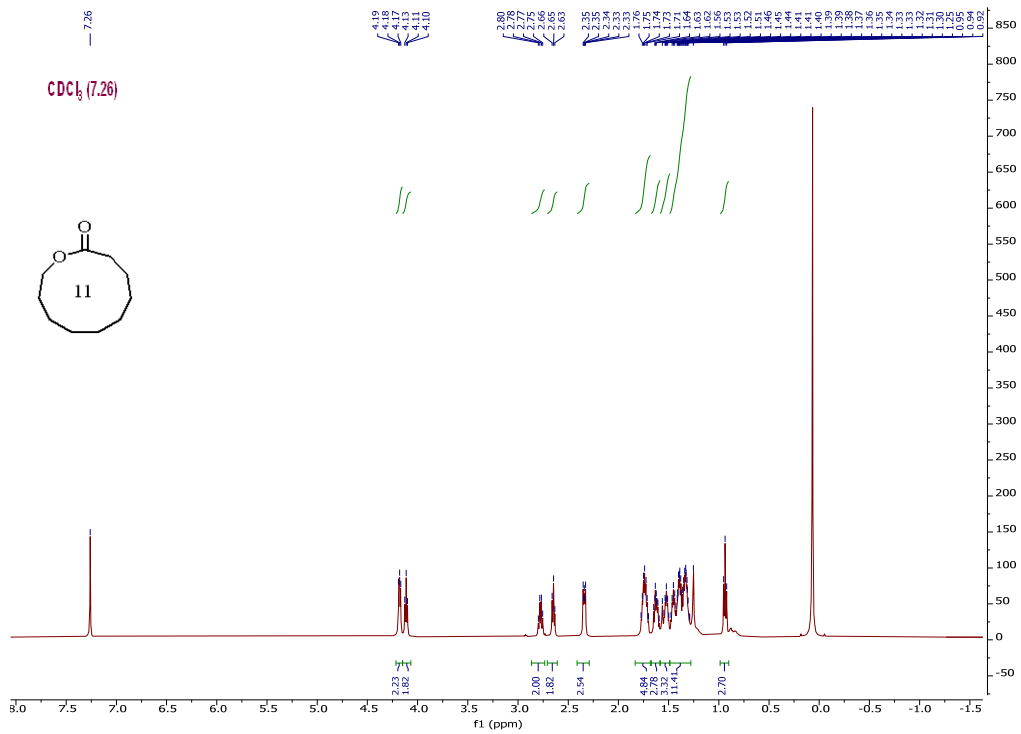


Figure S67. ^1H NMR Spectra of compound 2j. Chloroform-*d*1, 500 MHz for ^1H NMR.

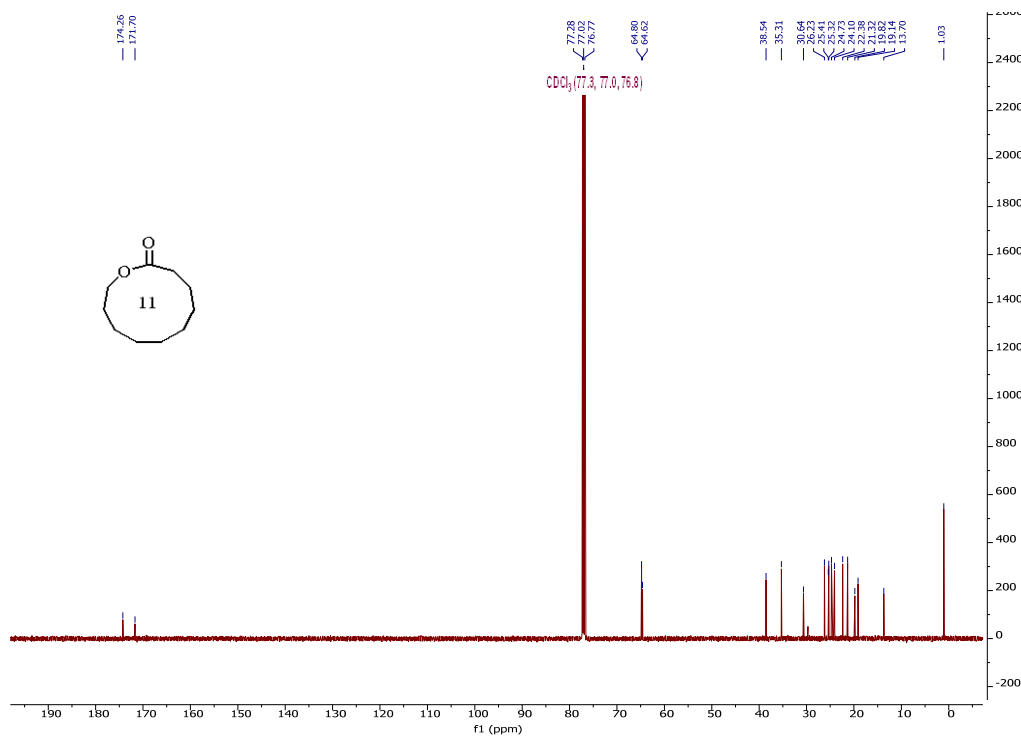


Figure S68. ^{13}C NMR Spectra of compound 2j. Chloroform-*d*1, 125 MHz for ^{13}C NMR.

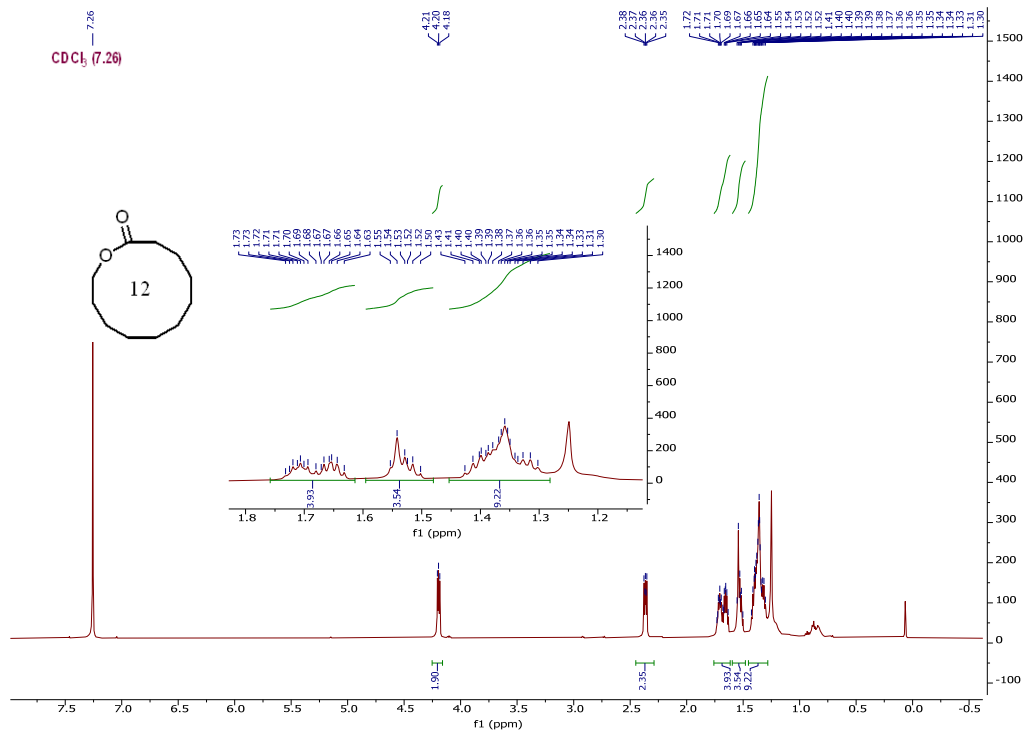


Figure S69. ^1H NMR Spectra of compound 2k. Chloroform-*d*1, 500 MHz for ^1H NMR.

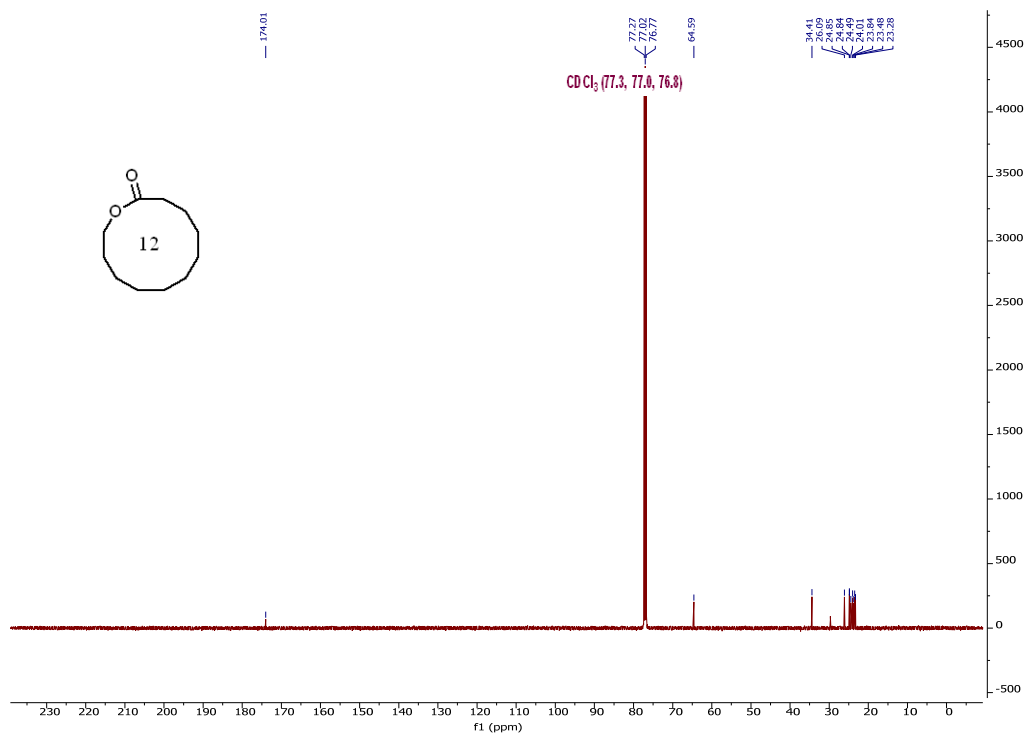


Figure S70. ^{13}C NMR Spectra of compound 2k. Chloroform-*d*1, 125 MHz for ^{13}C NMR.

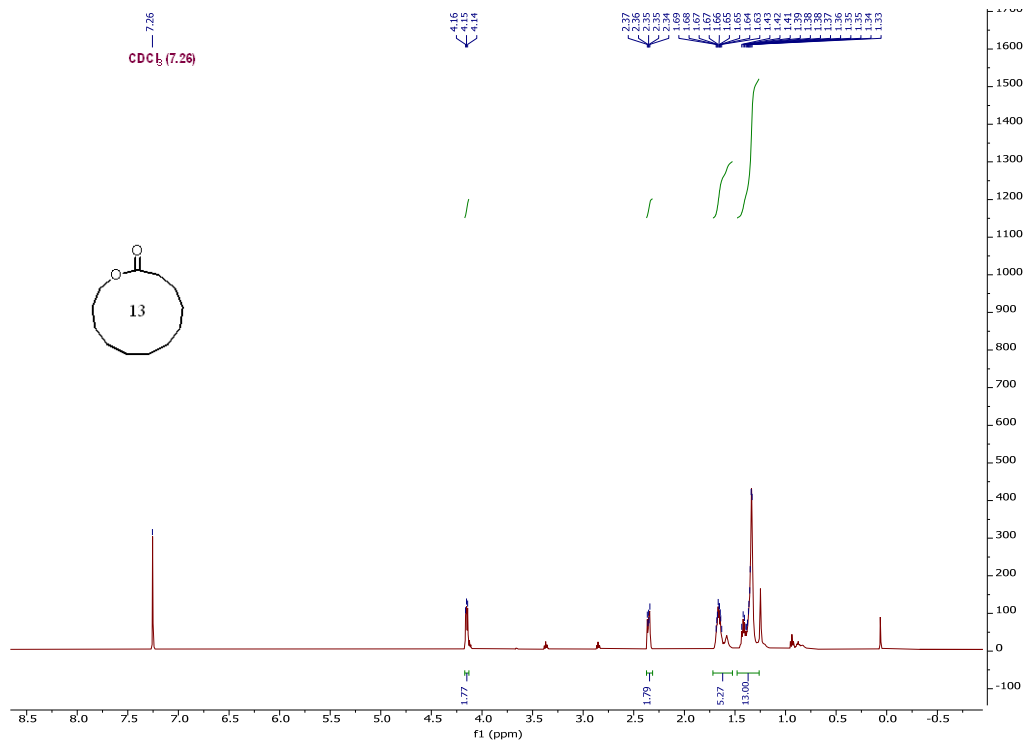


Figure S71. ¹H NMR Spectra of compound 21. Chloroform-*d*1, 500 MHz for ¹H NMR.

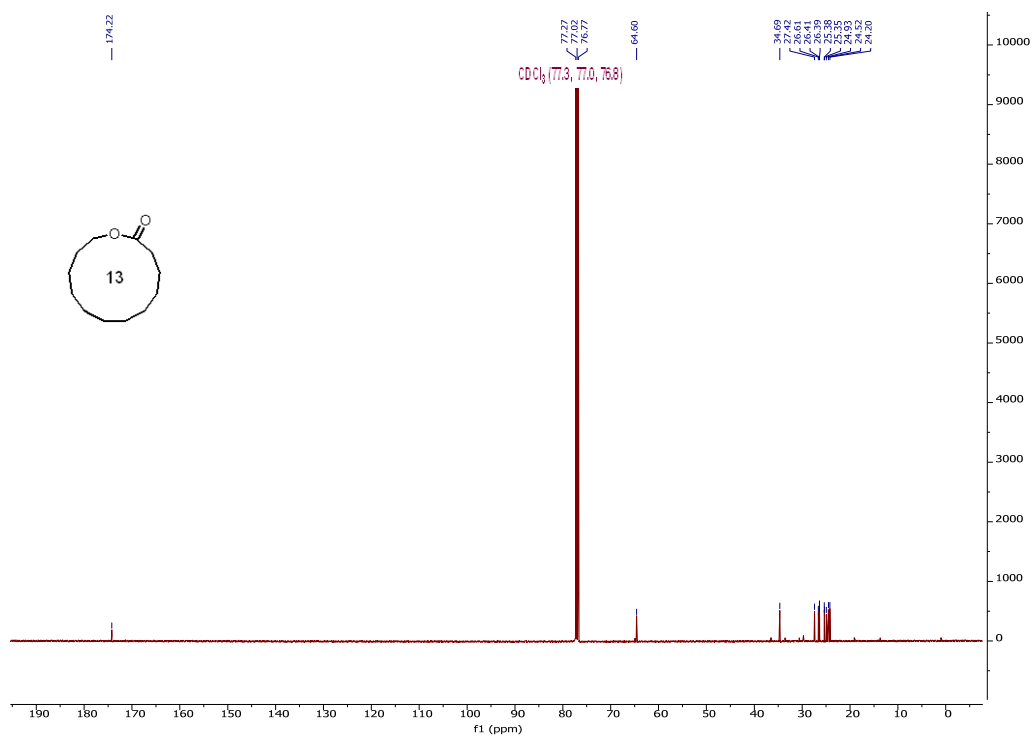


Figure S72. ¹³C NMR Spectra of compound 21. Chloroform-*d*1, 125 MHz for ¹³C NMR.

References

- (1) Sato, M.; Yagishita, F.; Mino, T.; Uchiyama, N.; Patel, A.; Chooi, Y. H.; Goda, Y.; Xu, W.; Noguchi, H.; Yamamoto, T.; Hotta, K.; Houk, K. N.; Tang, Y.; Watanabe, K. Involvement of Lipocalin-Like CghA in Decalin-Forming Stereoselective Intramolecular [4+2] Cycloaddition. *Chem. Bio. Chem.* **2015**, *16*, 2294–2298.
- (2) Li, L.; Yu, P.; Tang, M. C.; Zou, Y.; Gao, S. S.; Hung, Y. S.; Zhao, M.; Watanabe, K.; Houk, K. N.; Tang, Y. Biochemical Characterization of a Eukaryotic Decalin-Forming Diels-Alderase. *J. Am. Chem. Soc.* **2016**, *138*, 15837–15840.
- (3) Zou, Y.; Zhan, Z.; Li, D.; Tang, M.; Cacho, R. A.; Watanabe, K.; Tang, Y. Tandem Prenyltransferases Catalyze Isoprenoid Elongation and Complexity Generation in Biosynthesis of Quinolone Alkaloids. *J. Am. Chem. Soc.* **2015**, *137*, 4980–4983.
- (4) Yan, Y.; Liu, Q.; Zang, X.; Yuan, S.; Bat-Erdene, U.; Nguyen, C.; Gan, J.; Zhou, J.; Jacobsen, S. E.; Tang, Y. Resistance-Gene-Directed Discovery of a Natural-Product Herbicide with a New Mode of Action. *Nature* **2018**, *559*, 415–418.
- (5) Minor, W.; Cymboriwski, M.; Otwinowski, Z. & Chruszcz, M. HKL-3000: the integration of data reduction and structure solution-from diffraction images to an initial model in minutes. *Acta Crystallogr. Sect. D. Biol. Crystallogr.* **2006**, *62*, 859–866.
- (6) Kabsch, W. XDS. *Acta Crystallogr. Sect. D. Biol. Crystallogr.* **2010**, *66*, 125–132.
- (7) Winn, M. D.; Ballard, C. C.; Cowtan, K. D.; Dodson, E. J.; Emsley, P.; Evans, P. R.; Keegan, R. M.; Krissinel, E. B.; Leslie, A. G. W.; McCoy, A.; McNicholas, S. J.; Murshudov, G. N.; Pannu, N. S.; Potterton, E. A.; Powell, H. R.; Read, R. J.; Vagin, A.; Wilson, K. S. Overview of the CCP4 Suite and Current Developments. *Acta Crystallogr. Sect. D. Biol. Crystallogr.* **2011**, *67*, 235–242.
- (8) Adams, P. D.; Afonine, P. V.; Bunkóczi, G.; Chen, V. B.; Davis, I. W.; Echols, N.; Headd, J. J.; Hung, L. W.; Kapral, G. J.; Grosse-Kunstleve, R. W.; McCoy, A. J.; Moriarty, N. W.; Oeffner, R.; Read, R. J.; Richardson, D. C.; Richardson, J. S.; Terwilliger, T. C.; Zwart, P. H. PHENIX: A Comprehensive Python-Based System for Macromolecular Structure Solution. *Acta Crystallogr. Sect. D. Biol. Crystallogr.* **2010**, *66*, 213–221.
- (9) McCoy, A. J.; Grosse-Kunstleve, R. W.; Adams, P. D.; Winn, M. D.; Storoni, L. C.; Read, R. J. Phaser Crystallographic Software. *J. Appl. Crystallogr.* **2007**, *40*, 658–674.
- (10) Emsley, P.; Cowtan, K. Coot: Model-Building Tools for Molecular Graphics. *Acta Crystallogr. Sect. D. Biol. Crystallogr.* **2004**, *60*, 2126–2132.
- (11) DeLano, W. L. PyMOL: an Open-Source Molecular Graphics Tool. *Ccp4 Newslett. Protein Crystallogr.* **2002**, *40*, 82–92.
- (12) Schuck, P. Size-Distribution Analysis of Macromolecules by Sedimentation Velocity Ultracentrifugation and Lamm Equation Modeling. *Biophys. J.* **2000**, *78*, 1606–1619.
- (13) Heberlig, G. W.; Wirz, M.; Wang, M.; Boddy, C. N. Resorcylic Acid Lactone Biosynthesis Relies on a Stereotolerant Macrocyclizing Thioesterase. *Org. Lett.* **2014**, *16*, 5858–5861.
- (14) Hansen, D. A.; Koch, A. A.; Sherman, D. H. Substrate Controlled Divergence in Polyketide Synthase Catalysis. *J. Am. Chem. Soc.* **2015**, *137*, 3735–3738.
- (15) Morris, G. M.; Huey, R.; Lindstrom, W.; Sanner, M. F.; Belew, R. K.; Goodsell, D. S.; Olson, A. J. AutoDock4 and AutoDockTools4: Automated Docking with Selective Receptor Flexibility. *J. Comput. Chem.*

2009, 30 (16), 2785–2791.

- (16) Trott, O.; Olson, A. J. AutoDock Vina: Improving the Speed and Accuracy of Docking with a New Scoring Function, Efficient Optimization, and Multithreading. *J. Comput. Chem.* **2010**, 31 (2), 455–461.
- (17) Bannwarth, C.; Ehlert, S.; Grimme, S. GFN2-XTB—An Accurate and Broadly Parametrized Self-Consistent Tight-Binding Quantum Chemical Method with Multipole Electrostatics and Density-Dependent Dispersion Contributions. *J. Chem. Theory Comput.* **2019**, 15 (3), 1652–1671.
- (18) Lee, C.; Yang, W.; Parr, R. G. Development of the Colle-Salvetti Correlation-Energy Formula into a Functional of the Electron Density. *Phys. Rev. B* **1988**, 37 (2), 785–789.
- (19) Becke, A. D. Density-functional Thermochemistry. III. The Role of Exact Exchange. *J. Chem. Phys.* **1993**, 98 (7), 5648–5652.
- (20) Stephens, P. J.; Devlin, F. J.; Chabalowski, C. F.; Frisch, M. J. Ab Initio Calculation of Vibrational Absorption and Circular Dichroism Spectra Using Density Functional Force Fields. *J. Phys. Chem.* **1994**, 98 (45), 11623–11627.
- (21) Grimme, S.; Ehrlich, S.; Goerigk, L. Effect of the Damping Function in Dispersion Corrected Density Functional Theory. *J. Comput. Chem.* **2011**, 32 (7), 1456–1465.
- (22) Rassolov, V. A.; Pople, J. A.; Ratner, M. A.; Windus, T. L. 6-31G* Basis Set for Atoms K through Zn. *J. Chem. Phys.* **1998**, 109 (4), 1223–1229.
- (23) Frisch, M. J.; Trucks, G. W.; Schlegel, H. B.; Scuseria, G. E.; Robb, M. A.; Cheeseman, J. R.; Scalmani, G.; Barone, V.; Petersson, G. A.; Nakatsuji, H.; Li, X.; Caricato, M.; Marenich, A. V.; Bloino, J.; Janesko, B. G.; Gomperts, R.; Mennucci, B.; Hratchian, H. P.; Ortiz, J. V.; Izmaylov, A. F.; Sonnenberg, J. L.; Williams-Young, D.; Ding, F.; Lipparini, F.; Egidi, F.; Goings, J.; Peng, B.; Petrone, A.; Henderson, T.; Ranasinghe, D.; Zakrzewski, V. G.; Gao, J.; Rega, N.; Zheng, G.; Liang, W.; Hada, M.; Ehara, M.; Toyota, K.; Fukuda, R.; Hasegawa, J.; Ishida, M.; Nakajima, T.; Honda, Y.; Kitao, O.; Nakai, H.; Vreven, T.; Throssell, K.; Montgomery Jr., J. A.; Peralta, J. E.; Ogliaro, F.; Bearpark, M. J.; Heyd, J. J.; Brothers, E. N.; Kudin, K. N.; Staroverov, V. N.; Keith, T. A.; Kobayashi, R.; Normand, J.; Raghavachari, K.; Rendell, A. P.; Burant, J. C.; Iyengar, S. S.; Tomasi, J.; Cossi, M.; Millam, J. M.; Klene, M.; Adamo, C.; Cammi, R.; Ochterski, J. W.; Martin, R. L.; Morokuma, K.; Farkas, O.; Foresman, J. B.; Fox, D. J. Gaussian 16 Revision A. 03. 2016.